Representing the Car-Following Behaviour of Adaptive Cruise Control (ACC) Systems Using Parametric Car-Following Models

M. Blauw

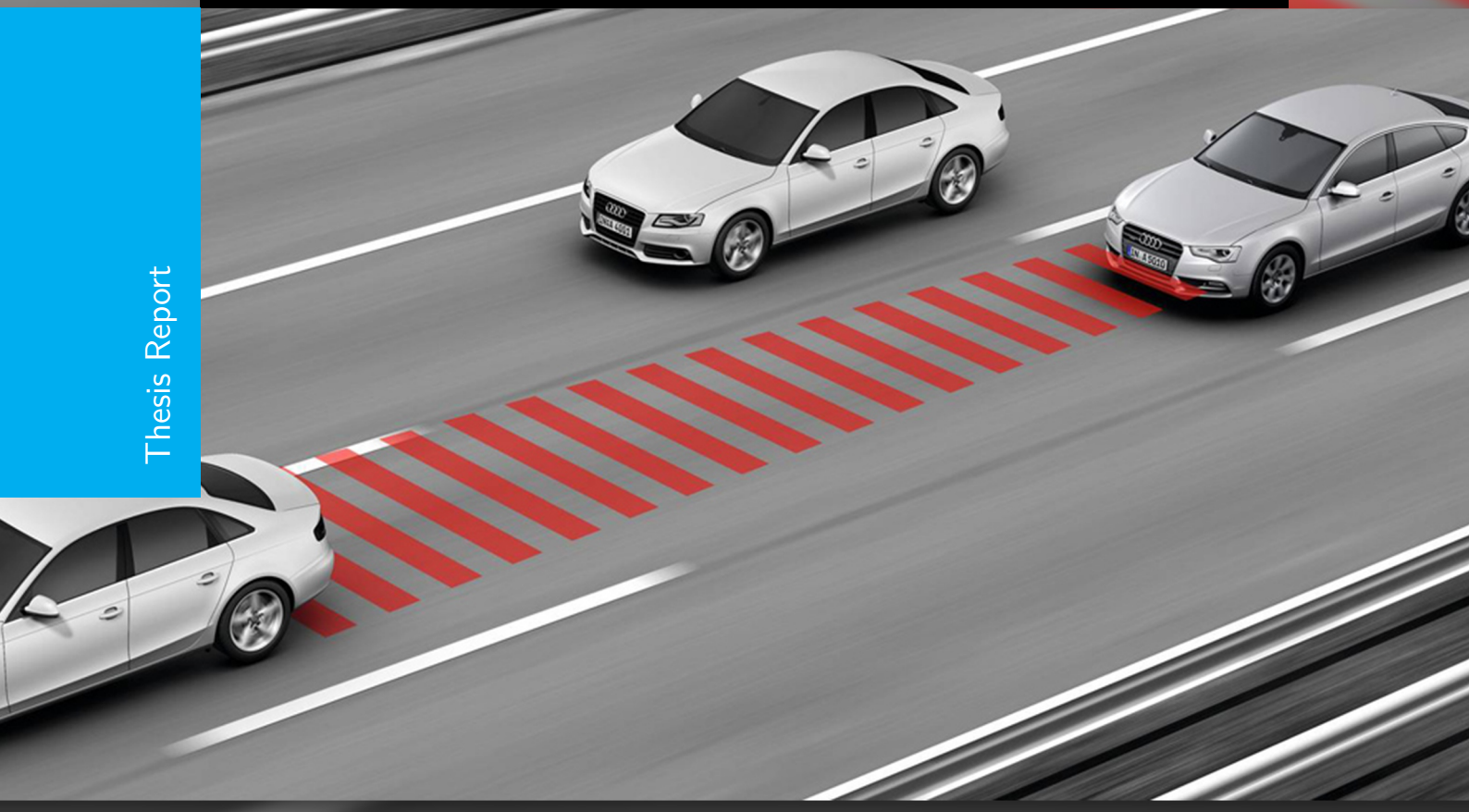

Thesis Report

TU Delft Delft University of Technology

Vehicle Engineering

Representing the Car-Following Behaviour of Adaptive Cruise Control (ACC) Systems Using Parametric Car-Following Models

by

M. Blauw

For the degree of Master of Science in Mechanical Engineering at Delft University of Technology

To be defended publicly on October 11th 2019, at 14:00h

Student Number	4195809	
Project Duration	September 1st, 2018 - October 11th, 2019	
Thesis Committee	Dr.ir. R. Happee	TU Delft, 3mE, CoR, Chairman
	Dr. V.L. Knoop	TU Delft, CITG, T&P, Associate Professor
	Dr.ir. M. Wang	TU Delft, CITG, T&P, Assistant Professor
	A. Spaans	Rijkswaterstaat, Guest

Faculty of Mechanical, Maritime and Materials Engineering (3mE) · Delft University of Technology

Rijkswaterstaat
Ministerie van Infrastructuur en Milieu

The work in this thesis was supported by Rijkswaterstaat. Their cooperation is hereby gratefully acknowledged.

TU Delft Delft University of Technology

Cognitive Robotics

Abstract

The Dutch governmental organisation Rijkswaterstaat contributes to the smooth and safe flow of traffic, as both traffic jams and accidents cost society large amounts of money each day. Roads are designed for the current traffic composition. Due to the promotion of Adaptive Cruise Control (ACC) systems, utilisation of these systems is expected to increase. Society benefits from insights into the effects these systems have on traffic flow, as they can help to reduce traffic jams and accidents.

ACC systems are designed to increase driving comfort by taking over throttling and braking from the human driver. For optimal driver acceptance, these systems show similar driving behaviour to that of human drivers. However, this is not entirely possible due to limited anticipation. To predict how differences in driving behaviour affect traffic flows, researchers usually perform simulations using parametric car-following models. However, research shows contradictory findings.

The goal of this research was to gain insights into the performance of commonly applied parametric car-following models on representing the driving behaviour of ACC systems. Optimal model calibration was obtained by investigating the sensitivity of the model calibration to synthetic data. Investigated were the calibration methodology and the quality and quantity of calibration data. Models are calibrated to real-world driving data from an Audi A4 from 2017. These models were used to assess the capability of representing typical highway scenarios: steady-state car-following, cut-in, cut-out, hard-braking and stop-and-go scenarios. The considered models were the Intelligent Driver Model (IDM) model, which has previously been applied to model the driving behaviour of human drivers, the newly developed simplified ACC (sACC) model and a variant on this model.

Insights in the sensitivity of the model calibration were obtained by performing a sensitivity analysis on synthetic data. Essential factors in achieving an optimal model calibration are: *1)* the model closely matches the driving behaviour in the data, *2)* noise levels are as low as possible and *3)* the data should contain as many situations as possible that are also included in the model. The dataset must be sufficiently long to include all these situations and to allow the model to develop its dynamics entirely.

Using these insights, a calibration was performed on real-world ACC driving data from an Audi A4 (2017). For the ACC system, it was found: *1)* the ACC system exhibits non-linear driving behaviour, *2)* the acceleration depends on the current velocity and distance to the desired velocity, *3)* the system does not consider an intelligent braking strategy and is thus not able of handling safety-critical driving situations and *4)* the model includes a sub-controller which ensures comfortable driving behaviour. Except for the comfortable sub-controller, the non-linear IDM model considers all of these factors and thus best represents the driving behaviour. The linear sACC model cannot represent standing conditions, which is resolved in the alternative version. The linearity allows for a better representation of the behaviour of the comfortable sub-controller. However, it disallows for an accurate representation of the dynamics by the models.

Table of Contents

Preface

Currently, you are reading the report: "Representing the car-following behaviour of Adaptive Cruise Control (ACC) systems using parametric car-following models". This thesis is written as part of my graduation for the masters Vehicle Engineering at the Delft University of Technology. The report is the result of approximately a year of analysing more than 10 GB of vehicle driving data. The research was executed in cooperation with Rijkswaterstaat.

During the masters Vehicle Engineering, much attention is paid on the design of vehicle automation systems and on proving their workings. For me, this raised questions about the feasibility and performance of these systems in actual driving situations. One of my supervisors, Victor Knoop, helped me to identify the state-of-the-art research and unanswered questions. Thanks to Rijkswaterstaat, I got access to an extensive recent data-set containing real-world driving behaviour of an Audi equipped with ACC, on which I could fit the models. The research has taught me a lot about traffic flows and comfortable driving, things one should definitely keep in mind as a designer of these systems.

This research is conducted under the supervision of Victor Knoop, Meng Wang and Riender Happee from the Delft University of Technology. I want to thank all of of my supervisors for their enthusiasm, criticism and valuable time. You were always very approachable and coached me to get the most out of myself. Without your supervision, I am sure the quality of the research would have never been of the same level.

I want to thank Rijkswaterstaat, the Ministry of Infrastructure and Water Management, the RDW and TNO for providing access to the SAE-L2 data-set. I also want to thank my supervisors from Rijkswaterstaat: André Spaans, who supervised my personal development during my graduation year, Tom Alkim and Henk Schuurman, who taught me a lot about the organisation. Next to this, I want to thank all of my direct colleagues, thanks to whom I have had a great year. I also want to thank Audi AG for providing the cover image.

Finally, I want to thank my family, friends and especially my girlfriend Maike for always supporting me and for every single moment we have ever had.

Mathieu Blauw
Utrecht, October 2019

"With four parameters I can fit an elephant, and with five I can make him wiggle his trunk."

— *John von Neumann*

Chapter 1

Introduction

1-1 Background

On a busy highway, each vehicle continuously reacts to other vehicles surrounding it. Therefore, the equilibrium flow of vehicles through a particular road segment and the dynamics of the flow result from the combination of all vehicles driving on the road. Adaptive Cruise Control (ACC) systems are designed to increase driving comfort by taking over the longitudinal Vehicle Motion Control (VMC) sub-task of the Dynamic Driving Task (DDT) (i.e. throttling and braking) from the human driver (Happee et al., 2018). The driver stays responsible for performing the remaining sub-tasks from the DDT and must supervise the ACC system. In case the driver prefers to deactivate the system, or the system requires or demands for deactivation, the longitudinal motion control sub-task can, and in most cases will be handed back to the driver.

ACC systems must show predictable behaviour for the human driver and other passengers in the vehicle to avoid motion sickness and increase driver acceptation (Viti et al., 2008). The gap-policy and dynamics of the system are therefore expected to be very similar to the non-linear control towards a constant time-gap often found for human drivers (Blauw, 2019). However, there are a few essential differences. The driving behaviour of ACC systems is more deterministic than that of human drivers. Moreover, while improvements have been made over the last years, temporal anticipation (the ability to look ahead in time) and spatial anticipation (the ability to look ahead on the road) are expected to be lower in most ACC systems than in human driving behaviour (Schakel et al., 2017).

Because of the similarity in driving behaviour with that of human drivers, disturbances in the traffic flow consisting of vehicles driving with ACC also have the ability to accumulate through a string of vehicles (Schakel et al., 2010). In case a disturbance, like a vehicle braking, is amplified throughout the string, the braking action will get stronger. If the effects continue, after some time a vehicle is brought to a complete stop, and a traffic jam will arise. Whenever a vehicle located at an arbitrary position in the string is not able to brake hard enough, even collisions can occur (Treiber and Kesting, 2013b).

Predictions on the effects of rising numbers of ACC on the road are generally obtained through simulations using the new traffic composition (for example in Liu et al. (2018); Kesting et al. (2006); Shladover et al. (2012)). Due to computational complexity, it is often undesirable to bring a complete vehicle model including control systems into the simulation environment. In some papers,

the designed controller is moved directly into a simulation environment. A second solution is to model each vehicle using a parametric car-following model, which is calibrated to vehicle data for optimal representation. Each model assumes a different (simplified) representation of the actual driving behaviour, influencing results of a simulation if the models are applied (Blauw, 2019). The models mostly applied to represent the driving behaviour of ACC systems are the Intelligent Driver Model (IDM) model, the simplified ACC (sACC) model and a variant of this model. The IDM model has previously been applied to model human driving behaviour.

1-2 Motivation

The Dutch governmental organisation Rijkswaterstaat contributes to the smooth and safe flow of traffic on the Dutch roads, as both traffic jams and accidents cost society large amounts of money each day. In the recently signed ADAS Covenant (ADAS Alliantie, 2019), among other things, the agreement was made to promote the use of ACC on the Dutch roads. To be able to anticipate on the effects resulting from changing traffic compositions, the organisation benefits from research performed on the topic of the effects of ACC on traffic flow.

Earlier performed research has shown that ACC usage increases road safety by a reduction in the number of head to tail accidents (Alkim et al., 2007). When it comes to traffic flow, however, the literature study has shown that current research shows contradictory findings (Blauw, 2019). Insufficient knowledge about the actual on-road performance of ACC systems in design studies often leads to an overestimation of their capabilities. Throughout empirical studies, the performance of the IDM model, which was initially designed to describe the driving behaviour of human drivers, and of the newly developed sACC model on representing the driving behaviour is still relatively unexplored field. Moreover, current studies often ignore the fact that the human driver can overrule the system and select different time-gap settings, the fact that systems have a limited operating range and the fact that different vehicles show different behaviour.

Models largely define the traffic flow dynamics, and equilibrium flow observed in traffic simulations. Therefore, profound knowledge on the driving behaviour of ACC systems and on the performance of these models on representing this driving behaviour must be present. The performance of a model on representing the driving behaviour is the result of the performance of the calibration process, in combination with the capability of the model on representing the behaviour of the system. Therefore, this thesis addresses the sensitivity of the model calibration and capability of optimally calibrated models on representing actual vehicle data. The research will be performed on a large data-set containing logged in-vehicle driving data of the ACC system from an Audi A4.

1-3 Research Questions

The goal of this research is to gain insights on the performance of existing parametric car-following models on representing the driving behaviour of ACC systems. To reach this goal, optimal calibration methodology will be determined from the results of the sensitivity analysis of the model calibration. Applying this optimal calibration methodology to the models allows for an investigation of the capability of the models on representing the driving behaviour of an actual ACC system. Performance on describing this system, together with findings from literature, will be used

to hypothesise on the performance on modelling other ACC systems. The goal will be achieved by answering the following research questions:

1. How is the calibration of existing parametric car-following models influenced by the calibration methodology and quality and quantity of calibration data?
   (a) How does the calibration methodology influence the results of the calibration procedure?
   (b) How do different pre-processing techniques influence the results of the calibration procedure?
   (c) How do the events present in the data influence the results of the calibration procedure?
   (d) How much data is needed for calibration?
2. How capable are existing parametric car-following models of representing the velocity and distance-gap of Adaptive Cruise Control (ACC) vehicles while car-following?
   (a) How to qualify the capability of car-following models?
   (b) What is the certainty of the estimated model parameters?
   (c) What is the overall fitting quality of the considered models?
   (d) Which events can or cannot be described by the considered models?

1-4 Research Approach

These research questions will be answered by applying the research approach shown in Figure 1-1. Literature is used to identify the current state-of-the-art in research. A synthesis from this literature review is already included at the beginning of this chapter. After structuring the problem and prioritising the issues, in the second step of the research, an issue analysis plan and research methodology will be defined. Before it is possible to perform an actual analysis of the in-vehicle data and answer the research questions, the data first has to be processed. After processing, application of the presented model calibration framework to synthetic data allows to answer research question 1. Findings from answering this research question forms the basis for the analysis of actual vehicle data. In this final step, the presented model calibration framework will again be applied, but this time to real-world vehicle data. Using the obtained results, research question 2 will be answered.

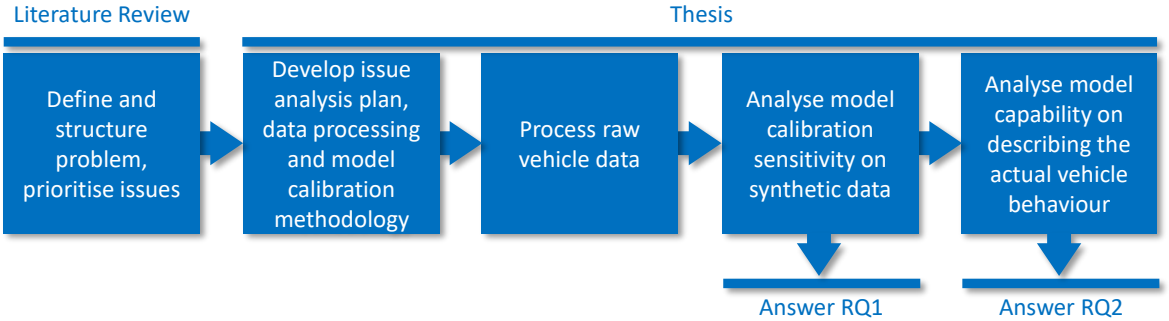

Figure 1-1: Schematic representation of the research approach.

1-5 Research Scope

This research will be focused on capturing the pure longitudinal car-following behaviour of the ACC system from an Audi A4 (2017) on highways. Only highway driving scenarios will be considered because, in urban driving conditions, the vehicle frequently interacts with the environment and infrastructure. Such situations cannot be represented by the considered car-following models and have to be removed from the considered data-set. This would result in lots of discontinuous intervals, whereas in highway driving these effects are less present, and thus longer continuous intervals can be retained. This research will furthermore be limited by the common driving scenarios that can be represented by the two models. Which means only constrained driving situations (car-following) will be considered. Finally, the research does not consider situations in which the human driver is involved with performing the longitudinal VMC sub-task of the DDT or in which actions undertaken by the human driver could influence the execution of longitudinal VMC. This means that situations such as human takeovers and lane-changing will not be considered.

1-6 Thesis Outline

Results from the research approach presented in the previous section will be included in this thesis report according to the structure represented in Figure 1-2. In this chapter, background introduction about the problem has been given, the current issues have been prioritised, and the research approach has been presented. Chapter 3 will introduce the applied issue analysis, data processing and model calibration methodology. In Chapter 4, processing steps performed on the in-vehicle data required for data analysis will be discussed. The analysis of synthetic data and actual vehicle data, with which both research questions will be answered, will be discussed in Chapters 5 and 6, respectively. Finally, Chapter 7 includes a conclusion on all findings, a discussion on the applied research methodology and obtained results, and recommendations upon further research.

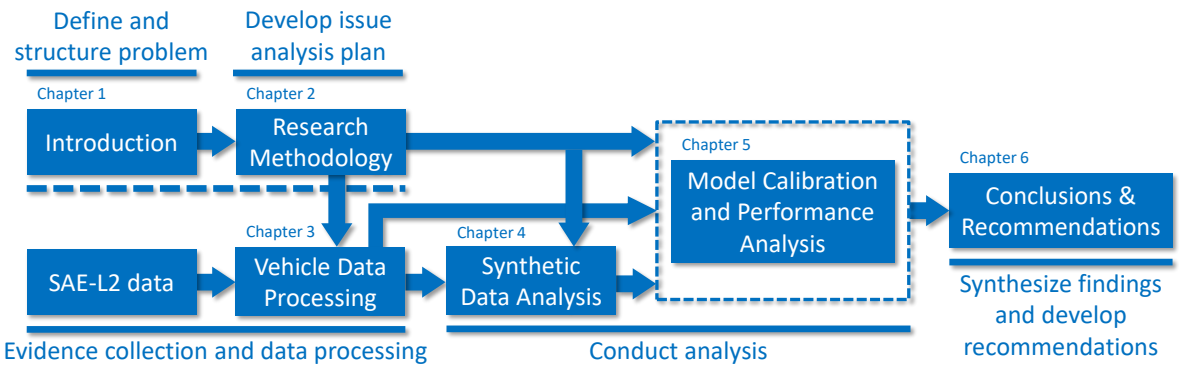

Figure 1-2: Schematic representation of the thesis outline.

Chapter 2

Parametric Car-Following Models

2-1 Introduction

The Intelligent Driver Model (IDM) and simplified ACC (sACC) models fall under the class of parametric continuous-time microscopic car-following models. Both models reactively define the current acceleration $\dot{v}_i$ as a function a_{mic} of the current velocity of the ego-vehicle v_i, the velocity of its direct leader v_{i-1}, and the current distance-gap between the vehicle and its direct leader s_i. Their mathematical expression is given in Equation 2-1, and a graphical interpretation is shown in Figure 2-1. The models are characterised by instantaneous accelerations, limited spatial anticipation (only to their direct leader) and deterministic behaviour towards the inputs.

$$\dot{v}(t) = a_{mic}(s_i(t), v_i(t), v_{i-1}(t)) \tag{2-1}$$

The considered models are commonly used throughout literature for representing the driving behaviour of Adaptive Cruise Control (ACC) systems. The IDM model was initially introduced in Treiber et al. (2000) for representing the driving behaviour of human drivers. The model is nowadays also applied by researchers for describing the driving behaviour of ACC systems (for example, by A. Kesting in Kesting et al. (2006); Kesting (2008)). The sACC model is a simplified version of the expected ACC control logic. In its current form, the model was introduced in Milanés and Shladover (2014), but variations have been applied before (for example, in Schakel et al. (2010)). The model is mainly used by V. Milanés (Milanés and Shladover, 2014, 2016) and L. Xiao (Xiao et al., 2017, 2018). In the next section, a more elaborate introduction to both models will be given.

2-2 Model Properties

The IDM model is a non-linear car-following model, characterised by the acceleration function shown in Equation 2-2. For notation simplicity, (t) has been dropped from the acceleration function in the rest of this chapter.

$$\dot{v}_{IDM}(s_i, v_i, v_{i-1}) = a \cdot \left[1 - \left(\frac{v_i}{v_0}\right)^4 - \left(\frac{s_d(v_i, v_{i-1})}{s_i}\right)^2\right], \qquad \text{where} \tag{2-2}$$

$$s_d(v_i, v_{i-1}) = s_0 + v_i T + \frac{v_i(v_i - v_{i-1})}{2\sqrt{ab}}$$

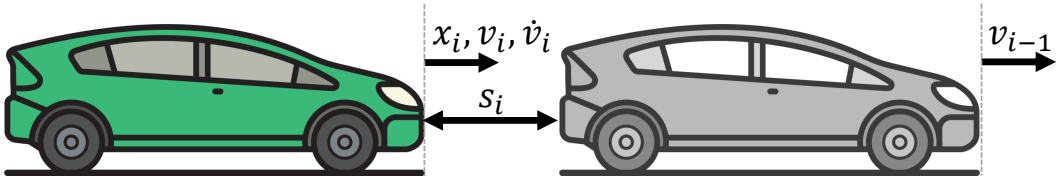

Figure 2-1: Figure showing the vehicle variables.

Five parameters allow for tuning of the driving behaviour as represented by the model. For each of the parameters, a short description and typical (published) values are included in Table 2-1. The model mainly has three operating modes. In unconstrained driving situations ($s_i \gg 0$), the model controls the vehicle to the desired velocity v_0, according to $\dot{v}_{i,ncon} \approx a \cdot [1 - (v_i / v_0)]$. In approaching and safety-critical braking conditions, the velocity difference between the vehicle and lead vehicle is generally large ($v_i - v_{i-1}$ = 'large'). The dynamics of the system are in these situations dominated by the intelligent braking strategy $\dot{v}_{i,appr} \approx -[(v_i(v_i - v_{i-1})) \ / \ (2\sqrt{b}s_i)]^2$. This strategy mainly allows for hard braking in safety-critical situations, avoiding possible collisions. Finally, in constrained driving situations ($s_i - s_d$ = 'small'), the model controls the vehicle to the desired distance-gap $\dot{v}_{i,con} \approx -a[(s_0 + v_i T)/s_i]^2$. The considered relation is quadratic and depends on the current distance-gap. This distance-gap is generally larger at higher velocities, thus resulting in lower accelerations. In most situations, the acceleration and deceleration profiles are symmetric, but they become asymmetric in case the intelligent braking strategy is activated. The model accepts slightly shorter following distances than s_d in case the distance to the desired velocity (v_i / v_0) is large.

The sACC model is a linear car-following model that considers a similar constant time-gap policy as the IDM model. The model is characterised by the acceleration function

$$\dot{v}_{ACC}(s_i, v_i, v_{i-1}) = k_p(s_i - s_d(v_i)) + k_d(v_{i-1} - v_i), \qquad \text{where} \tag{2-3}$$
$$s_d(v_i) = v_i t_d + s_0$$

The original sACC model includes three parameters (s_0 is not considered). In the analysis of real-world vehicle data, also a variation will be considered which includes s_0. A description of the model parameters and typical values is included in Table 2-1. Because of the linearity of the model, application is restricted to constrained driving situations. In contrast to the IDM model, the sACC model makes more assumptions about the driving behaviour. For example, the model considers a similar maximum acceleration at all velocities, considers no different braking strategy in safety-critical situations (risk of collisions), and considers a linear relation between a deviation in the distance-gap and resulting acceleration. Mathematically this is expressed as $\dot{v}_i(s_i^* + \delta_s) \equiv -\dot{v}_i(s_i^* - \delta_s)$, where δ_s is some small disturbance from the equilibrium. The same holds for disturbances in the velocity difference.

Table 2-1: An overview of the model parameters of the IDM and sACC models.

Parameters (IDM)	Description	Typical Value	Parameters (sACC)	Description	Typical Value
a, m/s^2	Maximum comfortable acceleration	1.25	k_p, s^{-2}	Distance-gap gain	0.23
b, m/s^2	Maximum comfortable deceleration	1.25	k_d, s^{-1}	Velocity gain	0.07
T, s	Desired time-gap	1.4	t_d, s	Desired time-gap	1.4
v_0, m/s	Desired velocity	55	s_0, s	Minimum standstill distance	0 or 3
s_0, m	Minimum standstill distance	3			

Chapter 3

Research Methodology

3-1 Introduction

In the previous chapter, the models which will be considered throughout this thesis research were introduced. The parameters of each of the models allow them to represent different behavioural variations within their considered driving style. The goal of the calibration procedure is to tune the model parameters such that the model optimally represents the driving behaviour captured in the data. The optimally calibrated model then allows for capability analysis using validation techniques.

In this chapter, the methodology for data processing, model calibration and model validation will be introduced. Performance of the calibration process is among others, determined by the properties of the calibration data-set. Therefore, the methodology for processing vehicle data will first be discussed. From the set of processed vehicle data, suitable trajectories for model calibration will be selected. Synthetic data created upon the chosen model trajectories will be used in a sensitivity analysis of the model calibration. The goal of this analysis is to define optimal calibration methodology for calibrating the models to real-world data. Optimal calibration methodology is finally used to calibrate the models to real-world vehicle data.

This chapter will start by introducing the methodology for processing the Adaptive Cruise Control (ACC) vehicle data in Section 3-2. Section 3-3 will discuss the general methodology for model calibration, which is applied to both synthetic and real-world data. Section 3-4 will discuss the methodology for determining the sensitivity of the model calibration. Finally, Section 3-5 will discuss methodology for determining model performance on representing real-world data.

3-2 Methodology for Processing ACC Vehicle Data

The data-set considered throughout this thesis contains in-vehicle measurements that were captured during a field test on June 13^{th}, 2018. A connection to the vehicle's On-Board Diagnostics (OBD)-port allows for reading communication sent over the Controller Area Network (CAN)

bus, a communication interface for microcontrollers in automobiles. The connection provides information from the vehicle's sensors, actuators and other electronic systems, see Figure 3-1. This connection is used to obtain the velocity of the vehicle from the speedometer, to determine the state of the ACC system and to find events in which the human intervenes with the system (manual throttling, braking, lane-changing etc.). A GPS sensor is used for positioning of the vehicle relative to the earth's surface. Together with the accelerometer signal, the speedometer and GPS signals allow for accurate vehicle state determination. Information about the vehicle driving in front, which will act as exogenous inputs for the car-following model, is obtained using a MobilEye system.

The measurement signals are noisy and are, due to this noise and bias, not always entirely consistent with one another. For optimal vehicle state estimation, a Kalman filter will be applied to fuse measurement signals from the ego-vehicle. After applying the Kalman filter, additional smoothing will be performed using a moving average filter. The moving average filter will also be applied to the MobilEye signals. After filtering, situations which cannot be described using the car-following models will be removed from the considered data-set. The necessity of filtering this noise becomes clear from the sensitivity of the model calibration to residual noise, which will be further elaborated in Section 5-5. The methodology for preparing data for filtering and sensor fusion will be discussed in Section 3-2-1. Methods for filtering and sensor fusion will be discussed in Section 3-2-2. Methods for ensuring consistency of the data-set will be discussed in Section 3-2-3 and finally methods for data selection will be discussed in Section 3-2-4.

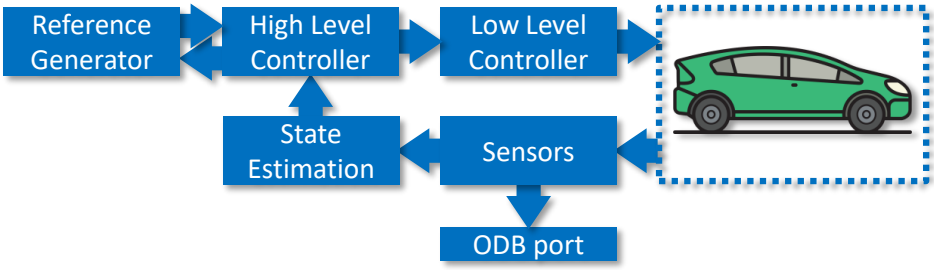

Figure 3-1: Schematic representation of the vehicle automation system.

3-2-1 Data Preparation

Model calibration requires continuous and smooth trajectories, in which all individual measurement signals are well in sync with each other. Measurements from the ego- and lead-vehicles will be filtered separately.

Ego-Vehicle Measurements

Measurements from the ego-vehicle are filtered using a Kalman filter. The Kalman filter enhances vehicle state estimation by fusing evidence from the GPS (x_{GPS}), speedometer (v_{CAN}) and accelerometer ($\dot{v}_{ACL}$) signals. While the Kalman filter is able to handle asynchronous measurement-times, the setup of the filter is greatly simplified if different signals are re-timed such that they are in sync and include a constant sampling interval. Re-timing signals will be performed by using linear interpolation, with a new sampling interval of Δt equal to the sampling interval of the speedometer and accelerometer measurements of 0.1 seconds. Times at which at least one of the

measurement signals is missing will be removed from the data-set. Data is considered missing if at least three consecutive measurements are not present. The sampling interval of the speedometer and accelerometer is higher than the one of the GPS signal. Therefore, more value is attached to the correct matching of these signals.

The GPS signal is used as evidence on the distance travelled by the vehicle. In the considered highway driving conditions, the vehicle is assumed to perform a purely longitudinal motion. Because of inconsistencies found in the sampling interval, differentiating the position measurements would result in high-frequency oscillations in the velocity signal. By integration of the velocity, this is avoided (Treiber and Kesting, 2013b). The measurements are sampled and thus require applying a proper stable numerical integration scheme, such as the trapezoidal rule (Wilson, 2001)

$$x_i(t+\Delta t) = x_i(t) + \Delta t \cdot \frac{v_i(t) + v_i(t+\Delta t)}{2} \tag{3-1}$$

A lag in the GPS signal causes it to be out-of-sync with the other measurement signals. It is assumed that this lag is caused by the time a GPS signal takes to travel from the satellite to the surface of the earth. Therefore, the lag is considered as non-stationary, and lag-compensation needs to be performed locally. The lag ($\delta^*_{GPS}(t)$) will be identified by sliding a window of width $300s$ over the data, for each time-step performing minimisation of the Root Mean Square Error (RMSE) between the speedometer signal and a time-shifted version of the GPS signal, see Figure 3-2. The RMSE between two measurement signals $\mathbf{z_i} \in \mathbb{R}^{N\times 1}, i = [1,\ 2]$ will be denoted as $\mathcal{F}_{RMSE}$ and is defined as:

$$\mathcal{F}_{RMSE}(\mathbf{z_1}, \mathbf{z_2}) = \sqrt{\frac{1}{N}\sum_{k=1}^{N}(z_1(k) - z_2(k))^2} \tag{3-2}$$

In case any discontinuities are present in the window, only the continuous region adjacent to the current point up to the discontinuity will be considered. In case discontinuities cause the range to drop below 20 seconds, the lag will be set to the mean of all observed lags.

The second signal considered in vehicle state estimation is the velocity from the speedometer. This signal is not compensated for low tire pressure or low traction between the tires and road surface. These factors, combined with an offset to avoid legal claims for indicating too low velocities, cause the signal to overestimate the actual velocity of the vehicle systematically. The bias of the speedometer signal δ^*_{CAN} is assumed to be proportional to the velocity of the vehicle $\mathbf{v}_i$ and to be constant in time (Treiber and Kesting, 2013b; Dogruer, 2014). Therefore, it is more convenient to view the problem as a Least Squares Estimation (LSE) problem and remove the bias before the filter.

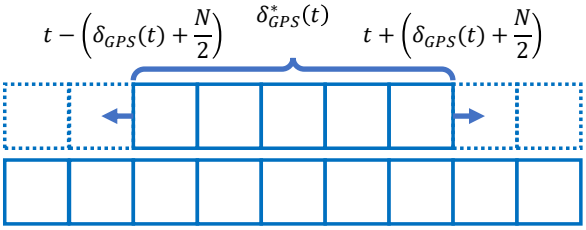

Figure 3-2: Figure showing a schematic representation of the applied sliding window methodology applied to determine the time-lag $\delta^*_{GPS}(t)$ in the GPS signal.

The compensated signal is defined as:

$$\mathbf{v}_{correct,i} = \delta^*_{CAN}\mathbf{v}_i \tag{3-3}$$

Since $\mathbf{v}^T_{CAN}\mathbf{v}_{CAN}$ is a scalar, δ^*_{CAN} is found by finding the least square estimate that minimises the error between the velocity from the speedometer and GPS signals (Verhaegen and Verdult, 2007), defined as:

$$\delta^*_{CAN} = 1 - (\mathbf{v}^T_{CAN}\mathbf{v}_{CAN})^{-1}\mathbf{v}^T_{CAN}\mathbf{v}_{GPS}$$

The last signal considered in the Kalman filter, the accelerometer signal, does only include drift which will be removed in the Kalman filter. Because the Kalman filter can only handle continuous intervals, locations at which data is missing will be marked.

Lead-Vehicle Measurements

Measurements on the distance-gap are originating from the MobilEye. In contrast to the measurements included in the Kalman filter, autocorrelation of noise sequences will be avoided by re-timing the measurements only after applying the filter. A change in the lead vehicle, resulting from passive or active lane-changes, causes a sudden jump in the velocity and distance-gap measurements from the MobilEye. Because of these jumps, it is not directly possible to filter these signals across these points. In line with Treiber and Kesting (2013a), points at which the lead vehicle changes and at which data is missing, will be marked.

3-2-2 Filtering and Sensor Fusion

The noise in all measurement signals is assumed to be zero-mean white only, meaning the noise sequence $\mathbf{X}$ has expectancy zero ($\mathbb{E}[\mathbf{X}] = 0$) and is nonautocorrelated ($R_X[n] = \sigma^2\delta[n]$). Furthermore, the noise between different measurement signals $\mathbf{z_1}$ and $\mathbf{z_2}$ is assumed to be uncorrelated ($\mathrm{Cov}[\mathbf{z_1}, \mathbf{z_2}] = 0$).

Kalman Filter

Only highway driving is considered in which the vehicle is assumed to perform a purely longitudinal motion. This allows definition of a similar, but greatly simplified version of the Kalman filter applied in (Magnusson and Odenman, 2012). The relations between states $\mathbf{x}(t)$ and $\mathbf{x}(t+\Delta t)$, and between sensor measurements $\mathbf{z}(t)$ and the vehicle state $\mathbf{x}(t)$ at time t, are defined as:

$$\underbrace{\begin{bmatrix} x \\ v \\ \dot{v} \end{bmatrix}}_{\mathbf{x}}(t+\Delta t) = \underbrace{\begin{bmatrix} 1 & \Delta t & \frac{1}{2}\Delta t^2 \\ 0 & 1 & \Delta t \\ 0 & 0 & 1 \end{bmatrix}}_{A} x(t) + \mathbf{w}(t), \qquad \underbrace{\begin{bmatrix} x_{gps} \\ v_{can} \\ \dot{v}_{acl} \end{bmatrix}}_{\mathbf{z}}(t) = \underbrace{\begin{bmatrix} 1 & 0 & 0 \\ 0 & 1 & 0 \\ 0 & 0 & 1 \end{bmatrix}}_{C} x(t) + \mathbf{v}(t) \tag{3-4}$$

where $\mathbf{w}(t)$ and $\mathbf{v}(t)$ represent the process and measurement noise, respectively. For notation simplicity, subscript i has been dropped from the equation.

The Kalman filter, as shown in Figure 3-3, allows one to obtain the filtered state estimate $\hat{\mathbf{x}}(t|t)$ using prior state information $\hat{\mathbf{x}}(t|t-\Delta t)$ and new measurement information $\mathbf{z}(t)$ as:

$$\hat{\mathbf{x}}(t|t) = \hat{\mathbf{x}}(t|t-\Delta t) + K^T(t)\left(\mathbf{z}(t) - C\hat{\mathbf{x}}(t|t-\Delta t)\right) \tag{3-5}$$

$\hat{\mathbf{x}}(t|t-\Delta t)$ is obtained by applying a time-update (Equation 3-6) to the filtered state estimate obtained in (previous) time step $t-\Delta t$:

$$\hat{\mathbf{x}}(t|t-\Delta t) = A\hat{\mathbf{x}}(t-\Delta t|t-\Delta t) \tag{3-6}$$

The aim is to define $K(t)$ in such a way that $\lim_{t\to\infty}(\hat{\mathbf{x}}(t)-\mathbf{x}(t)) = \mathbf{0}$. The acceleration signal from the accelerometer includes bias. By appending the state estimate with a bias state $\hat{\mathbf{x}} = [\hat{\mathbf{x}}^T,\ \dot{v}_{bias}]^T$ and replacing C in Equation 3-5 with $C = \left[C, [0,0,1]^T\right]$, the bias can be removed from the acceleration measurements (Magnusson and Odenman, 2012). Detailed derivation of the system matrices and a derivation of $K(t)$ to implement in MATLAB is given in Appendix A.

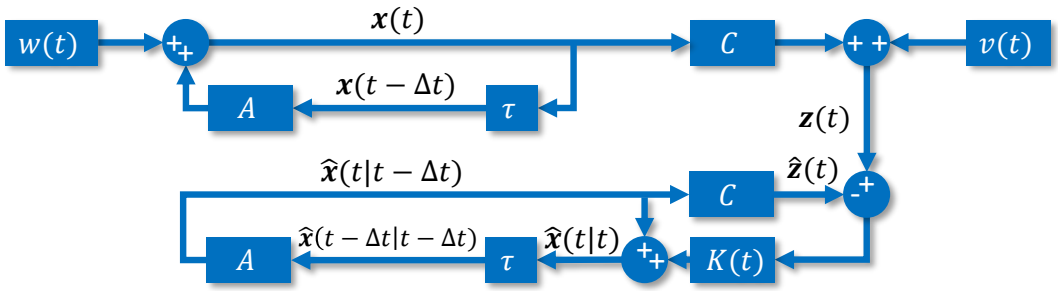

Figure 3-3: Schematic representation of the Kalman filter.

Moving Average Filter

The moving average filter utilises the fact that the noise in different measurement samples is uncorrelated to filter noise from the measurement signals. When differentiating noisy measurements, noise sequences are amplified. The optimal window size will therefore be determined by means of performing a jerk analysis on the obtained results. Drivers experience jerk as being uncomfortable if the level of jerk exceeds $1.5 m/s^3$ (Treiber and Kesting, 2013b). Two metrics are defined to assess the performance in noise reduction: *1)* acceleration behaviour: the jerk can only exceed the level of comfortable jerk in braking situations and *2)* the deviation of the velocity signal to the original signal must not exceed a certain threshold. This threshold will be determined in the filtering procedure by assessing the deviation between the original and the filtered signal. The window size will be changed iteratively until the required reduction of measurement noise is reached. The actual window size depends on the considered sampling interval. For sampling intervals of 0.1 seconds, the range of 3.5 seconds considered in Ossen (2008) seems a valid starting point.

3-2-3 Data Consistency

In addition to noise-free measurements, model calibration requires measurement signals from the data-set to be consistent to the equations of motion (often referred to as *internal consistency*). To ensure consistency, variables are derived after filtering and according to the methods in line with the methodology used in Treiber and Kesting (2013a). Internal consistency will be ensured by selecting the velocity from the Kalman filter as base variable, and deriving all dependent variables from this one variable. Because information from all measurement signals was fused in the Kalman filter, the information loss is small. The position x and acceleration $\dot{v}$ of the vehicle are derived using appropriate numerical integration and differentiation schemes. The applied numerical

integration scheme is the trapezoidal rule from Equation 3-1. The applied numerical differentiation scheme is the central finite difference scheme, defined as:

$$\dot{v}_i(t) = \frac{v_i(t+\Delta t) - v_i(t-\Delta t)}{2\Delta t} \tag{3-7}$$

Equivalent methods apply to derivation of the change in distance-gap $\dot{s}(t)$ from the gap $s(t)$. The position of the lead-vehicle is derived by applying the equation ensuring *platoon consistency*. The equation for platoon consistency relates the position of the ego vehicle to the position of the lead vehicle via the position of the front bumpers x_i and x_{i-1} and the length of the lead vehicle l_{i-1}. It is given by

$$s_i(t) = x_{i-1}(t) - x_i(t) - l_{i-1} \tag{3-8}$$

3-2-4 Data Selection

Selected data-sets must contain driving situations which both models can describe, in which the system does not interact with the environment or infrastructure, in which the ACC system is active and in which the human driver is not intervening (Treiber and Kesting, 2013a). Therefore, data will only be selected if ...

- ...longitudinal control is performed solely by the ACC system,
- ...the vehicle (only) reacts to the vehicle driving directly ahead, and
- ...only constrained driving situations are included

3-3 Methodology for Model Calibration

Because of the higher reliability, this thesis considers a global approach to model calibration (Treiber and Kesting, 2013a). In the global approach, optimal estimates for the model parameters $\hat{\boldsymbol{\beta}}$ are obtained from minimising a certain objective function $\mathcal{F}$, which defines the distance between predictions of the car-following model and actual vehicle data. Each iteration of the optimisation procedure consists of predicting a complete follower trajectory using the current set of estimated parameters. The objective function defines the performance on representing the actual data. Unless stated otherwise, the setup introduced in this section is used throughout the rest of this research.

In Section 3-3-1, methodology for obtaining model predictions will be discussed. Section 3-3-2 discusses the methodology for optimising these model predictions. Finally, Section 3-3-3 will discuss methodology for assessing the performance of the calibration procedure.

3-3-1 Obtaining Model Predictions

Follower trajectories generated by the model are obtained from running a simulation using the current set of parameter estimates $\hat{\boldsymbol{\beta}}$. Simulation starts by initiating the endogenous variables

$$\hat{v}_i(t_0) = 0, \qquad \hat{v}_i(t_0) = v(t), \qquad \hat{x}_i(t_0) = 0, \qquad \hat{s}_i(t_0) = s(t)$$

In each iteration of the simulation ($t = [t_0,\ t_0+\Delta t,\ \ldots,\ t_e]$), the acceleration $\hat{\dot{v}}_i(t)$ is computed by the model from the current set of endogenous and exogenous variables. Computation of the acceleration is followed by an update of the velocity $\hat{v}_i(t)$ and position $\hat{x}_i(t)$. Since the car-following models are in continuous-time and the simulation is in discrete-time, the velocity will be updated according to the equations of motion considering constant acceleration on the interval $t \in [t, t+\Delta t)$, defined as:

$$\hat{v}(t+\Delta t) = \hat{v}(t) + \hat{\dot{v}}(t)\Delta t \tag{3-9}$$

After computation of the velocity, the position will be updated using the trapezoidal rule from Equation 3-1.

Marks have been placed at the location where the lead-vehicle changed due to active or passive lane changes and at locations of missing data. In model calibration, at the location of these marks the current acceleration, velocity and distance-gap will be reset using a hard-reset, defined as:

$$\hat{\dot{v}}_i(t) = \dot{v}_i(t^+), \qquad \hat{v}_i(t) = v_i(t^+), \qquad \hat{s}_i(t) = s_i(t^+).$$

where t^+ indicates the time immediately after the location of the mark. Hard-resets allow for splitting the data-set into different sub-sets, which can be concatenated in any arbitrary order (Treiber and Kesting, 2013a). In the model validation or trajectory generation phase, a hard-reset will only be applied in case data is missing. In case the lead-vehicle changes, for example due to a cut-in or cut-out, a soft-reset will be applied. The soft-reset is defined as:

$$\hat{s}_i(t) = \hat{s}_i(t-\Delta t) + \left(s_i(t^+) - s_i(t^-)\right)$$

3-3-2 Optimisation of Model Predictions

The error-measure allows for defining the performance of the simulated follower trajectory on describing the trajectory of the same variable from the actual vehicle data. In the process of optimising model predictions, the objective is to minimise the value of the error function by varying the parameter values, see Equation 3-10. The error function is therefore usually referred to as objective function. The considered variable in the optimisation is referred to as calibration-variable. Until stated otherwise, the RMSE (Equation 3-2) will be considered using the distance-gap as calibration variable: $\mathcal{F}_{RMSE}(\mathbf{s}_i, \hat{\mathbf{s}}_i)$ or shortly noted as $\mathcal{F}_{RMSE,s}$. In literature, this combination is found to show most reliable results (Punzo and Simonelli, 2005).

$$\hat{\boldsymbol{\beta}} = \underset{\boldsymbol{\beta}}{\arg\min}\, \mathcal{F}(\mathbf{z}, \hat{\mathbf{z}}) \tag{3-10}$$

Figure 3-4 shows a typical result for the objective function for different combinations of variables β_1 and β_2. In case two parameters are considered, the obtained plot (left) is referred to as the fitness landscape. In case only a single parameter is considered, the obtained plot (right) is referred to as parameter sensitivity plot. In case a model can describe the driving behaviour, the objective function is generally smooth and shows only a single minimum (*). Therefore, gradient-based optimisation algorithms will be used for model calibration. However, the uniqueness of the results should always be checked by evaluating the fitness landscape. For optimal performance, the optimisation is constrained.

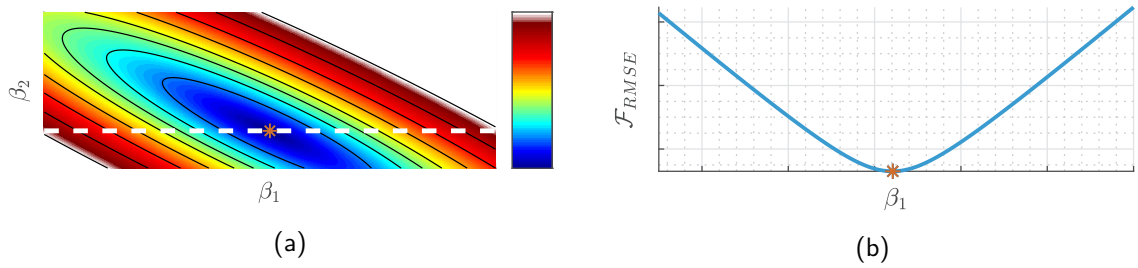

(a) (b)

Figure 3-4: Figure showing the fitness landscape of the error-measure or objective function for different combinations of parameters β_1 and β_2 (a) and parameter sensitivity at the dotted line (b).

In this thesis, the Sequential Quadratic Programming (SQP) algorithm will be used for model calibration. The SQP algorithm can solve constrained nonlinear optimisation problems and is built-in into the optimisation toolbox from MATLAB. Different algorithm settings considering smaller tolerances were tried, all resulting in similar performance as the default MATLAB algorithm settings. Therefore, these default algorithm settings will be used. Further elaboration on the exact workings of the algorithm is outside of the scope of this research. Using default settings, there are mainly four situations in which the algorithm ends its operation: *1)* first-order optimality is achieved (the found solution is both the local and global solution, the Jacobian is non-negative in all feasible directions), *2)* the improvement in the objective function when taking a step is below a certain limit (default: 10^{-6}), *3)* the number of iterations exceeds a certain limit (default: 400) and *4)* no feasible solution was found. Throughout this thesis, only algorithm termination due to situations 1 and 2 is considered as feasible.

3-3-3 Assessing the Calibration Performance

In line with Treiber and Kesting (2013a), the fitness landscape and parameter sensitivity plots introduced in the previous section will be used to assess the performance of the calibration procedure. Using the fitness landscape, one can check whether a minimum was present within the considered calibration region, and if the optimisation algorithm ended in this minimum. Furthermore, the plot indicates a possible correlation between different parameters. In case the optimisation was not able to end in a minimum, it is likely that in correlated parameters, parameters showing low sensitivity are sacrificed first.

This sensitivity is obtained from the parameter sensitivity plot, as shown in Figure 3-4b. The plot shows the cross-section of the fitness landscape at the found calibration value, in this figure indicated with the dashed line. The slope of this plot at the obtained value from the model calibration defines the sensitivity of the model parameters to correct calibration. The slopes at both sides are the first-order sensitivities and will be indicated by S^- (left) and S^+ (right). Only in case both S^- and S^+ are non-negative, an optimum is found for calibration of the parameter. Both sensitivities must be high in order to be sure that the calibrated parameter value is correct (Punzo et al., 2015).

3-4 Methodology for Investigating the Sensitivity of the Model Calibration

The sensitivity of the model calibration to various factors will be investigated using synthetic data. The formulation of the objective function (Equation 3-10) shows that the performance of the calibration procedure depends on: *1)* the selected optimisation algorithm *2)* the objective function, *3)* properties of the data-set, *4)* the method used for obtaining model predictions and *5)* the ability of the model to describe the data. These factors can be subdivided into methodological factors, data quality factors and data quantity factors. The methodological factors include: the method used to approach the optimum ($\arg\min_{\boldsymbol{\beta}}$), the error-measure ($\mathcal{F}$) and the model predictions ($\hat{\mathbf{z}}$). In this thesis, the sensitivity of the model calibration to three methodological factors will be investigated, being: the error-measure, the calibration variable weight and the simulation reset interval. The data quality and quantity factors consider the calibration data ($\mathbf{z}$). This thesis will investigate two data quality factors, being residual noise in the measurement signal and considering an incorrect model, and two data quantity factors, being: system excitation and the trajectory length. Before this investigation, commonly used settings are assumed for each of these factors.

To be able to assess the sensitivity of the model calibration to each of the considered factors, the analysis will be based on synthetic follower trajectories. These trajectories will be generated using a known model with known properties and allow for proper investigation (Ciuffo and Punzo, 2014; Montanino et al., 2012; Punzo et al., 2015). Different drivers are considered by creating many trajectories, each with different parameters. The ability of the calibration procedure of finding back the original parameters is used to define the sensitivity of the model calibration.

This section starts by introducing methods for creating synthetic trajectories in Section 3-4-1. Section 3-4-2 discusses the considered variations. Finally, Section 3-4-3 will discuss assessment criteria for the analysis.

3-4-1 Creation of Synthetic Data

The validity of the research is ensured by the leader trajectories resembling realistic driving situations. The accuracy of the filtered data from the ego-vehicle allows it to be used as a realistic leader trajectory in the generation of synthetic data. Four trajectories of vehicle data with different levels of excitation of the system will be selected, each consisting of 390 seconds of data, just above the minimum length of 300 seconds needed to calibrate models to human driving data (Treiber and Kesting, 2013a). Follower trajectories are generated by applying the methodology for obtaining model predictions. The only difference being the reset of the distance gap at marks, where the distance-gap is reset to the desired gap for the current model. For repeatability, parameters for the follower trajectories are selected (pseudo-)randomly from a range of suitable parameter values.

3-4-2 Factors Influencing the Calibration Performance

Methodological Factors

Error-Measure: When calibrating to synthetic data, the problem always shows a single optimum (Montanino et al., 2012). The error-measures do not change the position of the optimum, but only the sensitivity of the model calibration. Mainly two variations between error-measures exist. The

first difference is found between using relative or absolute error-measures; the second difference is found in between considering squared values and absolute values. In this thesis, sensitivity of the calibration to four different error-measures will be investigated, being: the Root Mean Square Error (RMSE) (equation 3-2), Root Mean Square Relative Error (RMSRE), Mean Absolute Error (MAE) and Mean Absolute Relative Error (MARE), defined as:

$$\mathcal{F}_{RMSRE,s} = \sqrt{\frac{1}{N}\sum_{k=1}^{N}\left(\frac{\hat{s}_i(k) - s_i(k)}{\hat{s}_i(k)}\right)^2}, \quad \mathcal{F}_{MAE,s} = \frac{1}{N}\sum_{k=1}^{N}|\hat{s}_i(k) - s_i(k)|, \quad \mathcal{F}_{MARE,s} = \frac{1}{N}\sum_{k=1}^{N}\frac{|\hat{s}_i(k) - s_i(k)|}{|s_i(k)|} \tag{3-11}$$

Calibration variable weight: In case the ACC system does not behave exactly according to the considered car-following model, calibrating to either the distance-gap or velocity can result in a mismatch on representing the other. A consensus can be made by considering a mixed error-measure, where a weight is assigned to both the distance-gap w_s and the velocity w_v. In this thesis, sensitivity of the calibration to 5 different weights will be investigated (w_s/w_v): 100/0, 75/25, 50/50, 25/75, 0/100. The mixed error variant of the RMSE is defined as:

$$\mathcal{F}_{RMSE,mix} = \frac{\mathcal{F}_{RMSE,s}}{w_s} + \frac{\mathcal{F}_{RMSE,v}}{w_v}, \qquad \frac{1}{w_s} + \frac{1}{w_v} = 1 \tag{3-12}$$

Simulation reset interval: Errors that arise earlier will most probably persist in the data for a longer time. These errors count heavier than an error arising just before a reset point. This temporal correlation possibly affects the results of the calibration procedure. On the other hand, models possibly need some time to react to sub-ideal initial conditions. To investigate the effects of temporal correlation and the time both models take to respond to the initial conditions and the effect this has on the calibration, reset points will be added at different interval lengths. The considered reset intervals are: Inf., 50, 25, 10, 1 and 0.2 seconds (after each iteration of the simulation).

Data Quality

Residual noise: In case residual noise is present in the measurement signals of the ego- and/or lead vehicle(s), this could cause the model trying to represent this noise, instead of only the dynamics captured in the data-set. In this thesis, sensitivity of the calibration to 4 different noise-variances will be investigated: 0.1, 0.05, 0.01 and 0.001 (m/s and m). Because multiple redundant measurement signals are available for the ego-vehicle, the possibility of completely filtering out all noise is higher. Therefore, the sensitivity of residual noise will be investigated for two different cases: only for the lead-vehicle and both for the ego- and lead-vehicles.

Incorrect car-following model: In real-world scenarios, the considered car-following model is never entirely in line with the driving behaviour. The effects of considering an incorrect model will be investigated by calibrating the IDM model on trajectories generated using the simplified ACC (sACC) model and vice versa.

Data Quantity

In the considered car-following models, the parameters in the model describe the dynamics and equilibrium of the car-following behaviour. Model calibration using parametric car-following models is essentially performing a grey-box optimisation. The calibration data-set must include sufficient excitation of the system in order to allow for observation of the system dynamics and tuning

of the model parameters. The amount of excitation present in the considered trajectory is determined by: 1) the presence of excitation itself, 2) the length of the considered trajectory. Furthermore, trajectories should be sufficiently long to distinguish between the probabilistic and deterministic part of driving behaviour.

The sensitivity to different combinations of trajectory length and system excitation will be assessed simultaneously by applying a sliding window model calibration over the desired length. The trajectory lengths considered are: 390, 300, 250, 200, 150, 100, 50, 25 and 10 seconds. The performance will be split over different ranges for $\mathbf{v}_i$ and $\dot{\mathbf{v}}_i$, with the purpose of finding a relation between the present variation in these variables and the possibility of correctly tuning the parameters.

3-4-3 Assessing the Calibration Sensitivity

The sensitivity of the model calibration will be assessed by means of assessing the parameter sensitivity, the location of the minimum and by comparing the resulting distance of the calibrated parameters to the actual parameters. Instead of the relative distance used in Ossen (2008), the absolute value of the relative distance for each of the calibrated parameters to the actual ones will be used $|(\hat{\beta}_i - \beta_i^*)/\beta_i^*|$. This allows for logarithmic axes, improving the visibility of improvements close to the optimum. The amount of created synthetic trajectories allows for visualisation of the result using box-plots. A graphical representation of the considered methodology is shown in Figure 3-5.

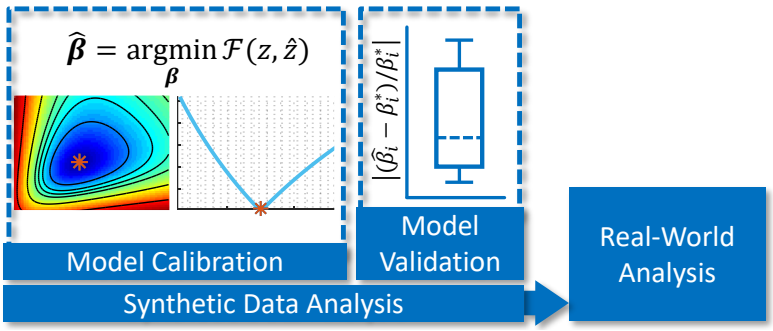

Figure 3-5: Schematic representation of the research methodology for investigating the sensitivity of the model calibration.

3-5 Methodology for Real-World Model Validation

Findings from the sensitivity analysis on the model calibration will be applied in the analysis of real-world data to ensure optimal calibration. The real-world model validation will also consider a variant on the sACC model which includes a parameter s_0 defining the minimum standstill distance, as was already considered in Xiao et al. (2017). Real-world validation of the models will be performed by assessing model performance on five different driving situations. The considered driving situations will be typical highway scenarios commonly considered when investigating string stability, road capacity and comfortable behaviour of the ACC system. The considered driving situations are steady-state car-following, cut-in, cut-out, hard-braking and stop-and-go scenarios. Proper representation of each of these trajectories is important to draw valid and reliable conclusions using the models (Xiao et al., 2017; Mullakkal-Babu et al., 2016; Wang, 2014).

The validity of the model calibration procedure will be assessed using the fitness landscape and parameter sensitivity plots. Because of the model not completely being in line with the driving behaviour included in the data, the sensitivity of each of the parameters to a correct calibration is expected to be lower than when considered trajectories are generated using the same model (Montanino et al., 2012).

For proper assessment of the capability of the model on representing the driving behaviour, the considered calibration trajectory must not be equal to the considered validation trajectory. Classical cross-validation methodology considers a single sub-trajectory of the complete trajectory for model validation (Wang et al., 2018). When the sub-trajectory used for validation contains easy (hard) data to represent, this results in overestimating (underestimating) the capability of the models. In this thesis, k-fold cross-validation techniques will be used. In the considered technique, k folds will be generated, which are iteratively selected for model validation. The remaining data is used for calibration. A fold is a continuous sub-trajectory, of which the minimum length should be sufficient for the model to respond to the initial conditions. The length of the fold will be determined using the results on the sensitivity of the model calibration to the reset interval. The average performance throughout all iterations is reported as the final performance. A low number of folds ($k \leq 2$) results in biased results, whereas a high number of folds ($k \geq 15$) means the considered trajectory should be very long and would result in large variances. In an early analysis, a right balance was found for $k \in [5,\ 10]$. This balance will be used in defining the final length of the considered trajectories.

A more comprehensive assessment is achieved by extending cross-validation methods with a cross-comparison between model parameters and trajectories and with an assessment of the model capabilities on representing specific events. In cross-comparison, each of the obtained parameter sets will be used to describe the other trajectories. Most papers consider the same model using different parameter values for representing different drivers, but assume these parameters to be fixed in time (Ossen, 2008). Therefore, it is favourable that all or most driving situations can be (optimally) described using a single set of parameters. To investigate this, also the mean and published parameters and the "best" calibrated parameters on all trajectories together will be considered. Since non-overlapping trajectories are selected in the analysis of real-world data, the validation trajectories in cross-comparison are not used for model calibration making application of cross-validation methods unnecessary. A graphical representation of the considered methodology is shown in Figure 3-6.

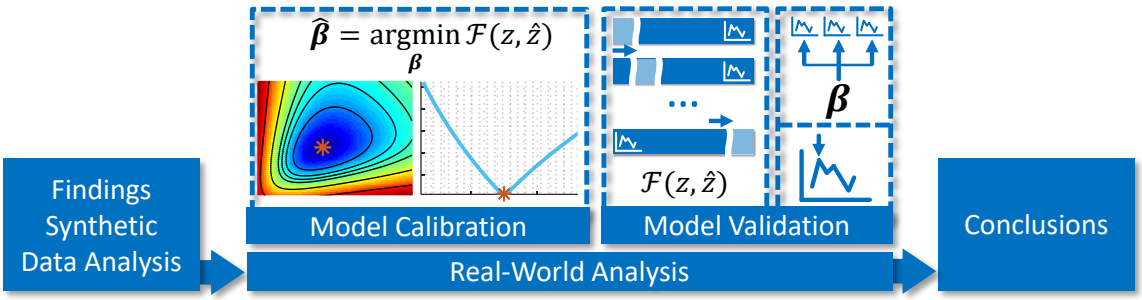

Figure 3-6: Schematic representation of the research methodology for the real-world analysis.

Chapter 4

Vehicle Data

4-1 Introduction

In the previous chapter, the methodology for assessing the sensitivity of the model calibration and performance of parametric car-following models on representing driving behaviour was introduced. The research requires a consistent and noise-free data-set containing realistic Adaptive Cruise Control (ACC) driving behaviour. This chapter provides an introduction to the considered data-set and undertaken processing steps with which consistency and noise reduction are achieved. The processed data-set serves as a basis from which trajectories are selected in subsequent chapters.

This chapter will start by introducing the considered data-set in Section 4-2. Data preparation steps required for filtering will be discussed in Section 4-3, after which the actual filtering will be discussed in Section 4-4. Finally, Section 4-5 will discuss the selection of data from which trajectories will be extracted in subsequent chapters.

4-2 The SAE-L2 Data-Set

Throughout this thesis, data will be used from the Audi A4 (2017) vehicle from the SAE-L2 (SAE level 2) platoon-test day. The SAE-L2 test-day was an initiative from Rijkswaterstaat, the Ministry of Infrastructure and Water Management, the RDW and TNO and was organised by AON on Wednesday June 18th, 2018. The goal of the day was to let (inexperienced) drivers experience the driving behaviour of ACC systems. Participants drove with seven vehicles from Groningen, via Amsterdam and Helmond, to the city of Rotterdam, see Figure 4-1. Drivers were instructed to select the shortest following distance available and set their desired velocity slightly above the speed limit, making the vehicle string prone to instabilities. The ACC system of the Audi allows selection of five time-gap settings (1, 1.3, 1.8, 2.4 and 3.6 seconds) and allows drivers to set their desired velocity between 30 to 150km/h. If the situation requires, the system can handle situations below 30 km/h.

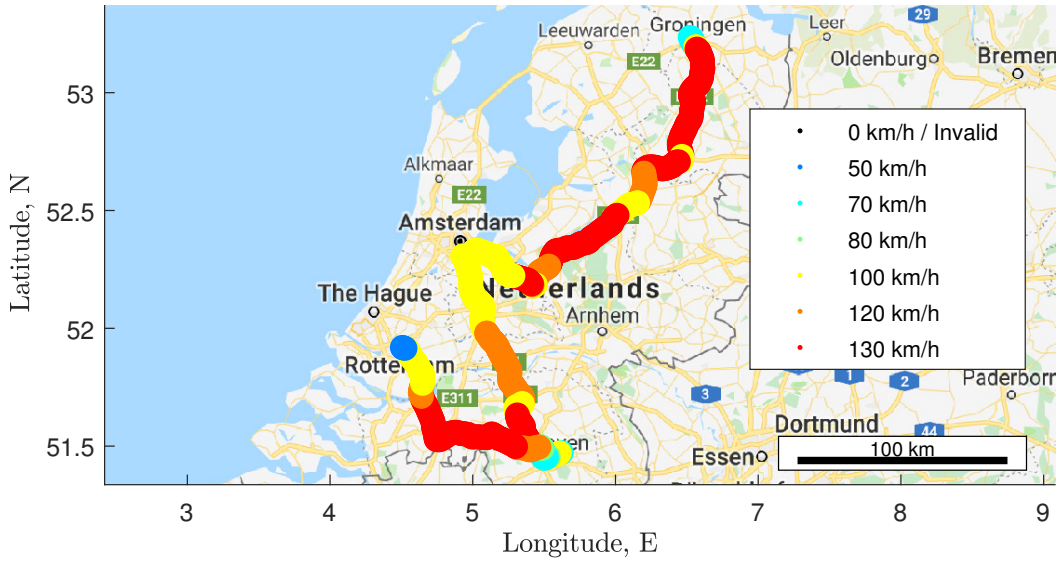

Figure 4-1: Figure showing the route driven during the SAE-L2 test-day on June 13th, 2018.

The sensor layout of the Audi vehicle is shown in Figure 4-2. The CAN bus, accelerometer and MobilEye system are all sampled at approximately $10Hz$, whereas the GPS signal was sampled at approximately $1Hz$.

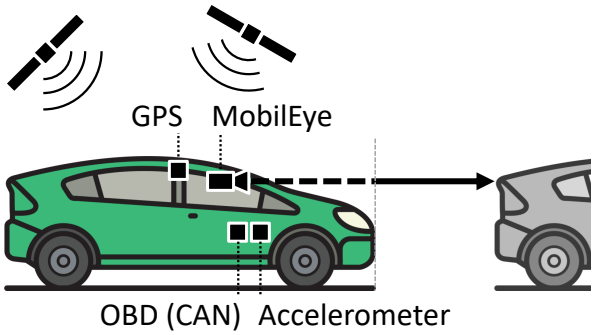

Figure 4-2: Figure showing a schematic representation of the installed sensors on the Audi A4 during the SAE-L2 field test form June 13th, 2018.

4-3 Data Preparation

In the previous chapter, the inconsistencies present in the GPS and speedometer signals have been introduced. These inconsistencies require removal before the Kalman filter can be applied to fuse the measurement signals. Figure 4-3 shows the inconsistencies found in the sampling interval of the GPS signal. The histogram plots indicate the distribution of sampling-intervals for $\Delta t < 5s$. Various conclusions are drawn from this Figure: *1)* The default sampling interval is approximately 1 second and *2)* long sampling intervals of approximately 1.5 seconds are followed by short sampling intervals of approximately 0.5 seconds. The incorrect sampling interval is corrected by moving measurements that are logged too late to an earlier time by setting the sampling time of the

incorrect measurements to the mean time of the two measurements surrounding it.

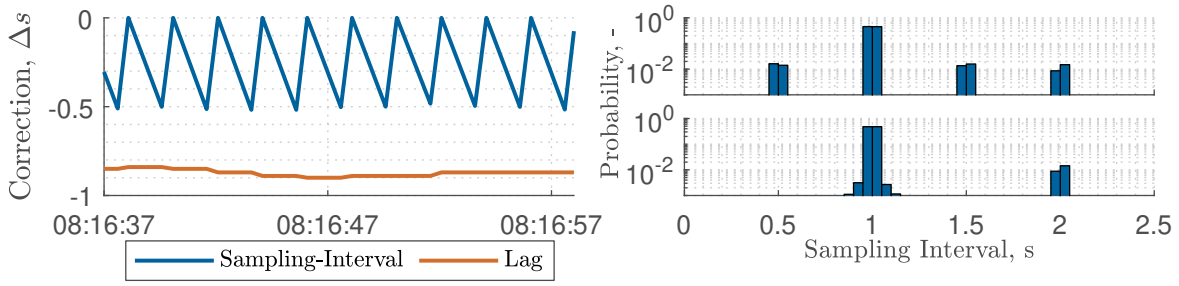

Figure 4-3: Figure showing the applied correction in the time-vector of the GPS signal in seconds (left), and the distribution of sampling times before (right top) and after (right bottom) correction.

After removing the sampling error, the lag in the GPS signal, which is assumed to be induced by the time signals take to travel from the satellite to the surface of the earth, needs to be removed. For a GPS satellite located directly above the GPS receiver travelling at an orbital height of 20.180 km and considering that the signal travels at the speed of light, the lag would be around $67ms$. An average signal lag of $789ms$ was found, which is much higher than expected. Figure 4-3 shows the observed lag in the GPS signal. Figure 4-4 shows that the corrected GPS signal is well in sync with the corrected speedometer signal. The bias factor for this signal (δ^*_{CAN}) was found to be 0.984.

Reset marks have been added at points where data is missing and at points where the lead vehicle was changed. The bottom plot from Figure 4-4 shows the distance-gap signal obtained from the MobilEye. Within the shown interval, two reset-points are included in the signal. In total, 295 reset-points are added to the data, making the average time between two consecutive reset points 65 seconds.

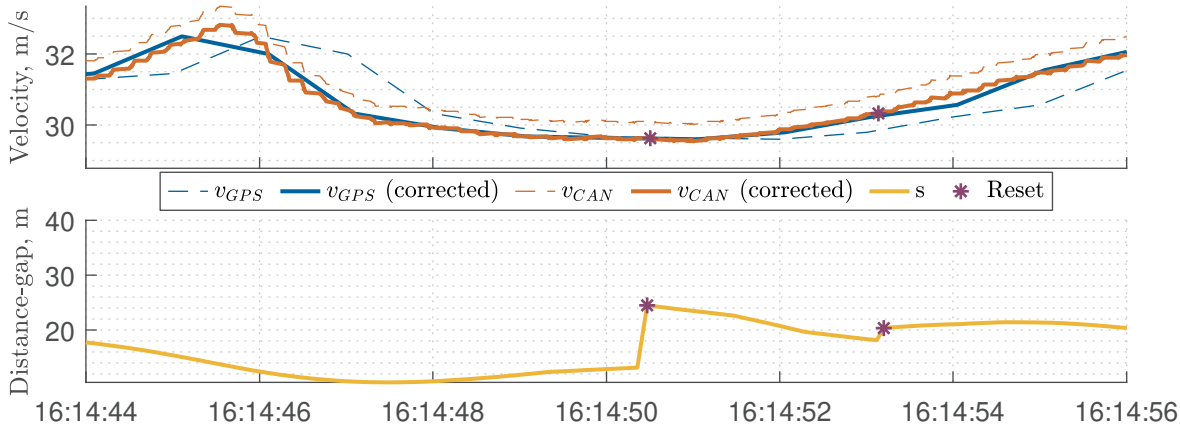

Figure 4-4: Figure showing velocities from the GPS (v_{GPS}) and speedometer (v_{CAN}) signals before and after correction (top) and the distance-gap from the MobilEye (s) with reset points (bottom).

4-4 Filtering and Sensor Fusion

4-4-1 Ego Vehicle

All continuous measurement signals from the ego-vehicle are re-timed to a sampling-interval of $\Delta t = 0.1s$, which is the original sampling interval of the speedometer and accelerometer signals. The data-set is split at the point where discontinuities are present. An additional bias state $\dot{\mathbf{v}}_{bias}$ allows for the removal of the bias in the acceleration signal.

Computation of the Kalman gain $\mathbf{K}(t)$ requires the noise covariance matrices from the measurement and process noise sequences. A GPS sensor has a typical error σ_{GPS} of about 4 meters (Gavrila and Kooij, 2017). The variance of the speedometer and accelerometer signals are computed using MATLAB and are found to be $2.32 \cdot 10^{-1} m/s$ and $1.91 \cdot 10^{-2} m/s^2$. Since all measurements originate from different sources, the off-diagonal terms are set to zero. Obtained values are used to construct the measurement noise covariance matrix R. Defining the process noise covariance matrix Q is a bit less straightforward since these noise variances are unknown. The matrix is found by minimising the Root Mean Square Error (RMSE) between velocities resulting from each of the measurement signals. The matrix is fine-tuned using trial-and-error methods. Again, all off-diagonal terms are kept zero. Both matrices are shown in Equation 4-1. The resulting performance of the Kalman filter of removing noise from the measurement signals and bias from the accelerometer signal is shown in Figure 4-5.

$$R = \begin{bmatrix} 4^2 & 0 & 0 \\ 0 & \left(2.32 \cdot 10^{-1}\right)^2 & 0 \\ 0 & 0 & \left(1.91 \cdot 10^{-2}\right)^2 \end{bmatrix}, \quad Q = \begin{bmatrix} 9.85 & 0 & 0 & 0 \\ 0 & 9.35 \cdot 10^{-4} & 0 & 0 \\ 0 & 0 & 2.46 \cdot 10^{1} & 0 \\ 0 & 0 & 0 & 2.96 \cdot 10^{-2} \end{bmatrix} \tag{4-1}$$

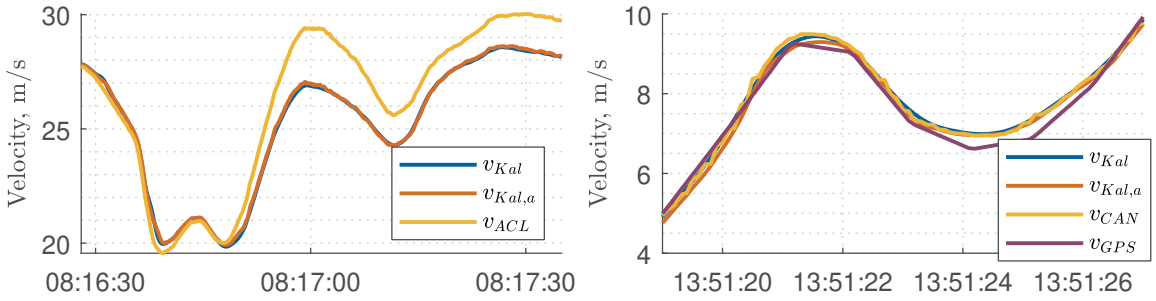

Figure 4-5: Figure showing the performance of the Kalman filter on removing the bias from the accelerometer signal (a) and fusing the different measurement signals (b).

After fusing and filtering the measurements using the Kalman filter approach, the jerk analysis shows residual noise resulting in jerk levels of over $3m/s^3$. The threshold for maximum deviation of the resulting velocity from the Kalman filter to the smoothed measurement signal is set to 2%. By means of visual comparison between noise reduction considering different filter widths, a width of 4 measurement samples is found to result in optimal results. This is significantly shorter than the considered width of 35 measurement samples considered in Ossen (2008). Improvements by the filter on the velocity can be seen in Figure 4-6a. Results for other variables are included in Appendix B.

4-4-2 Lead Vehicle

Under the assumption that all remaining noise has been removed from the measurements of the ego-vehicle, the state variables of the lead vehicle can be determined by applying the equation for platoon consistency (Equation 3-8). Performing the jerk analysis for the lead vehicle results in a filter width of 101 measurement samples, which removes many of the observed dynamics from the data. Therefore, the right balance between preserving the dynamics and removing noise from the data needs to be found. Up to a filter width of 9 samples, the observed jerk levels reduce with increasing filter width, where the error does only increase moderately. After this point, performance improvements from increasing filter width become less significant. Therefore, a filter width of 9 measurement samples is chosen for the MobilEye signal, which is again significantly shorter than the considered width in Ossen (2008). Improvements by the filter on the distance-gap can be seen in Figure 4-6b. Histograms of jerk levels before and after filtering and results for other variables are included in Appendix B.

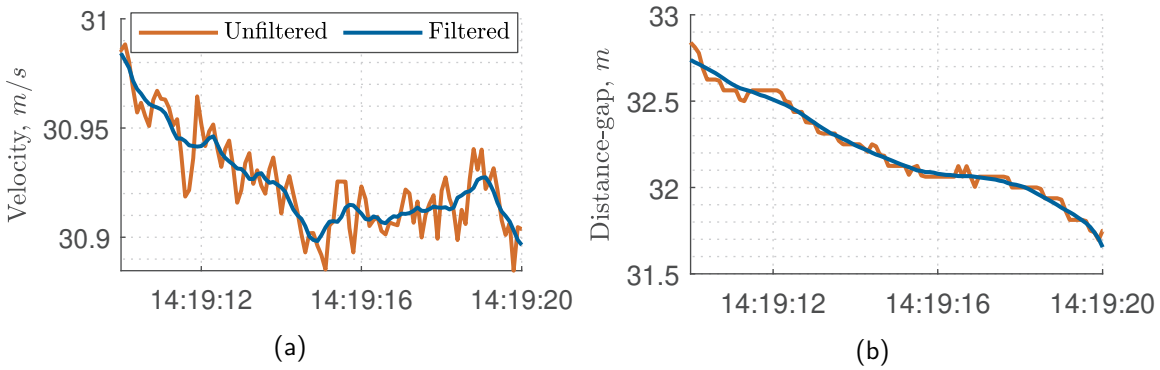

Figure 4-6: Figure showing the final results of the jerk analysis for the velocity measurements of the ego-vehicle (a) and distance-gap measurements from the ego to the lead vehicle (b).

4-5 Data Selection

The previously executed steps in data processing ensure consistency in the measurement signals. The final step is to remove data which is not suitable for model calibration purposes. The situations of driving situations which the model cannot describe and are being removed from the considered data-set are human intervention (ACC overruling and (de)activation), lane-changing, interaction with the environment and non-constrained driving. Before removal of specific data, a total time of 5:20.48h of driving data is available for the Audi vehicle. The first considered situation is the intervention of human drivers with the ACC system. Considering user acceptation, the driving behaviour of ACC systems should be predictable. Which could be interpreted as: "at least the intent of the action should be equal between the human driver and ACC system". Considering the maximum levels of comfortable acceleration of $2 m/s^2$ and jerk of $1.5 m/s^2$ (Treiber and Kesting, 2013b), this means that effects of the human driver are in worst-case scenario diminished after $t = \dot{v}/j = 1.33$ seconds. Adding the reaction time of the ACC system of 0.9 - 1.3s (Makridis et al., 2018) and considering a small safety margin, a time of 1 second before up to 5 seconds after the event is removed from the data. In total, ACC (de)activation and human intervention with the ACC system accounts for removal of 44.41m of vehicle data.

The second situation to be removed is lane-changing. Situations in which the vehicle performed a lane-change are identified by combining evidence from the CAN-bus and MobilEye system. The CAN-bus includes activation times of the indicator signal. The MobilEye system includes the distance to the left and right lane markings, which are re-initiated when a lane-change has occurred. As for ACC system (de)activation and overruling, a total time of 1 second before the event to 5 seconds after the event has ended is removed from the data to ensure all effects of the lane-change are removed. Lane-changes account for additional removal of 13.21m of vehicle data. A derivation of the times when the ACC system was active is included in Appendix C-1. A graphical interpretation of the removal of human intervention and lane-changing situations is included in Appendix C-2.

Finally, situations in which the vehicle does not solely react to its direct predecessor are removed from the data. This implies two cases: non-constrained driving and interaction with the environment. Driving is considered to be constrained if either the time-gap is below 2.5 seconds, or the velocity is below $10 m/s$, and at the same time, the distance-gap is below 25 meters. Urban driving situations, traffic lights and tight corners are all identified by manually evaluating the driven route and marking each of these situations in the data. This final step accounts for additional removal of 31.21m of vehicle data. After removal, a total time of 3:50.15h of vehicle data is left which can be used for analysis.

Chapter 5

Sensitivity of the Model Calibration

5-1 Introduction

In order to be able to investigate the sensitivity of the model calibration procedure to various factors, at first, a consistent, noise-free data-set is required. This data-set, the SAE-L2 data-set, was introduced and processed in the previous chapter. From the processed data, various trajectories are selected which are used to investigate the sensitivity of the model calibration.

This chapter investigates the sensitivity for the Intelligent Driver Model (IDM) and simplified ACC (sACC) models to the calibration methodology, and the quality and quantity of calibration data will be investigated. The investigation will be performed through calibrating parametric car-following models to synthetically generated trajectories. The first goal of this chapter is to obtain insights into the process of setting up an optimal model calibration on Adaptive Cruise Control (ACC) driving data. These insights are used to define a single calibration methodology yielding optimal results for the considered models to real-world trajectory data. The second goal is to create an understanding of the validity of the resulting calibrated models.

This chapter will start by introducing the trajectories selected for the creation of synthetic vehicle trajectories in Section 5-2. Sections 5-4 to 5-6 will discuss the sensitivity to the calibration methodology and quality and quantity of calibration data. Finally, Section 5-7 will discuss the conclusions of the performed analysis.

5-2 Creation of Synthetic Data

An optimal investigation on the sensitivity of the model calibration requires the selection of multiple trajectories containing different velocity and acceleration ranges. Four trajectories with different levels of system excitation are selected. The trajectories, including the reset points in the trajectories, are shown in Figure 5-1. Statistics for each of the trajectories are shown in Figure 5-2. The selected trajectories are: “Car-Following” (CF) containing steady-state car-following with minor accelerations, “Oscillating” (OSC) containing car-following with moderate accelerations, “Stop-and-Go 1” (SG1) containing a complete stop-and-go manoeuvre with relatively low oscillatory behaviour and “Stop-and-Go 2” (SG1) also containing a complete stop-and-go manoeuvre,

but with more oscillatory behaviour. The OSC trajectory is only 170 seconds and is therefore appended with 219 seconds of data from the CF trajectory. Unless stated otherwise, indicated results are based on the SG1 trajectory, which contains various velocities and acceleration levels while containing minimal reset points.

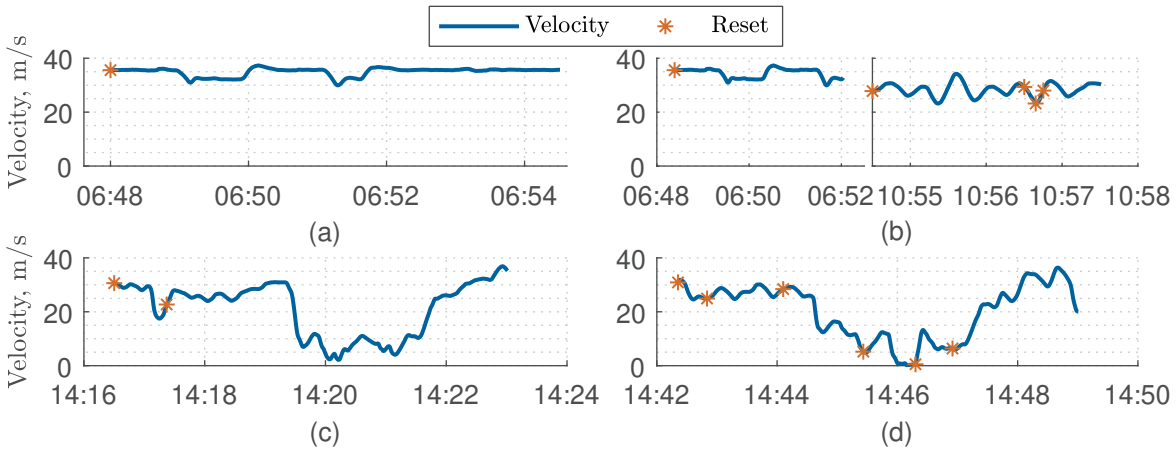

Figure 5-1: Figure showing the four selected trajectories where the sensitivity analysis will be based upon, being: "Car-Following" (a), "Oscillating" (b), "Stop-and-Go 1" (c) and "Stop-and-Go 2" (d).

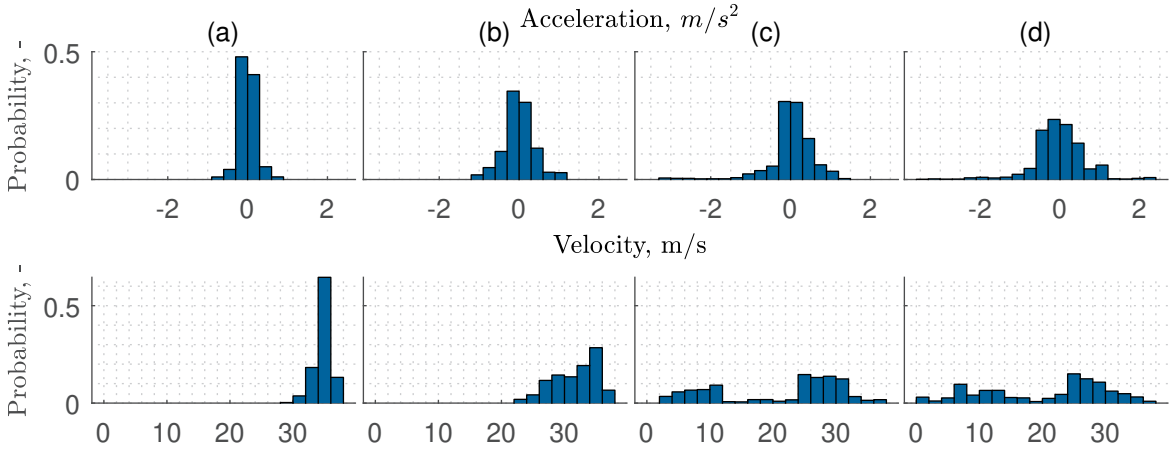

Figure 5-2: Figure showing statistics for the four selected trajectories where the sensitivity analysis will be based upon, being: "Car-Following" (a), "Oscillating" (b), "Stop-and-Go 1" (c) and "Stop-and-Go 2" (d).

Considered ranges of parameter values for the creation of synthetic data, and also constraints for the calibration algorithm are shown in Table 5-1. Most parameters are constrained to logically or psychical limits. Since it is not yet sure if the ACC system contains an intelligent braking strategy, constraints on b are very loose. This also yields for the constraints on k_p and k_d, but is more the result of the non-intuitiveness of these parameters. Using the number of variations indicated in the table for each parameter, a total of 243 trajectories are created using the IDM model, and a total of 216 trajectories are created using the sACC model. Example follower trajectories for the SG1 trajectory are included in Figure 5-3. For the other trajectories, example follower trajectories are included in Appendix D.

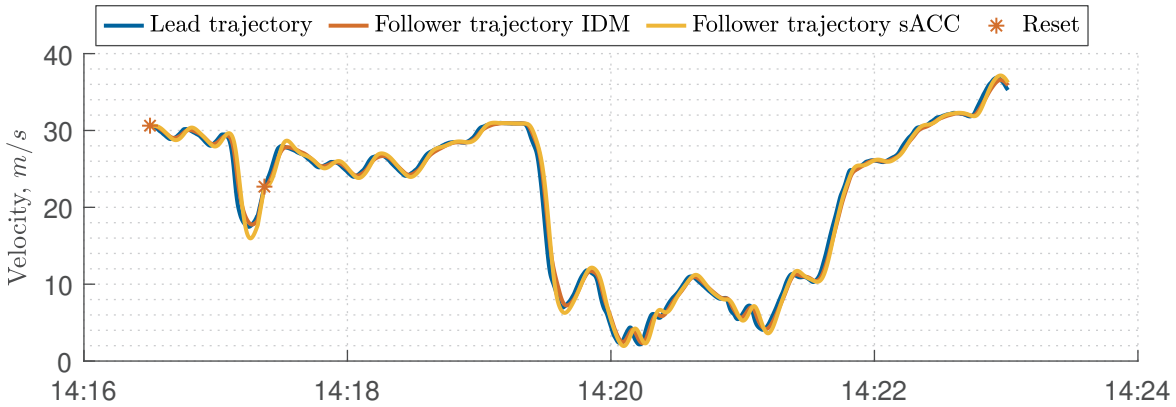

Figure 5-3: Plot showing an example of generated follower trajectories on the SG1 trajectory for the IDM model using parameters $p_{IDM} = [2.63,\ 2.81,\ 1.33,\ 54.13,\ 3.53]^T$ and sACC model using parameters $p_{sACC} = [0.28,\ 0.09,\ 1.33]^T$.

Table 5-1: Table showing an overview of the considered ranges of parameter values used for the creation of synthetic follower trajectories, as well as constraints considered for the calibration algorithm in the process of recovering the original parameters.

	IDM Parameters					sACC Parameters		
	$a, m/s^2$	$b, m/s^2$	T, s	$v_0, m/s$	s_0, m	k_p, s^{-2}	k_d, s^{-1}	t_d, s
Variations	3	3	3	3	3	6	6	6
Generation range	[1.0, 3.0]	[1.0, 3.0]	[1.0, 3.6]	[45, 55]	[1.0, 5.0]	[0.2, 0.3]	$[10^{-3}, 0.1]$	[1.0, 3.6]
Calibration ub*	8.0	10^4	10	69.4	10	30	10	10
Calibration lb**	10^{-5}	10^{-5}	10^{-5}	$4.6\cdot10^{-4}$	10^{-5}	$2.0\cdot10^{-5}$	$1.0\cdot10^{-6}$	$1\cdot10^{-4}$

* ub - upper bound, ** lb - lower bound

5-3 Benchmark Calibration Performance

In Figure 5-4, the parameter sensitivity for the defined calibration methodology from the previous chapter is shown. As can be seen, the sensitivity of both models on correctly calibrating the parameter defining the equilibrium gap T/t_d is relatively high. The IDM model is least sensitive to a correct calibration of v_0, followed by b and s_0. For the sACC model, parameter k_d is found least sensitive.

The IDM model considers different operating modes. Parameter a is outside of the parentheses, therefore present in all modes and affects the complete driving behaviour. In constrained driving at highway conditions, s_0 is only a small value representing the standstill-distance which adds to the term $v(t)T$. Therefore, the sensitivity of T in the considered trajectory is high. To obtain high sensitivity for s_0, driving situations at low velocities must be considered. b is mainly active in hard-braking situations, which are not included in the considered trajectory. Therefore, the sensitivity to a correct calibration is not very high, which is also the case for unconstrained driving situations and parameter v_0.

In the sACC model, only three parameters influence the model behaviour. All parameters influence the overall dynamics in all driving situations. Therefore the lowest obtained calibration sensitivity is higher than in the IDM model. A similar reasoning as for T in the IDM model yields for t_d.

The ability of the model calibration to retrieving the original model parameters is shown in Figure 5-5. In general, for parameters with higher sensitivity, the ability to retrieve the original parameter

values is higher. However, for the performance on retrieving v_0 and s_0 this is not true. The landscape plots, included in Figure 5-6, show small parameter correlation for IDM parameters a and b, parameters T and v_0 and parameters T and s_0. The correlation between T and v_0 and between T and s_0 could be a reason for this behaviour.

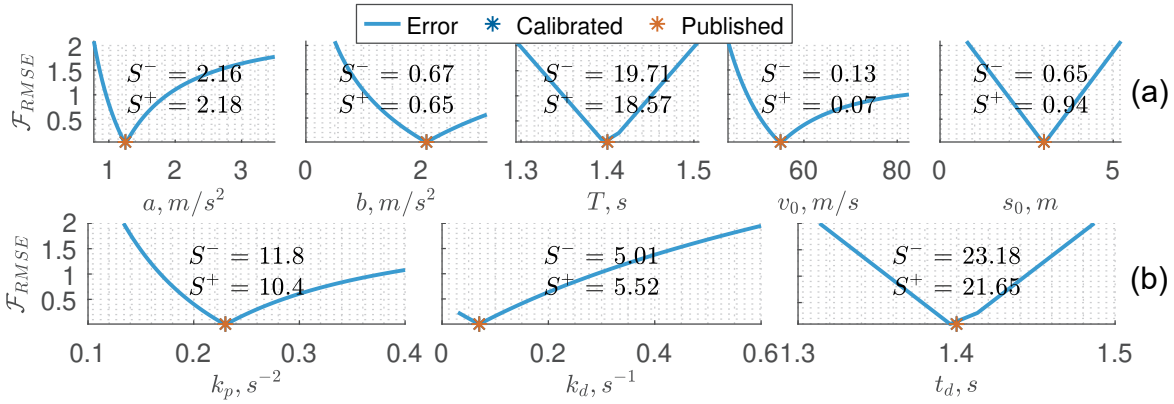

Figure 5-4: Figure showing the parameter sensitivity of the IDM (a) and sACC (b) models for the benchmark case. Calibrated parameter values overlap with the published ones.

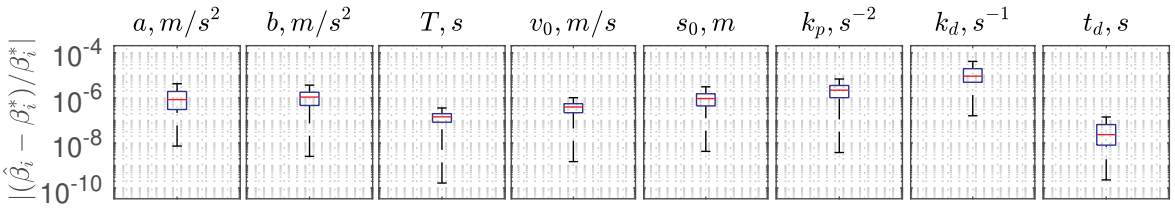

Figure 5-5: Figure showing the distribution of the distances of the calibrated parameters to the actual model parameters of the IDM (a) and sACC (b) models for the benchmark case.

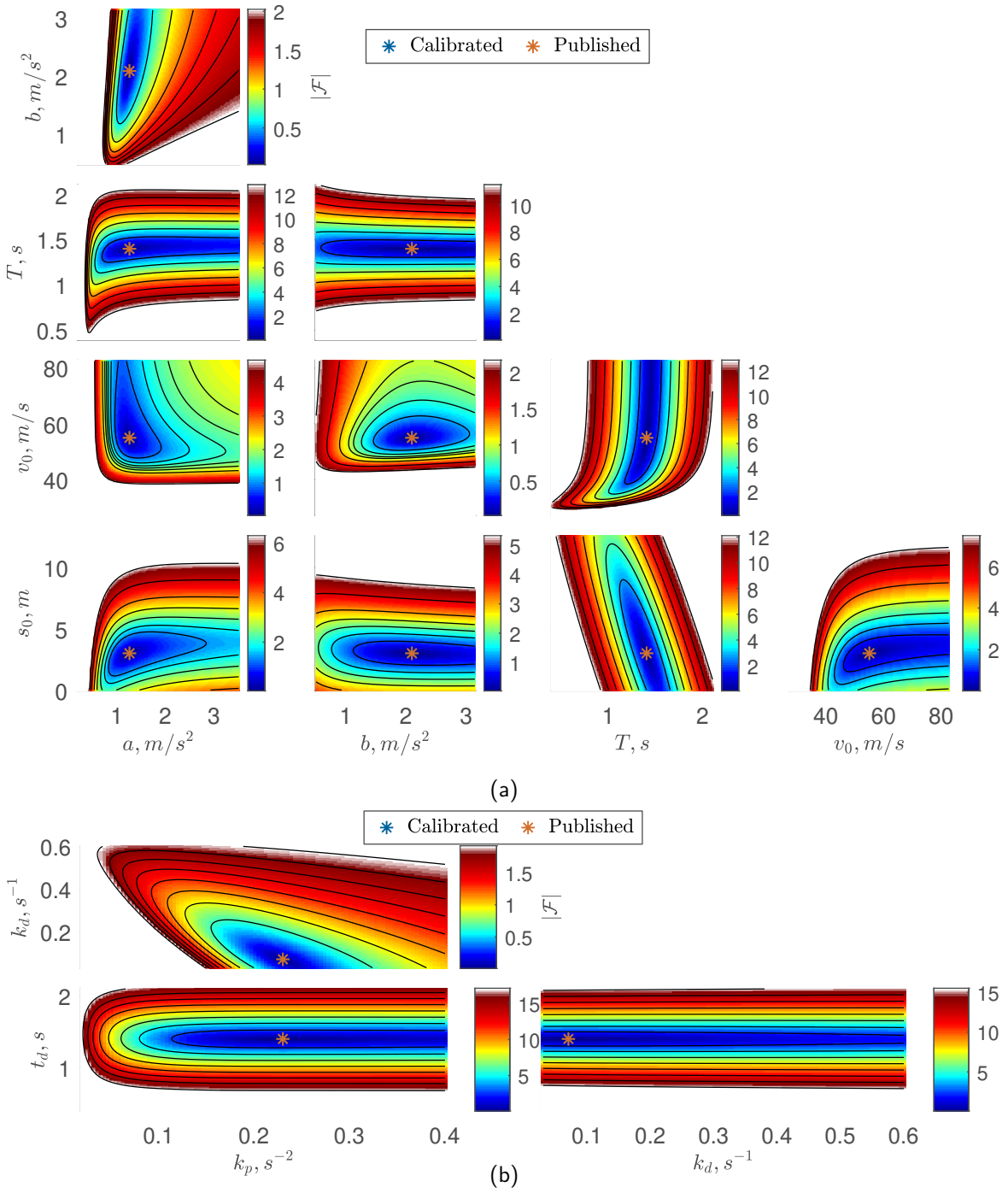

Figure 5-6: Figure showing the fitness landscape of the IDM (a) and sACC (b) models for the benchmark case. Calibrated parameter values overlap with the published ones.

5-4 Impact of the Calibration Methodology

In this section, the sensitivity of the model calibration to three different methodological factors will be investigated, being: the selected error-measure in Section 5-4-1, the assigned weight to each of the variables in the error-measure and general calibration performance in Section 5-4-2 and the interval at which simulations are reset in Section 5-4-3.

5-4-1 Error-Measure

The first methodological factor investigated is the error-measure. Relative error-measures, as compared to absolute error-measures, are more sensitive to the same errors at small distance-gaps. The sensitivity plots included in Appendix D-2-1 show that the considered error-measure indeed does not change the position of the optimum, but only the sensitivity of the model calibration. The parameter sensitivity of the IDM model decreases with approximately 97% when relative error-measures are selected over absolute error-measures. When considering the Mean Absolute Error (MAE) instead of the Root Mean Square Error (RMSE), the sensitivity decreases with 5-40%, depending on the parameter. Although less present, these effects are also visible for the sACC model, where the sensitivity in most cases decreases with more than 90% when considering relative error-measures instead of absolute error-measures.

Figure 5-7 shows box-plots indicating the performance for different error-measures on retrieving the original parameters. For both models, a decrease in parameter sensitivity causes the performance of the calibration to be lower. In the sACC model, something that cannot be explained from the sensitivity and landscape plots causes calibration performance using the MAE to be very bad. Best parameter sensitivity and calibration performance were found when considering the RMSE.

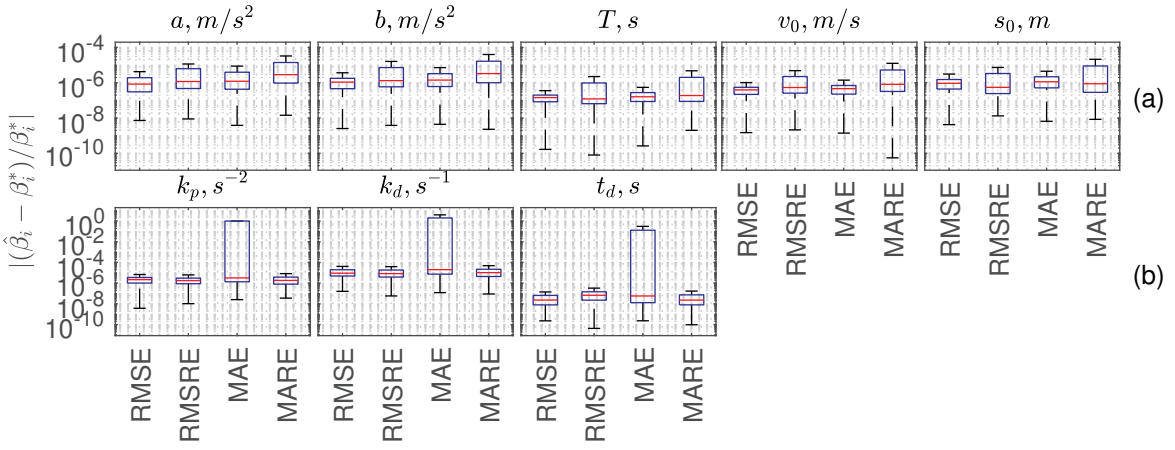

Figure 5-7: Figure showing the distribution of the distances of the calibrated parameters to the actual model parameters of the IDM (a) and sACC (b) models for different error-measures. The calibration was performed on the noise-free SG1 trajectory using full weight on the distance-gap ($w_s = 1$).

5-4-2 Variable Weight

In case the considered model is not completely in line with the driving behaviour, the weight attached to each of the calibration variables influences the model's ability to represent either the distance-gap or velocity. However, here, this is not the case. Considering full weight on the velocity ($w_v = 1$) does decrease the parameter sensitivity of the IDM model with a minimum of 80% and the parameter sensitivity of the sACC model with a minimum of 65% as compared to the benchmark. Considering equal weight on both variables ($w_s = w_v = 0.5$) decreases the parameter sensitivity in both models with approximately 40%. The fitness landscape remains unchanged.

The box-plots included in Figure 5-8 indicate for most parameters only minor effects on the ability of the model calibration on retrieving the original parameters. For the IDM model, the performance on retrieving the original model parameters is slightly higher when considering full weight on the velocity. For the sACC model, good performance is obtained in case relatively more weight is put on the distance-gap, while the best performance is obtained when full weight is on the distance-gap. Some events that cannot be explained cause calibration performance to be bad when considering a weight distribution $w_s/w_v = 25/75$.

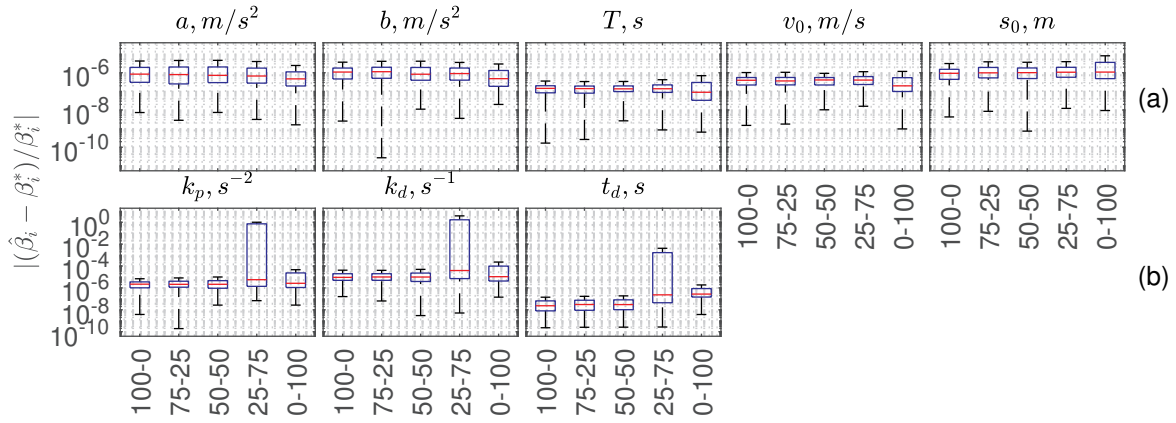

Figure 5-8: Figure showing the distribution of the distances of the calibrated parameters to the actual model parameters of the IDM (a) and sACC (b) models for different calibration variable weights ($w_s - w_v$). The calibration was performed on the noise-free SG1 trajectory using the RMSE error-measure.

5-4-3 Reset Interval

The reset interval defines the time after which the simulation of the model trajectories is reset to the measurement data. In case long reset intervals are considered, there exists a temporal correlation between errors at different steps of the simulation. Temporal correlation can be avoided by applying shorter intervals. Because of transient behaviour, models take some time to respond to the (sub-optimal) initial conditions. Applying reset intervals shorter than the response time of the models to the initial conditions could result in models not being able to respond to these conditions. This response time can be seen in case the model is initiated at a noisy measurement, such as is the case for the sACC model in Figure 5-12b on page 34. In this figure, the trajectory is initiated at a noisy measurement. As can be seen, the effects of the incorrect initiation are only gone after almost 19 seconds have passed. This response time is furthermore important because the selected

reset interval will be used as validation trajectory length in the validation of model performance on real-world data.

The parameter sensitivity and fitness landscape remains approximately unchanged for most parameters in case reset intervals up to 1 second are considered. In Figure 5-9, results on the performance of the calibration procedure can be found. From the box-plots, it can be seen that the performance of the calibration on retrieving the original IDM and sACC parameters is negatively affected in case reset intervals below 10 (IDM) and 25 (sACC) seconds are applied.

Something interesting happens when changing the variable weight for the sACC model from a full weight on the distance-gap to an equally distributed weight of $w_s/w_v = 50/50$. Here, the calibration performance, when using the smallest reset interval, improves significantly. This improvement is possibly the result of a faster response of the velocity than the response of the distance gap, which is $2/\Delta t$ times slower. A box-plot image showing these results is included in Appendix D-2-2.

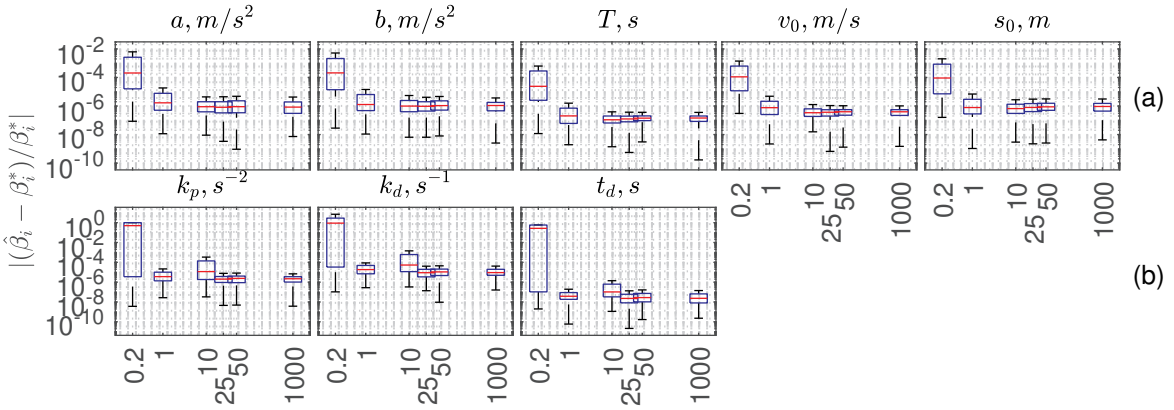

Figure 5-9: Figure showing the distribution of the distances of the calibrated parameters to the actual model parameters of the IDM (a) and sACC (b) models for different simulation reset intervals. The calibration was performed on the noise-free SG1 trajectory using the RMSE error-measure with full weight on the distance-gap ($w_s = 1$).

5-5 Impact of Varying Data Quality

5-5-1 Noise: Lead Vehicle

When only noise in the measurements from the lead vehicle is considered, this effectively means the measured distance-gap is varying very fast. In order to follow these variations, models have to be able to react very fast. The parameter sensitivity plots indicate that the IDM model is trying to represent the noise in the data. Compared to the benchmark case, the sensitivity has only been reduced by 25-40% for parameters a, b and T. The optimum, however, is not found at the original location anymore and the sensitivity of parameters v_0 and s_0 is about 70% lower. Model parameter b is showing a higher correlation to all other parameters than was observed before. The parameter sensitivity plot and fitness landscape for the IDM model are included in Appendix D-3-1.

The sACC model is not able to represent the noise. Because of the fast variations in the distance-gap, extra or less damping only has few effects. The noise causes the sensitivity on the model

damping parameter k_d to be about 90% lower than in the benchmark case. The sensitivity of model parameter k_p is about 40% lower, while the sensitivity of t_d is almost unchanged. The fitness landscape of the model is also unchanged.

In Figure 5-10, results on the performance of retrieving the original model parameters can be found. In line with the expectations, for both models, the calibration is sensitive to residual noise in the measurement signals of the lead vehicle. Also, the sensitivity of the IDM model is higher than the sensitivity of the sACC model. The model responses of the two models included in Figure 5-11a confirms that the IDM model is trying to mimic the data and that the sACC model is still trying to represent the noise-free data.

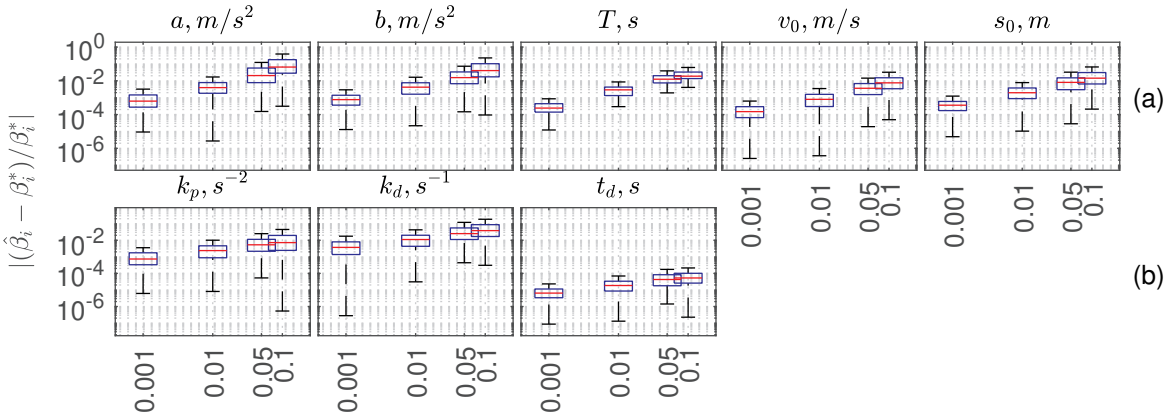

Figure 5-10: Figure showing the distribution of the distances of the calibrated parameters to the actual model parameters of the IDM (a) and sACC (b) models for different levels of noise variance in the distance-gap measurements. The calibration was performed on the SG1 trajectory using the RMSE error-measure with full weight on the distance-gap ($w_s = 1$).

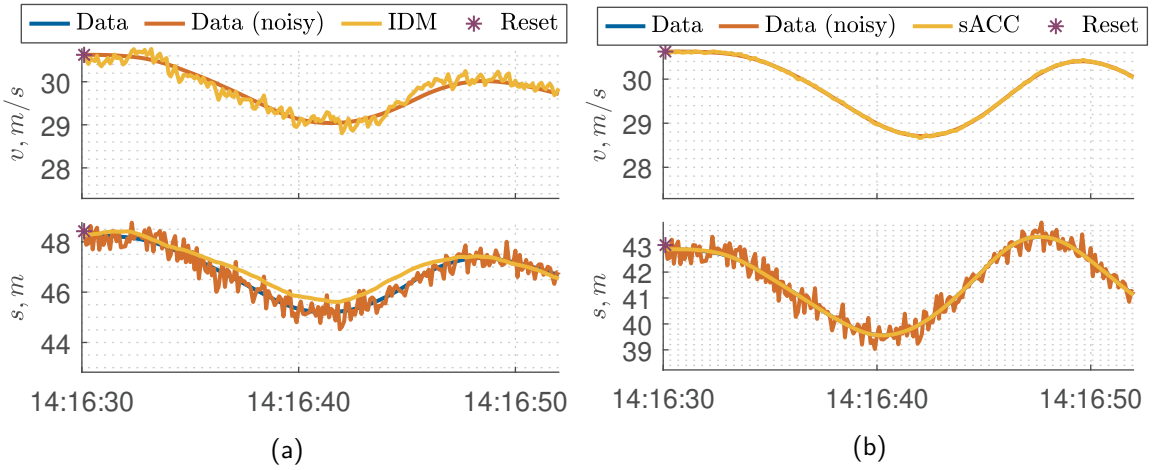

Figure 5-11: Figure showing the response of the IDM (a) and sACC (b) models on a sub-set of the SG1 trajectory where noise ($\mathcal{N}(0, 0.1)$) is injected to the distance-gap measurements. The generating model is calibrated using the RMSE error-measure with full weight on the distance-gap ($w_s = 1$).

5-5-2 Noise: Lead and Follower Vehicle

In the second case considered, residual noise is present in trajectories of both the velocity and distance-gap measurements. The found sensitivity of the model calibration is a bit worse than, but very similar to, the ones obtained when considering noise in the trajectories of the lead vehicle. The fitness landscape and the ability of the calibration on retrieving the original model parameters are for both models similar to the ones obtained in the previous section.

The response of both models is included in Figure 5-12. For the IDM model, the results of the model trying to represent the noise become even more apparent. The model response of the sACC model shows that the model needs some time to respond to the initial conditions. This has to be taken into account when determining the final length of the reset interval.

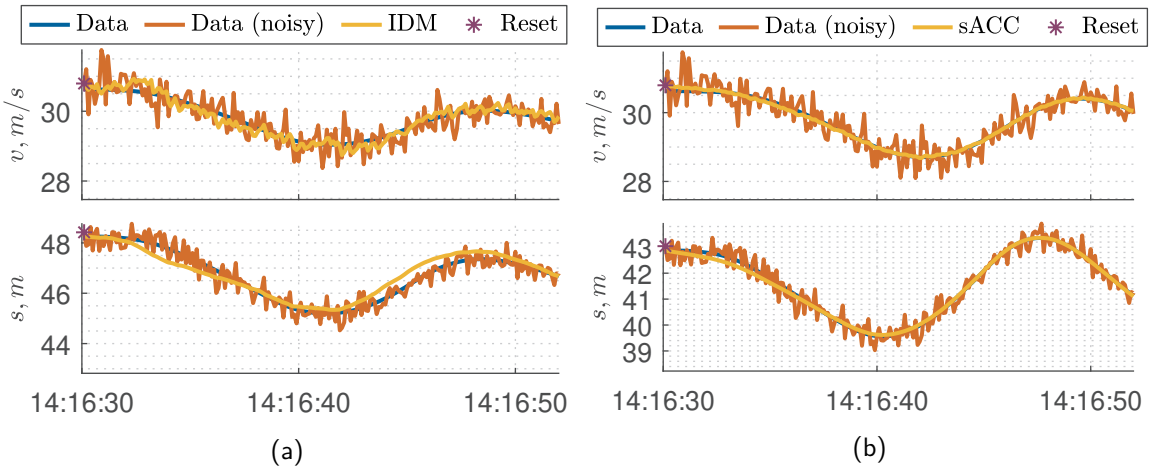

Figure 5-12: Figure showing the response of the IDM (a) and sACC (b) models on a sub-set of the SG1 trajectory where noise ($\mathcal{N}(0,0.1)$) is injected to the velocity and distance-gap measurements. The models are calibrated using the RMSE error-measure with full weight on the distance-gap ($w_s = 1$).

5-5-3 Incorrect Car-Following Model

In real-world situations, it is almost certain that the model is never completely in line with the actual behaviour. To find out what the effects of this are, in Figure 5-13, the parameter sensitivity is shown for the case the model trajectories are generated using the other model (i.e. IDM generated, sACC calibrated and vice versa). The obtained fitness landscape for both models is included in Appendix D-3-2.

As discussed earlier, the acceleration in the sACC model does not depend on the current velocity nor the distance to the desired velocity, the model does not consider an intelligent braking strategy, and the model considers no minimum standstill distance s_0. The absence of an intelligent braking strategy causes that for the IDM model, no optimum for b was found within the considered calibration region. While the disability of correctly calibrating b is in this case caused by the sACC model lacking an intelligent braking strategy, in real-world calibration this could also be the result of the considered trajectory data not considering any events in which this intelligent braking is needed. As for parameter b, the velocity-independent accelerations and absence of a minimum

standstill distance cause that model parameters v_0 and s_0 cannot be calibrated. The result is that the optimal region in the fitness landscape is now spread out towards very high parameter values.

The other way around, the IDM model does consider a parameter s_0, considers different acceleration and deceleration profiles and considers velocity-dependent acceleration. In the calibration of the sACC model, this results in a relatively low parameter sensitivity of model parameters k_p and k_d. For all three parameters, a single minimum is still present. The considered minimum standstill distance results in an overestimation of the desired distance-gap.

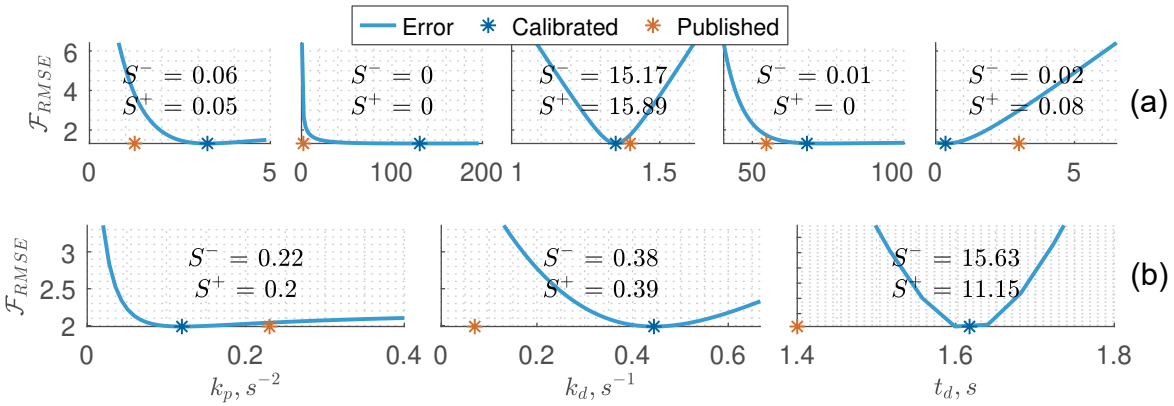

Figure 5-13: Figure showing the parameter sensitivity of the IDM (a) and sACC (b) models on a sub-set of the SG1 trajectory where the trajectory data is generated using the other model. The analysis was performed using the RMSE error-measure with full weight on the distance-gap ($w_s = 1$).

5-6 Impact of Varying Data Quantity

In this section, conclusions will be drawn on the minimum trajectory length and excitation required for proper calibration. This section start by investigating the sensitivity of the model calibration to various trajectory lengths in Section 5-6-1, after which the sensitivity to different levels of system excitation will be discussed in Section 5-6-2. In practice, both are always interlinked and cannot be considered entirely separate. Therefore some findings will coincide between the two sections.

5-6-1 Trajectory Length

Selecting the location and length of a calibration trajectory is a complex choice. Long trajectories have more change of including sufficient system excitation, allow for better filtering of the probabilistic part and allow for more validation steps to be performed, while short trajectories have less chance of including behavioural changes. In case too short trajectories are considered, the sensitivity of the parameters to a correct calibration decreases significantly, while the shape of the fitness landscape remains about unchanged.

In Figure 5-14, results on the performance of retrieving the original model parameters can be found. For short trajectory lengths, the reported performance is the total performance on the trajectory, which is subdivided into sub-trajectories of the considered length. Performance of the

IDM model seems to increase more gradually with increasing trajectory length than the performance of the sACC model. For the IDM model, good performance is observed from trajectory lengths of 200 seconds and higher, while for the sACC model, this is true from a minimum of 100 seconds. This gradual increase in performance is the result of the linearity of the considered models. The non-linear IDM model contains different operating modes which are active depending on the magnitude of the excitation of the system. Calibration of the linear sACC model does not rely on the amplitude of the excitation, but more on the included frequency range. In general laboratory conditions, a model is calibrated to a system by exciting the system at its input using an input signal constructed from one or more sine waves. Generally, one frequency is considered per calibration parameter. With increasing trajectory length, the magnitude of present excitation, therefore, increases more gradually than the number of frequencies.

Box-plots indicating the performance of the model calibration for other trajectories are included in Appendix D-4-1. For the IDM model, less excitation in the considered trajectory causes the different modes to be less visible. The minimum trajectory length required for optimal calibration remains about unchanged, but the calibration performance decreases with a factor 300 for the CF trajectory, 10 for the OSC trajectory and increases with a factor 2 for the SG2 trajectory. The latter is the result of the trajectory containing actual low-velocity conditions, which increase the calibration performance of s_0 and thereby increases the calibration performance of the other parameters. For the sACC model, considering other trajectories causes the minimum length required for proper calibration to be longer. However, the same performance is obtained when sufficient length is considered. These findings confirm what was stated before.

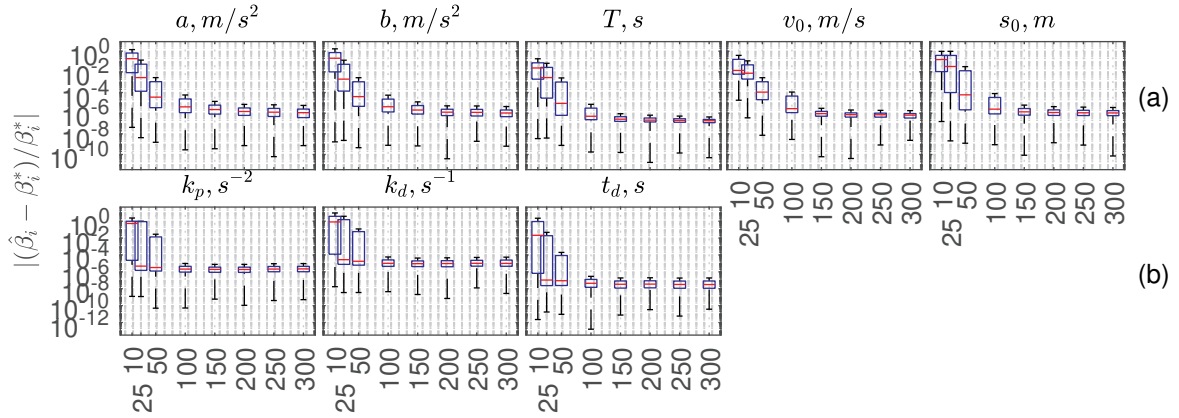

Figure 5-14: Figure showing the distribution of the distances of the calibrated parameters to the actual model parameters of the IDM (a) and sACC (b) models for different trajectory lengths. The calibration was performed on the noise-free SG1 trajectory using the RMSE error-measure with full weight on the distance-gap ($w_s = 1$).

5-6-2 System Excitation

For proper model calibration, the system must be sufficiently excited in order to include the full dynamical behaviour. In the previous section, some preliminary statements were made about what levels can be considered as sufficient. For a more detailed investigation, the sensitivity of the model calibration to different levels of system excitation is performed by considering the smallest trajectory length of 10 seconds. In this way, the absolute performance of the model calibration will be

lower, and the chance of including only a single type of system excitation is higher. This increases the difference in relative sensitivity which will be observed between different sub-sets of the trajectory.

In Figure 5-15, the ability of the model calibration on retrieving the original model parameters is shown over time for the SG1 trajectory. For the IDM model, the length considered is too short to calibrate parameter v_0 correctly. For the other parameters, braking actions or both braking and acceleration actions in the calibration trajectory seem to result in better performance than when only acceleration actions are considered. Moreover, the performance is better at low velocities. For the sACC model, the calibration seems to perform better in case braking actions are present. Splitting the calibration performance over different levels of minimum acceleration a_{min}, maximum acceleration a_{max} and average velocity v_{avg} included in each of the trajectories confirm these observations. Figures of this investigation are included in Appendix D-4-2. The IDM model shows best performance in case the calibration trajectory consist of deceleration levels below $-1 m/s^2$ at velocities below $10 m/s$. For the sACC model, the best performance is found when at least deceleration levels below $-1 m/s^2$ are present, independent on the acceleration levels or present velocities.

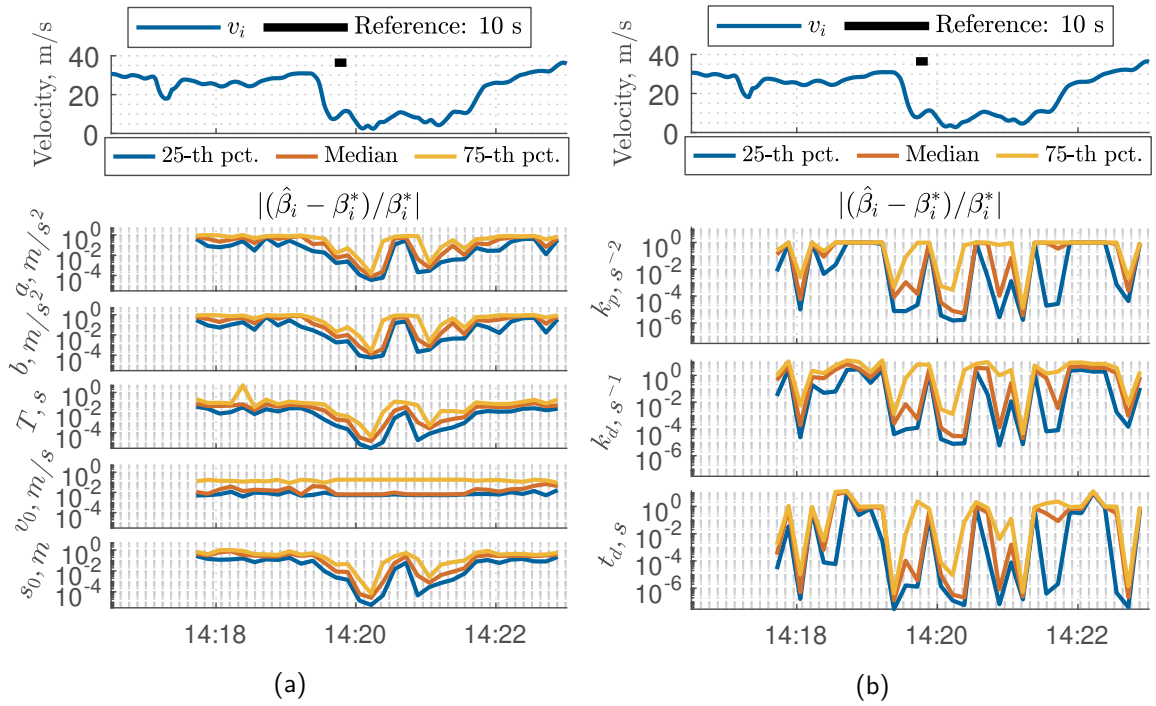

Figure 5-15: Figure showing the distribution of the distances of the calibrated parameters to the actual model parameters of the IDM (a) and sACC (b) models for a trajectory length of 10 seconds over time. The calibration was performed on the SG1 trajectory using the RMSE error-measure with full weight on the distance-gap ($w_s = 1$).

5-7 Conclusions

The goal of this chapter was to obtain insights in the process of setting up an optimal model calibration on ACC data and to create an understanding of the validity of the resulting calibrated models. Differences were found between the sensitivity of both models to some of the investigated factors. This raises the question of whether using a single approach for model calibration of both models could be considered as best practice, or that different models need different approaches. This thesis will consider an approach will which suits the calibration of both models, allowing for optimal comparison of the obtained results.

In the model calibration, the parameters having the most influence in defining the equilibrium distance-gap (T and t_d) are found to be most sensitive to correct calibration, followed by s_0 and the parameters directly involved when an error in the distance-gap arises (a and k_p). The least sensitive were the parameters connected with an error in the velocity-difference (b and k_d). Selecting a model of which the driving behaviour is in line with the behaviour captured in the data is found to be the most important factor in model calibration. For a linear model, calibrating a model that considers incorrect driving behaviour affects calibration performance of all parameters. Causing calibrated models not to be applicable in any other driving situations than the considered situation used in model calibration. For a non-linear model, only parameters included in modes that are not in line with the considered driving behaviour are affected. Still making the model applicable in other situations, but including such modes is unnecessary.

A proper model calibration requires the data to include sufficient system dynamics which are clearly visible. Because the trajectory length restricts the amount of included system excitation, the two are interconnected. For proper calibration, the considered trajectory must be at least 200 seconds in which at least decelerations below $-1 m/s^2$ are present. For the IDM model, these decelerations must take place at velocities below $10 m/s$.

Noise decreases the visibility of the dynamics. In case a model is able to do so, it will try to represent noise in the measurement signals. This results in a shift of the optimal calibration parameters from the actual parameter values. Because the parameter sensitivity and calibration error remain reasonable, one must not blindly trust these results. In case a model is not able to represent measurement noise, the actual dynamics will be represented. However, the parameter sensitivity will severely decrease and therefore, also the quality of the calibration. This emphasises the importance of accurately processing the data-set.

In the same way as that it is important that the data includes sufficient dynamics, it is also important that the model is able to develop and show its dynamics. Temporal correlation was only found to have only minor effects. Therefore, there is no need to include additional reset points in the trajectories. The parameter sensitivity was found to degrade severely when relative error-measures are considered. These measures should, therefore, not be used in model calibration. The model calibration was furthermore not found to be very sensitive to considering the velocity in the model calibration. The model calibration on real-world data will consider the RMSE using equal weight on the velocity and distance-gap and without extra reset-points being added. The length of the folds in model validation will be equal to the minimum required reset interval for accurate model calibration of 25 seconds.

Chapter 6

Real World Validation of Adaptive Cruise Control (ACC) Models

6-1 Introduction

In the previous chapter, the sensitivity of the model calibration to the calibration methodology and the quality and quantity of calibration data was investigated. From the SAE-L2 data-set, five trajectories will be selected in this chapter of which three satisfy the (minimum) requirements determined in the previous chapter.

In this Chapter, the validity of the IDM and sACC models on representing the driving behaviour of the ACC system from an Audi A4 will be assessed. The investigation will be performed by means of calibrating the models to the different vehicle trajectories, each including one or more interesting events. The goal of this chapter is to gain insights on the capability of each of the considered car-following models on representing the overall velocity and distance-gap, and on the representation of the specific events.

This chapter will begin by examining the obtained parameter values, validation errors and event representation for each of the trajectories in Sections 6-3 to 6-6. After obtaining optimal parameters for both models for each of the trajectories, cross-comparison of model performance for each of the parameter sets on all trajectories will be performed in Sections 6-7, 6-8 and Section 6-9. Finally, Section 6-10 will discuss the conclusions of the performed analysis.

6-2 Trajectory Selection

The considered trajectories are shown in Figure 6-1. Statistics about the selected trajectories are shown in Figure 6-2. The first trajectory contains steady-state car-following at highway velocities. The trajectory will be referred to as CF. Good representation in steady-state car-following is important in determining the estimated road capacity and driving comfort when using the ACC system. The following distance can furthermore be used to predict the number of cut-ins, which

affect user acceptation of the system (Nowakowski et al., 2011). At a cut-in, the distance-gap is suddenly reduced. When the ACC system reacts too nervous to cut-in scenarios, this can have a big impact on comfort and driver acceptation (Happee et al., 2018). The same holds for the reaction to a sudden increase in distance-gap caused by a cut-out. Both cut-in and cut-out events are included in the second and third trajectory, which will be referred to as CI and CI2, respectively. The fourth trajectory contains a hard-braking event and will be referred to as HB. A hard-braking event causes a large magnitude disturbance in the vehicle string. The way in which the vehicle reacts is often a determining factor in if the vehicle gets an accident or if instabilities are triggered. Finally, the fifth trajectory contains a stop-and-go manoeuvre, containing both hard-braking and (almost) free acceleration, combined with low-velocity conditions. Proper representation on this trajectory is important for reliable simulations using the model at different velocities. This trajectory will be referred to as SG.

To meet the requirements in excitation for the simplified ACC (sACC) model, the car-following trajectory has been appended with 120 seconds of data in which the system was more excited. There was no data nearby with which the requirements for the Intelligent Driver Model (IDM) model could be met. The same holds for the CI trajectory, which also does not include sufficient excitation for calibration of the IDM model. In the CI2 trajectory, a sub-trajectory with a length of 60 seconds is appended with which sufficient excitation is ensured for all models. The considered hard-braking event is constructed from approximately the same data as considered in the SG2 trajectory from the previous chapter and contains sufficient excitation to calibrate all models. The selected stop-and-go trajectory is a sub-section from the SG1 trajectory used in the previous chapter and contains sufficient excitation to calibrate all models.

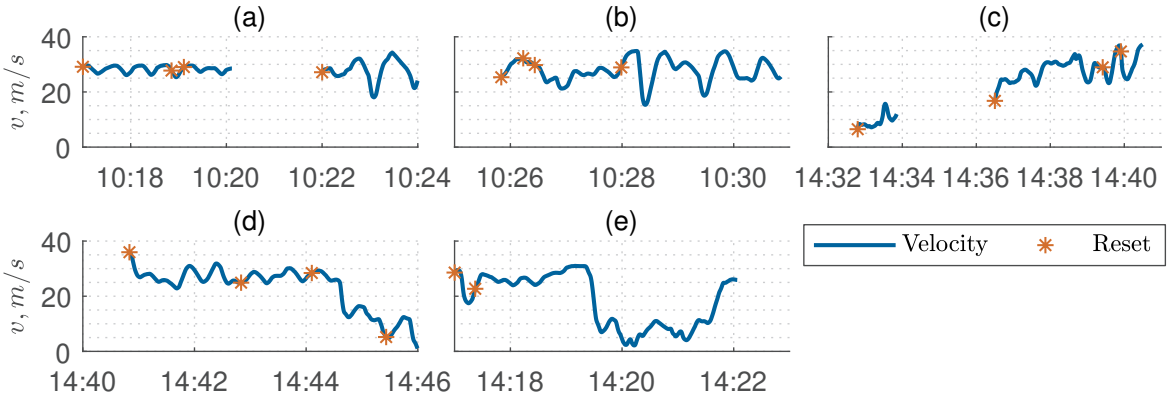

Figure 6-1: Figure showing the five selected trajectories where the real-world analysis will be based upon, being: "Steady-State Car-Following" (a), "Cut-In" (b), "Cut-In 2" (c), "Hard-Braking" (d) and "Stop-and-Go" (e).

6-3 Steady-State Car-Following

Figure 6-3 shows the considered trajectory and the obtained model trajectories using calibrated parameters. Because of the lack of excitation for the IDM model, it is expected that correct calibration is not possible. The obtained model response will be compared with the model response using the mean parameters of all calibration trajectories that contain sufficient excitation. The fitness

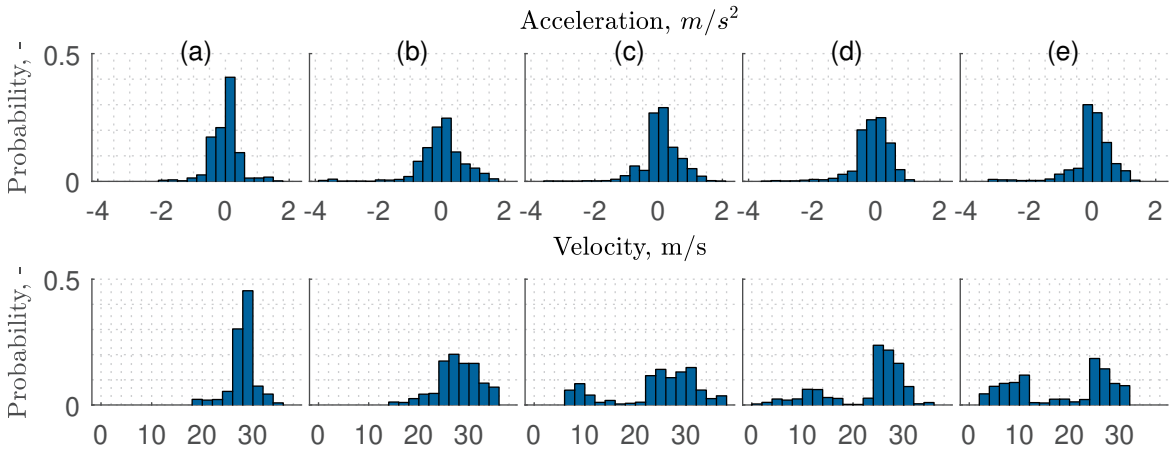

Figure 6-2: Figure showing statistics for the five selected trajectories where the real-world analysis will be based upon, being: "Steady-State Car-Following" (a), "Cut-In" (b), "Cut-In 2" (c), "Hard-Braking" (d) and "Stop-and-Go" (e).

landscape, parameter sensitivity plots and model response using mean parameters are included in Appendix E-1. They indicate that the there is an optimum present for all parameters except for b (IDM) and s_0 (alternative sACC). The parameter sensitivity of most parameters is rather low. The found calibration parameters are included in Table 6-1. The calibrated alternative sACC model will thus show similar behaviour as the regular sACC model.

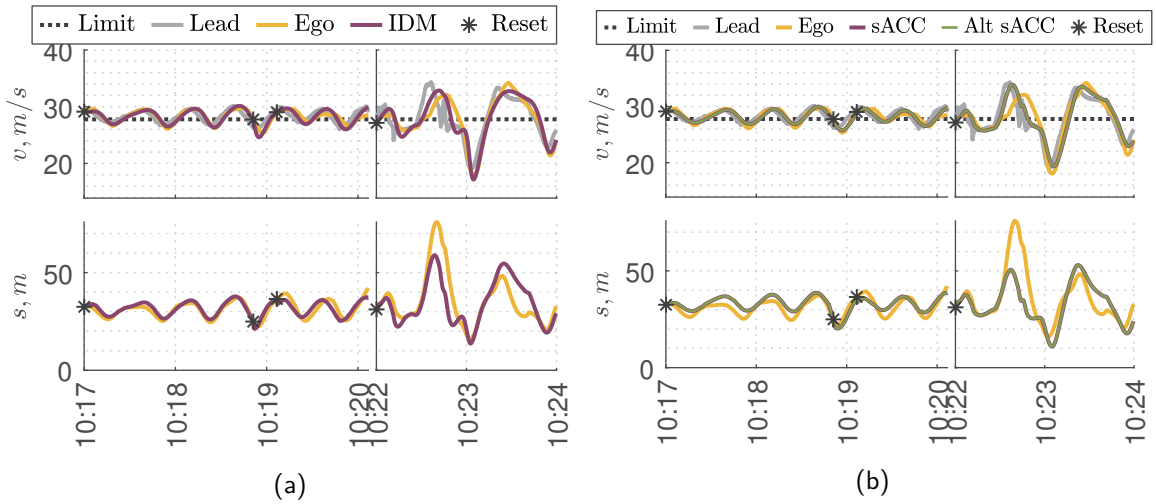

Figure 6-3: Figure showing the response of the IDM (a) and sACC (b) models on the CF trajectory. The models are calibrated using the RMSE error-measure with equal weight on the velocity and distance-gap ($w_s = w_v = 0.5$).

From the model response plot, the IDM model seems to better match the velocity of the ego-vehicle, and seems better able to reproduce the steepness of the velocity signal. Considering the mean parameters causes the model to react more sensitive to deviations from the desired gap, but performance is very similar. The errors of the IDM model on the first sub-trajectory are generally bounded by $e_v \in [-6.21, 3.43]$ % (velocity error) and $e_s \in [-14.7, 13.2]$ % (distance-gap error). Con-

sidering the mean parameters, e_v remains unchanged while distance-gap errors mainly shift towards underestimation ($e_s \in [-22.2, 9.94]$ %). The sACC models slightly overestimate the distance-gap and show a damped version of the actual behaviour. The errors on the first sub-trajectory are bounded by $e_v \in [-3.60, 3.11]$ % and $e_s \in [-12.2, 19.6]$ %, which is approximately equal to the ones from the IDM model. The actual vehicle shows cautious behaviour as it approaches the equilibrium time-gap, most probably to avoid overshoot and thereby enhance comfort and fuel efficiency. Both models are not able to reproduce the asymmetry this causes in the velocity profile. In the second sub-trajectory, especially the sACC models react too sensitive to the gap that is opened and seem to overshoot the desired velocity. This causes less variation in the distance-gap to be present and causes the errors of the IDM model to increase to $e_v \in [-13.3, 10.2]$ % and $e_s \in [-44.0, 52.7]$ %, while for the sACC models they rise to $e_v \in [-12.1, 15.1]$ % and $e_s \in [-46.9, 37.4]$ %.

The trajectory allows for the creation of 7 folds of 25 seconds for model validation, which is sufficient based on earlier findings. The results for the model validation are included in Table 6-1. In contrast to what was expected, the performance of the models on representing the distance-gap is comparable. The IDM model outperforms the sACC model on representing the velocity.

Table 6-1: Table showing obtained model parameters and cross-validation results for the CF trajectory. The considered error-measure in the model calibration is the RMSE using equal weight on the velocity and distance-gap $w_s = w_v = 0.5$.

	Calibration Model		
	IDM	sACC	Alternative sACC
$\mathcal{F}_{RMSE,mix}$	3.33	4.06	4.06
$\mathcal{F}_{RMSRE,v}$	$3.45 \cdot 10^{-2}$	$3.78 \cdot 10^{-2}$	$3.78 \cdot 10^{-2}$
$\mathcal{F}_{RMSRE,s}$	$1.36 \cdot 10^{-1}$	$1.95 \cdot 10^{-1}$	$1.95 \cdot 10^{-1}$
Parameters	$a = 2.97$, $b = 1.86 \cdot 10^3$, $T = 0.734$, $v_0 = 35.57$, $s_0 = 3.42$	$k_p = 0.0301$, $k_d = 0.294$, $t_d = 1.20$	$k_p = 0.0301$, $k_d = 0.294$, $t_d = 1.20$, $s_0 = 0^*$

* Parameter calibrated to bound of calibration region.

In summary, even while the requirements for excitation were not met, both models show good behaviour in representing the velocity. The found performance on representing the distance-gap is not that good. The behaviour of the IDM model seems to be most in line with the actual vehicle behaviour. The damped behaviour of the two sACC models causes the maximum representation error in both the velocity and distance-gap signal to be higher than in the IDM model. Both models were not able to reproduce the asymmetry in the velocity signal.

6-4 Cut-In and Cut-Out

Figure 6-4 shows the considered trajectory and the obtained model trajectories. The fitness landscapes and parameter sensitivity plots are of similar shape as for the CF trajectory, only the position of their optimum has been changed. The obtained parameter sensitivity plots for all models and the model response using mean parameters for the CI trajectory are included in Appendix E-2. The found calibration parameters are included in Table 6-2

The first trajectory contains one cut-in (around 10:26:15) and two cut-outs (around 10:26:30 and 10:28:00). At the cut-in, the velocity of the cut-in vehicle is just below the velocity of the ego-vehicle

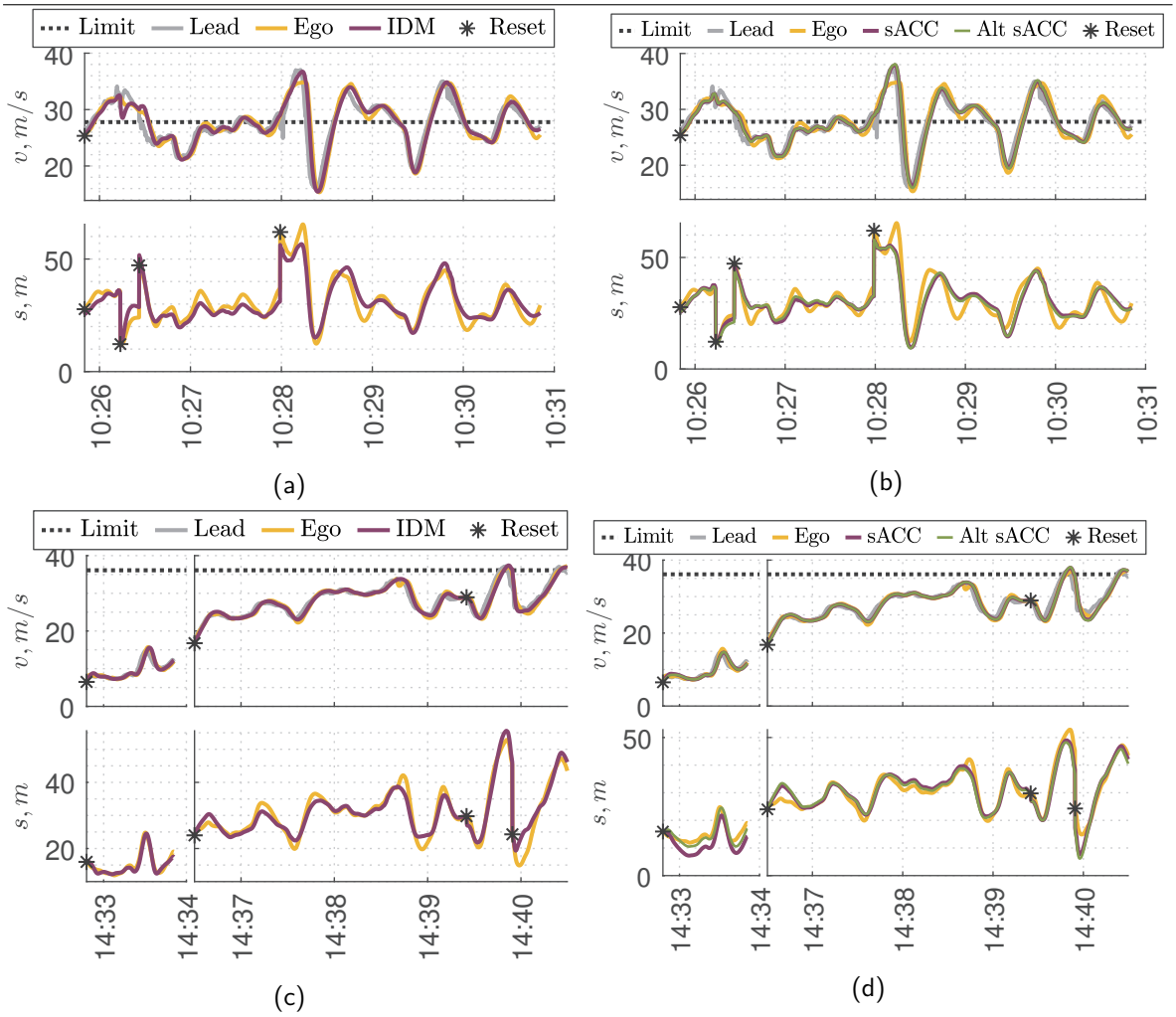

Figure 6-4: Figure showing the response of the IDM (left column) and sACC (right column) models on the CI (top row) and CI2 (bottom row) trajectories. The models are calibrated using the RMSE error-measure with equal weight on the velocity and distance-gap ($w_s = w_v = 0.5$).

($\Delta v = -0.35 m/s$), such that only a slight deceleration is necessary to avoid a collision. The second trajectory contains a single cut-in (just before 14:40:00), in which the cut-in vehicle has to brake very hard immediately after the cut-in to equal the velocity of its lead vehicle, resulting in a large velocity difference of $5 m/s$.

The IDM model shows a relatively good representation of the two cut-out events and closes the opened gap in the same manner as observed for the actual vehicle. The sACC models let more time pass before the gap is closed. This is something that is noticed in both trajectories, where the sACC model seems to show damped behaviour and therefore is not able to show all dynamics. Both models furthermore overshoot the velocity after the second cut-out. This same behaviour is found in the reaction after cut-ins. The IDM model is too sensitive to a small distance-gap and is not able to show the comfortable behaviour of the actual ACC system. The sACC model, on the other hand, shows a good representation of the first cut-in. At the second cut in the model lets the time-gap decrease to 0.3 seconds, as compared to 0.6 seconds for the actual vehicle, which means there is almost a collision.

Looking at the errors in the model response, the errors of the IDM model are generally bounded by $e_v \in [-3.65, 5.51]\,\%$ and $e_s \in [-15.2, 33.3]\,\%$. The errors at the cut-in and cut-out events are larger, where $e_v \in [-9.47, 7.42]\,\%$ and $e_s \in [-23.2, 34.5]\,\%$. Considering the mean parameters, the general errors remain approximately unchanged, while the specific errors at the cut-in and cut-out events increase to $e_v \in [-26.9, 8.30]\,\%$ and $e_s \in [-50.2, 65.5]\,\%$. Errors in the sACC model are approximately equal to the observed errors in the IDM model, where in general $e_v \in [-3.40, 6.40]\,\%$ and $e_s \in [-28.3, 14.5]\,\%$. Errors at the cut-in and cut-out events are lower than in the IDM model, where $e_v \in [-13.3, 9.52]\,\%$ and $e_s \in [-31.3, 42.1]\,\%$.

The trajectories allow for the creation of 11 (CI) and 7 (CI2) folds of 25 seconds for model validation. The results for the model validation are included in Table 6-2. In both trajectories, the IDM model outperforms the sACC model in terms of the RMSE measure and the two Root Mean Square Relative Error (RMSRE) measures considered. Performance on representing the velocity is much higher than performance on representing the distance-gap. Including s_0 in the sACC model, only increases representation performance on the distance-gap from the CI2 trajectory by 2%.

Table 6-2: Table showing obtained model parameters and cross-validation results for the CI (a) and CI2 trajectories. The considered error-measure in the model calibration is the RMSE using equal weight on the velocity and distance-gap $w_s = w_v = 0.5$.

(a)

	Calibration Model		
	IDM	sACC	Alternative sACC
$\mathcal{F}_{RMSE,mix}$	2.22	2.68	2.61
$\mathcal{F}_{RMSRE,v}$	$2.51 \cdot 10^{-2}$	$2.74 \cdot 10^{-2}$	$2.79 \cdot 10^{-2}$
$\mathcal{F}_{RMSRE,s}$	$1.13 \cdot 10^{-1}$	$1.55 \cdot 10^{-1}$	$1.45 \cdot 10^{-1}$
Parameters	$a = 1.96$, $b = 8.75$, $T = 0.515$, $v_0 = 40.9$, $s_0 = 10.0^*$	$k_p = 0.0465$, $k_d = 0.500$, $t_d = 1.08$	$k_p = 0.0447$, $k_d = 0.505$, $t_d = 0.712$, $s_0 = 10.0^*$

* Parameter calibrated to bound of calibration region.

(b)

	Calibration Model		
	IDM	sACC	Alternative sACC
$\mathcal{F}_{RMSE,mix}$	$9.43 \cdot 10^{-1}$	1.26	1.12
$\mathcal{F}_{RMSRE,v}$	$1.66 \cdot 10^{-2}$	$1.70 \cdot 10^{-2}$	$1.66 \cdot 10^{-2}$
$\mathcal{F}_{RMSRE,s}$	$5.45 \cdot 10^{-2}$	$9.77 \cdot 10^{-2}$	$7.55 \cdot 10^{-2}$
Parameters	$a = 1.79$, $b = 12.5$, $T = 0.692$, $v_0 = 46.7$, $s_0 = 7.45$	$k_p = 0.0719$, $k_d = 0.316$, $t_d = 1.09$	$k_p = 0.0715$, $k_d = 0.318$, $t_d = 0.918$, $s_0 = 4.58$

* Parameter calibrated to bound of calibration region.

In summary, both models are sensitive to overshoot in case the actual vehicle approaches the desired velocity. The IDM model shows fast response in adapting its velocity in case of both a cut-in and cut-out and outperforms the sACC model in representing the overall vehicle dynamics. While the damped response of the sACC model ensures good performance at cut-in events, it causes the model to lack the ability to represent all dynamics in the data accurately.

6-5 Hard-Braking

Figure 6-5 shows the considered trajectory and the obtained model trajectories. The trajectory starts with a closing action from a time-gap of just above 1.8 seconds, after which the vehicle is in constrained, slightly oscillating driving conditions. At around 14:44:30, the vehicle in front suddenly performs a hard-braking action ($\dot{v}_{max} = 3.33 m/s^2$), after which the vehicles decelerate to a standstill at the end of the trajectory. For all models, the fitness landscape is smooth and of similar shape as in the CF trajectory. The parameter sensitivity plots are included in Appendix E-2. The found calibration parameters are included in Table 6-3.

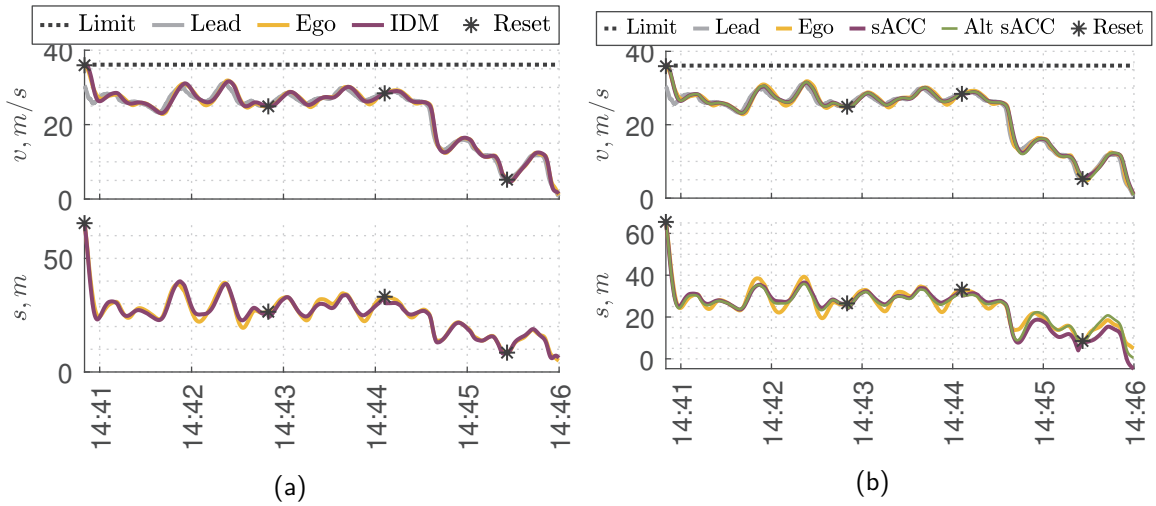

Figure 6-5: Figure showing the response of the IDM (a) and sACC (b) models on the HB trajectory. The models are calibrated using the RMSE error-measure with equal weight on the velocity and distance-gap ($w_s = w_v = 0.5$).

During the section before the hard-braking action, the behaviour represented by the IDM model is relatively good in line with the actual vehicle behaviour. The model allows slightly less distance-gap variations. Errors of the IDM model on representing the distance-gap and velocities are generally bounded by $e_v \in [-2.50, 4.41]\,\%$ and $e_s \in [-9.19, 17.4]\,\%$, respectively. Performance on representing the hard-braking action itself is approximately similar, where the observed errors are $e_v \in [-2.94, 4.14]\,\%$ and $e_s \in [-6.26, 5.58]\,\%$. The two sACC models show very similar behaviour in representing the velocity of the vehicle. At low velocities, parameter mainly parameter s_0 causes the distance-gap representation of the alternative sACC model to be much better. The sACC model even shows negative distance-gaps. Errors for the models on representing the velocity and distance-gap before the braking action are generally bounded by $e_v \in [-3.31, 3.37]\,\%$ and $e_s \in [-6.92, 22.7]\,\%$. Representation on the vehicle behaviour around the hard-braking event is quite bad, where the model is not able to reproduce the intensity of the braking action. As a result, the distance-gap becomes much smaller than observed in the data. The found errors are $e_v \in [-3.15, 15.0]\,\%$ and $e_s \in [-45.0, 5.10]\,\%$.

The trajectory allows for the creation of 6 folds of 25 seconds for model validation. The results for the model validation are included in Table 6-3. The visual performance and calibration errors of both models on representing the velocity and distance-gap, suggests that the performance on representing the velocity is approximately equal for both models, whereas performance on repre-

sentation the distance-gap is much less for the sACC model. However, the validation errors indicate that the performance of the two sACC models on representing the velocity and distance-gap is about two times worse for the IDM model.

Table 6-3: Table showing obtained model parameters and cross-validation results for the HB trajectory. The considered error-measure in the model calibration is the RMSE using equal weight on the velocity and distance-gap $w_s = w_v = 0.5$.

	Calibration Model		
	IDM	sACC	Alternative sACC
$\mathcal{F}_{RMSE,mix}$	$9.59 \cdot 10^{-1}$	1.57	1.35
$\mathcal{F}_{RMSRE,v}$	$1.31 \cdot 10^{-2}$	$2.42 \cdot 10^{-2}$	$2.29 \cdot 10^{-2}$
$\mathcal{F}_{RMSRE,s}$	$5.97 \cdot 10^{-2}$	$1.19 \cdot 10^{-1}$	$9.70 \cdot 10^{-2}$
Parameters	$a = 1.31$, $b = 17.3$, $T = 0.797$, $v_0 = 69.4^*$, $s_0 = 6.03$	$k_p = 0.110$, $k_d = 0.349$, $t_d = 1.07$	$k_p = 0.0978$, $k_d = 0.359$, $t_d = 0.771$, $s_0 = 7.72$

* Parameter calibrated to bound of calibration region.

In summary, both models show sufficient performance on representing the overall velocity of the actual vehicle. The IDM model can react faster to sudden changes than the over-damped sACC model and furthermore seems to perform better in balancing the magnitude of its reaction. It, therefore, performs better on representing the hard-braking event, where the sACC model shows overshoot in the distance-gap caused by this overly damped reaction.

6-6 Stop-and-Go

Figure 6-6 shows the considered stop-and-go trajectory and the obtained model trajectories. The calibration landscape is for the IDM and alternative sACC model of similar shape as for the CF trajectory. For the sACC model, the shape is different, showing a small correlation between parameters k_p and k_d that was not there before. This fitness landscape, and the parameter sensitivity plots of this and the other models are included in Appendix E-2. The found parameters are included in Table 6-4. Because of lacking a parameter s_0 in the sACC model, higher accelerations are needed in the low-velocity region to match the velocity of the actual vehicle. This results in k_p being larger than k_d.

Representation of the dynamics by the IDM and alternative sACC models is very good. The errors of the IDM model are generally bounded by $e_v \in [-2.10, 4.40]$ % and $e_s \in [-7.37, 6.23]$ % in the high velocity region. When considering the low-velocity region, the absolute error approximately stays the same, such that the relative error increases to $e_v \in [-22.4, 28.1]$ % and $e_s \in [-15.7, 28.2]$ %. Performance of the two sACC models on representing the velocity in the high-velocity region is approximately equal to the performance of the IDM model, where the errors are bounded by $e_v \in [-3.33, 7.35]$ %. Due to the lack of a parameter s_0, the sACC model can only accurately represent the distance-gap at a single location. Errors for the distance-gap are bounded by $e_s \in [-10.9, 13.1]$ % for the sACC model and $e_s \in [-10.4, 10.3]$ % for the alternative sACC model. In the low velocity region these errors increase significantly to $e_s \in [-100, -18.0]$ % for the sACC model and $e_s \in [-72.5, 27.0]$ % for the alternative sACC model.

Within the trajectory, 10 folds of 25 seconds are created for model validation. The results for the model validation are included in Table 6-4. In contrast to what was expected from the represen-

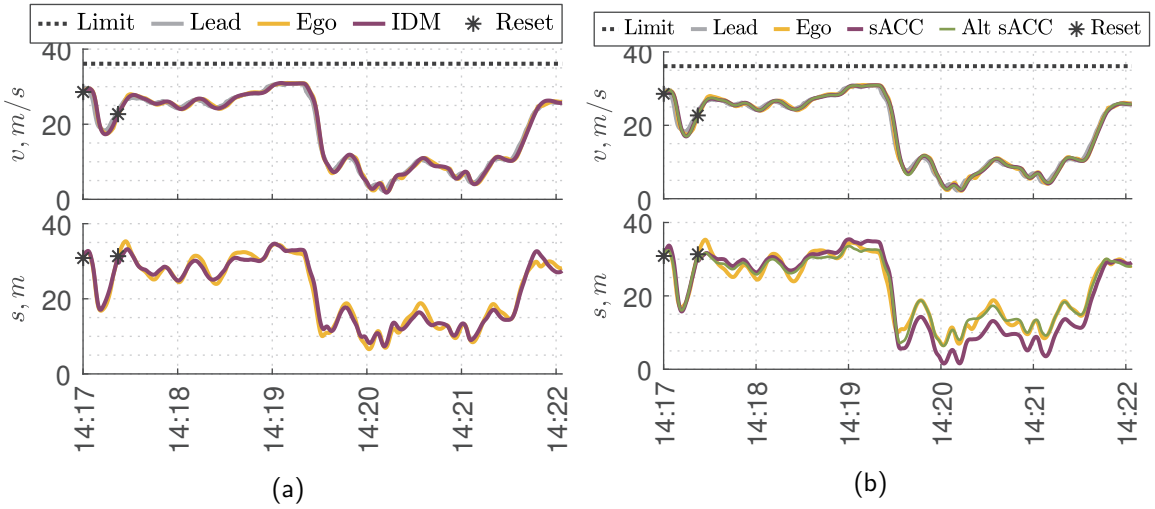

Figure 6-6: Figure showing the response of the IDM (a) and sACC (b,c) models on the SG trajectory. The models are calibrated using the RMSE error-measure with equal weight on the velocity and distance-gap ($w_s = w_v = 0.5$).

tation errors, the performance of the IDM and alternative sACC model is very similar. The models outperform the sACC model on representing the distance-gap with almost 3 times the performance and on representing the velocity with over 1.5 times the performance.

Table 6-4: Table showing obtained model parameters and cross-validation results for the SG trajectory. The considered error-measure in the model calibration is the RMSE using equal weight on the velocity and distance-gap $w_s = w_v = 0.5$.

	Calibration Model		
	IDM	sACC	Alternative sACC
$\mathcal{F}_{RMSE,mix}$	$8.92 \cdot 10^{-1}$	1.95	$8.55 \cdot 10^{-1}$
$\mathcal{F}_{RMSRE,v}$	$3.24 \cdot 10^{-2}$	$5.17 \cdot 10^{-2}$	$3.21 \cdot 10^{-2}$
$\mathcal{F}_{RMSRE,s}$	$8.19 \cdot 10^{-2}$	$2.36 \cdot 10^{-1}$	$8.08 \cdot 10^{-2}$
Parameters	$a = 2.15$, $b = 32.8$, $T = 0.774$, $v_0 = 50.9$, $s_0 = 6.74$	$k_p = 0.245$, $k_d = 0.156$, $t_d = 1.13$	$k_p = 0.181$, $k_d = 0.303$, $t_d = 0.830$, $s_0 = 6.86$

* Parameter calibrated to bound of calibration region.

In summary, the IDM and alternative sACC models show good performance on representing the driving behaviour of the considered vehicle in a stop-and-go scenario, partly due to the presence of a term defining the minimum distance at standstill s_0. Lacking such a parameter in the sACC model causes underestimation of the gap at low velocities. This increases the instability of traffic flow in these conditions, which could lead to too many accidents in the model simulation.

6-7 Cross-Comparing Results from the IDM Model

Table 6-5 gives an overview of all obtained calibration parameters, as well as published, best and mean parameter values for the CI2, HB and SG trajectories. For the validity of the investigation, the parameters defining the equilibrium distance-gap (T and s_0) are replaced by the mean parameters. Variations in most parameter values on the trajectories that were sufficiently exciting are limited. Inconsistencies in parameter calibration are only found in the trajectories that could not be used for calibration and v_0 in the hard-braking trajectory.

The parameter with the largest sensitivity in all trajectories is T, the parameter having the most influence in determining the equilibrium distance-gap. Followed by a, s_0 and v_0 and finally b. The sensitivity of a increases with increasing accelerations, the sensitivity of s_0 at low velocities are considered, and the sensitivity of v_0 when the considered velocity-range becomes smaller. The most remarkable results are however found for b, of which the sensitivity is low in every trajectory. This could either mean that the considered ACC system does not include an intelligent braking strategy, or that situations in which this strategy was active were just not present enough to result in a sensitive calibration. For $b \to \infty$, the performance on representing the SG trajectory shows an absolute decrease of 21% in the distance-gap and 28% in the velocity. This is just above the minimum improvement required for considering an additional parameter of 20% (Ossen, 2008). However, it looks like the intelligent braking strategy itself is not considered in the system.

Table 6-5: Table showing results for the calibrated parameters for each of the trajectories for the IDM model. The considered error-measure is the RMSE using equal weight on the velocity and distance-gap $w_s = w_v = 0.5$.

	a, m/s^2	b, m/s^2	T, s	v_0, m/s	s_0, m
Car-Following	2.97	$1.86 \cdot 10^3$	0.734	35.6	3.42
Cut-In	1.96	8.75	0.515	40.9	10.0*
Cut-In 2	1.79	12.5	0.692	46.7	7.45
Hard-Braking	1.31	17.3	0.797	69.4*	6.04
Stop-and-Go	2.15	32.8	0.774	50.9	6.74
Published	1.25	2.09	0.754**	33.3	6.74**
Mean (CI2/HB/SG)	1.75	20.9	0.754	55.7	6.74
Best	1.98	12.1	0.657	41.5	7.77

* Parameter calibrated to bound of calibration region.

** Parameters defining equilibrium (T and s_0) are set to the mean of the calibrated parameters.

Table 6-6 shows the results for the cross-comparison of the obtained IDM parameters on other trajectories. What is noticeable immediately, is that model performance using published parameter values is in most considered trajectories not inferior to the performance using obtained parameters from model calibration. A maximum deviation from the optimal performance of only 7% is observed. However, the model response is much too sensitive to deviations from the desired distance-gap. Considering the mean of the calibration parameter values often performs as one of the best parameter sets with on average sub-percentage worse and maximum 5% worse results from the optimal performance. Except for the SG trajectory, the performance of the mean parameter set is lower than for the set calibrated on that trajectory. Mainly because of the high sensitivity to deviations from the desired distance-gap. Because of the increased sensitivity, deviation in model trajectories is mostly visible at cut-in and cut-out manoeuvres. As compared to the calibrated parameters, the errors at these events increase with $|e_v| = +5\%$ and $|e_s| = +30\%$. Moreover, the increased desired velocity causes a slight overshoot in the velocity of the car-following manoeuvre, where $|e_v| = +8\%$ and $|e_s| = +30\%$.

Compared to the mean parameters, the "best" parameters show more agile driving behaviour while keeping a relatively shorter following distance. The observed sensitivity to deviations from the desired distance-gap is a bit less than for the mean parameter set. As compared to the calibrated parameters, the error at cut-in increases with $|e_v| = +1\%$ and $|e_s| = +25\%$. The overshoot from the desired velocity increases with $|e_v| = +6\%$ and $|e_s| = +20\%$. For both situations, this is less than when considering the mean parameter set.

In terms of local performance, the mean and "best" parameter show comparable performance on the CF and HB trajectories. The mean outperforms the "best" parameter set on the CI2 trajectory and the "best" parameter set outperforms the mean on the other two trajectories. In terms of global performance, Table 6-6 indicates slightly different results. Except for the HB and SG trajectories, the "best" parameter set outperforms the mean parameters. Representation of the HB trajectory is best for both models. Calibrated parameters from the CI2 trajectory relatively show the best performance on representing the other trajectories. As compared to common values for the RMSRE in the distance-gap of 15% for model calibration (Brockfeld et al., 2005) and just above 20% for model validation (Punzo and Simonelli, 2005) on human driving data, the obtained results are much better. Plots indicating the mismatch in vehicle trajectories when considering the mean and "best" parameter sets are included in Appendix E-5.

Table 6-6: Table showing cross-comparison results for the IDM model. The considered error-measure in the model calibration is the RMSE using equal weight on the velocity and distance-gap $w_s = w_v = 0.5$. Shown are the RMSRE errors for the velocity and distance-gap of the obtained trajectories. $\mathcal{F}_{RMSRE,s}$ is abbreviated as $\mathcal{F}_s$ and $\mathcal{F}_{RMSRE,v}$ as $\mathcal{F}_v$.

	Trajectory									
	Car-Following		Cut-In		Cut-In 2		Hard-Braking		Stop-and-Go	
Parameter Set	$\mathcal{F}_s$	$\mathcal{F}_v$	$\mathcal{F}_s$	$\mathcal{F}_v$	$\mathcal{F}_s$	$\mathcal{F}_v$	$\mathcal{F}_s$	$\mathcal{F}_v$	$\mathcal{F}_s$	$\mathcal{F}_v$
Car-Following	0.136*	0.0345*	0.318	0.0518	0.319	0.0499	0.148	0.0388	0.212	0.0713
Cut-In	0.153	0.0379	0.113*	0.0251¶	0.101	0.0231	0.130	0.0543	0.151	0.0487
Cut-In 2	0.141	0.0391	0.135	0.0315	0.0545*	0.0166*	0.0807	0.0369	0.0857	0.0430
Hard-Braking	0.150	0.0405	0.206	0.0417	0.105	0.0293	0.0597*	0.0131¶	0.109	0.0488
Stop-and-Go	0.144	0.0427	0.193	0.0441	0.123	0.0274	0.0853	0.0392	0.0819*	0.0324*
Published**	0.149	0.0417	0.168	0.0376	0.109	0.0279	0.130	0.0286	0.111	0.0462
Mean (CI2/HB/SG)	0.148	0.0420	0.160	0.0404	0.104	0.0265	0.0699	0.0367	0.0766	0.0432
Best	0.115*	0.0285¶	0.109*	0.0221¶	0.0535*	0.0158¶	0.0734*	0.0218¶	0.0826*	0.0310*

* Validation error.

** Parameters defining equilibrium (T and s_0) are set to the mean of the calibrated parameters.

6-8 Cross-Comparing Results from the sACC Model

In Table 6-7, an overview of all obtained calibration parameters is shown. The table also includes published, best and mean parameter values. For the published parameter values, the parameter defining the equilibrium distance-gap (t_d) is replaced by the mean. Obtained parameter values vary more between different trajectories than for the IDM model. The range of accelerations and velocities included in the models increases in the order the trajectories are discussed throughout this chapter. An exception is the HB trajectory, which considers a wider velocity range than the SG trajectory. The non-completeness of the sACC model is considered as a limiting factor in the selection of trajectories. As discussed earlier, this model is linear and therefore, does not have

orthogonal parameters and only a single operating mode. Each of the parameters can, therefore, uniquely be determined in each trajectory.

When considering a larger range, the weight of the gains seems to shift from k_d in case small ranges are considered, to k_p in case large ranges and low-velocity conditions are considered. The parameter sensitivity for t_d is found to be constant, regardless of the considered ranges. The parameter with the largest sensitivity in most trajectories is t_d. Followed by k_p and finally k_d. The sensitivity of k_p is higher in case a limited velocity range is present, and the sensitivity of k_d is, except for the SG trajectory, approximately constant.

Table 6-7: Table showing results for the calibrated parameters for each of the trajectories for the sACC model. The considered error-measure is the RMSE using equal weight on the velocity and distance-gap $w_s = w_v = 0.5$.

	k_p, s^{-2}	k_d, s^{-1}	t_d, s
Car-Following	0.0301	0.294	1.20
Cut-In	0.0465	0.500	1.08
Cut-In 2	0.0719	0.316	1.09
Hard-Braking	0.110	0.349	1.07
Stop-and-Go	0.245	0.156	1.13
Published	0.230	0.0700	1.10*
Mean (CI2/HB/SG)	0.142	0.274	1.10
Best	0.0757	0.403	1.12

* Parameter defining equilibrium (t_d) is set to the mean of the calibrated parameters.

Table 6-8 shows the results for the cross-comparison of the obtained sACC parameters on other trajectories. What is noticeable immediately, is that optimal model calibration using a mixed error does not have to mean that the validation error on representing the velocity and distance-gap is also optimal. Model performance differs much among different trajectories, and there is not a single parameter set that yields good performance on all trajectories. The trajectory that comes closest is the HB trajectory, with a maximum deviation from the optimal performance of 22.7%. Low performance is especially obtained using parameters of the CF trajectory, of which the performance is up to 49.7% lower than the optimal performance found.

The high gain on deviations from the desired gap k_p from the published parameter set results in many occasions of overshoot in both the velocity and distance-gap. On the other hand, considering the mean parameter results in too sensitive model behaviour, where the model often overshoots and shows negative distance-gaps. Except for the CF trajectory, the performance of the mean parameter set is lower than for the set calibrated on that trajectory. Deviation in model trajectories is mostly visible at cut-in and cut-out manoeuvres when approaching the desired-velocity and during low-velocity conditions. As compared to the calibrated parameters, the errors increase with $|e_v|$ = +9% and $|e_s|$ = +15 (overshooting desired-velocity) to $|e_s|$ = +40% (low velocity) and $|e_s|$ = +65% (cut-in).

As for the mean parameter set, performance of the "best" parameter set varies per trajectory. At high velocities, the same damped representation of the dynamics is present. At low velocities, the dynamics seem better represented, but the distance-gap still becomes negative. As compared to the calibrated parameters, the errors at the cut-ins increase with $|e_v|$ = +2.5% and $|e_s|$ = +35. The errors at low-velocity conditions are the highest with $|e_v|$ = +17% and $|e_s|$ = +60%, as compared to the calibrated parameters.

The mean parameter set is derived from the trajectories, including driving situations at low velocities. Since the model shows different optimal parameter values for different velocity ranges, this results in worse local performance in trajectories only considering high velocities, as compared to the "best" parameter set. In terms of global performance, the "best" parameter set outperforms the mean parameter set on all trajectories. As for the IDM model, validation performance on most trajectories is better than for human driving data. Plots indicating the mismatch in vehicle trajectories when considering the mean and "best" parameter sets are included in Appendix E-6.

Table 6-8: Table showing cross-comparison results for the sACC model. The considered error-measure in the model calibration is the RMSE using equal weight on the velocity and distance-gap $w_s = w_v = 0.5$. Shown are the RMSRE errors for the velocity and distance-gap of the obtained trajectories. $\mathcal{F}_{RMSRE,s}$ is abbreviated as $\mathcal{F}_s$ and $\mathcal{F}_{RMSRE,v}$ as $\mathcal{F}_v$.

	Trajectory									
	Car-Following		Cut-In		Cut-In 2		Hard-Braking		Stop-and-Go	
Parameter Set	$\mathcal{F}_s$	$\mathcal{F}_v$	$\mathcal{F}_s$	$\mathcal{F}_v$	$\mathcal{F}_s$	$\mathcal{F}_v$	$\mathcal{F}_s$	$\mathcal{F}_v$	$\mathcal{F}_s$	$\mathcal{F}_v$
Car-Following	0.195*	0.0378*	0.282	0.0378	0.198	0.0369	0.344	0.122	0.594	0.108
Cut-In	0.147	0.0403	0.155*	0.0274*	0.141	0.0268	0.237	0.0597	0.375	0.0707
Cut-In 2	0.143	0.0409	0.198	0.0260	0.0977*	0.0170*	0.289	0.0643	0.396	0.0762
Hard-Braking	0.149	0.0430	0.170	0.0306	0.159	0.0253	0.119*	0.0242*	0.324	0.0577
Stop-and-Go	0.159	0.0473	0.236	0.0557	0.205	0.0373	0.227	0.0581	0.0970*	0.0229*
Published**	0.159	0.0498	0.249	0.0668	0.213	0.0434	0.257	0.0796	0.284	0.0521
Mean (CI2/HB/SG)	0.151	0.0448	0.191	0.0375	0.171	0.0283	0.244	0.0485	0.303	0.0526
Best	0.126*	0.0309*	0.123*	0.0237*	0.0989*	0.0173*	0.146*	0.0292*	0.263*	0.0562*

* Validation error.

** Parameter defining equilibrium (t_d) is set to the mean of the calibrated parameters.

6-9 Cross-Comparing Results from the Alternative sACC Model

In Table 6-9, an overview of all obtained calibration parameters is shown. Again, the table includes published, best and mean parameter values. For the published parameter values, the parameters defining the equilibrium distance-gap (t_d, s_0) are replaced by the mean. What can immediately be noticed from the calibration results is that $k_d > k_p$ for all trajectories. Obtained parameter values for s_0 are relatively close to the ones obtained for the IDM model. As compared to the sACC model, variations in parameter values have decreased. However, there is still a factor 6 difference between the smallest and largest parameter values for k_p. Parameter values for the published, mean and "best" parameters are very similar to the ones from the sACC model.

As in the other models, parameter values for t_d are found to be most sensitive to correct calibration. Followed by k_p, k_d and finally s_0. The sensitivity of k_p is the highest when large variations in the velocity are considered, the sensitivity of k_d is constant, and the sensitivity of s_0 is highest in case low-velocity conditions are considered.

Table 6-10 shows the results for the cross-comparison of the obtained sACC parameters on other trajectories. In contrast to obtained results form the sACC model, model performance using the calibrated parameters is now not much worse than for the IDM model, and for the SG trajectory, even better results are obtained. While model performance using published parameters is not very good in most cases, considering the mean of the calibration parameter values performs at maximum 5.5% worse than the parameter set resulting in optimal performance.

Table 6-9: Table showing results for the calibrated parameters for each of the trajectories for the alternative sACC model containing s_0. The considered error-measure is the RMSE using equal weight on the velocity and distance-gap $w_s = w_v = 0.5$.

	k_p, s^{-2}	k_d, s^{-1}	t_d, s	s_0, m
Car-Following	0.0301	0.294	1.20	0.00*
Cut-In	0.0447	0.505	0.712	10.0*
Cut-In 2	0.0715	0.318	0.918	4.58
Hard-Braking	0.0978	0.359	0.771	7.72
Stop-and-Go	0.181	0.303	0.830	6.86
Published	0.230	0.0700	0.840**	6.38**
Mean (CI2/HB/SG)	0.117	0.327	0.840	6.38
Best	0.0707	0.419	0.901	5.76

* Parameter calibrated to bound of calibration region.
** Parameters defining equilibrium (t_d and s_0) are set to the mean of the calibrated parameters.

Since the parameters defining the dynamics are similar, observed dynamics are approximately equal to the ones obtained using the sACC model. Most differences in performance are found in case low-velocity conditions are considered. The large variation in parameter values k_p indicate that the model is still prone to overshoot and negative distance-gaps. Negative distance-gaps are observed for the "best" parameter set in the HB trajectory. As compared to the calibrated parameters, the errors for the mean parameter set increase with $|e_v|$ = +5% and $|e_s|$ = +45 at low-velocity conditions. This is an improvement of 5% on the velocity and equal performance for the distance-gap, as compared to the sACC model. The errors of the "best" parameter set increase with $|e_v|$ = +9% and $|e_s|$ = +60 at low velocity conditions. This is an improvement of 8% on the velocity and equal performance for the distance-gap, as compared to the sACC model. Plots indicating the mismatch in vehicle trajectories when considering the mean and "best" parameter sets are included in Appendix E-7.

Table 6-10: Table showing cross-comparison results for the alternative sACC model containing s_0. The considered error-measure in the model calibration is the RMSE using equal weight on the velocity and distance-gap $w_s = w_v = 0.5$. Shown are the RMSRE errors for the velocity and distance-gap of the obtained trajectories. $\mathcal{F}_{RMSRE,s}$ is abbreviated as $\mathcal{F}_s$ and $\mathcal{F}_{RMSRE,v}$ as $\mathcal{F}_v$.

	Trajectory									
	Car-Following		Cut-In		Cut-In 2		Hard-Braking		Stop-and-Go	
Parameter Set	$\mathcal{F}_s$	$\mathcal{F}_v$	$\mathcal{F}_s$	$\mathcal{F}_v$	$\mathcal{F}_s$	$\mathcal{F}_v$	$\mathcal{F}_s$	$\mathcal{F}_v$	$\mathcal{F}_s$	$\mathcal{F}_v$
Car-Following	0.191*	0.0373*	0.282	0.0378	0.198	0.0369	0.344	0.122	0.594	0.108
Cut-In	0.146	0.0405	0.145*	0.0279*	0.164	0.0269	0.157	0.0498	0.231	0.0651
Cut-In 2	0.145	0.0417	0.194	0.0270	0.0755*	0.0166*	0.214	0.0572	0.276	0.0743
Hard-Braking	0.158	0.0442	0.165	0.0322	0.112	0.0253	0.0970*	0.0229*	0.157	0.0561
Stop-and-Go	0.160	0.0475	0.191	0.0481	0.139	0.0317	0.113	0.0460	0.0808*	0.0321*
Published**	0.169	0.0538	0.262	0.0808	0.186	0.0468	0.167	0.0999	0.0921	0.0601
Mean (CI2/HB/SG)	0.155	0.0452	0.171	0.0358	0.110	0.0263	0.135	0.0405	0.136	0.0526
Best	0.125*	0.0309*	0.114*	0.0232*	0.0826*	0.0175*	0.124*	0.0244*	0.161*	0.0454*

* Validation error.
** Parameters defining equilibrium (t_d and s_0) are set to the mean of the calibrated parameters.

6-10 Conclusions

The goal of this chapter was to obtain insights on the capability of commonly used parametric car-following models on representing the driving behaviour of the considered ACC system. By selecting different trajectories containing typical highway scenarios commonly considered when investigating string stability, the capability of the models on representing five different types of events, and the overall fitting quality of the models on different trajectories of vehicle data was investigated.

An extensive capability investigation pointed out that a proper model calibration or validation error does not necessarily imply good model performance on representing other trajectories and specific events. Cross-comparison using different parameter sets on different trajectories provides information about the model being the correct model to represent the driving behaviour.

In the model calibration process, selection of a model correctly matching the behaviour, a proper calibration trajectory containing sufficient system excitation and a calibration trajectory which is as complete as the model, is critical. Events in the calibration trajectory that cannot be represented by the model by default induce parameter value changes to match the observed behaviour. Incorrectly calibrated and non-identifiable parameters have the possibility of influencing calibration values of other parameters. A model calibrated on an improper trajectory cannot be used to represent model performance on other trajectories. A trajectory containing sufficient excitation and considering a correct representation of the driving behaviour causes the order of parameter sensitivities to be equal to the found order in the analysis of synthetic data. The relatively low error in model calibration and model validation indicates the driving behaviour is more in line with the proposed models. Indicating more deterministic driving behaviour and/or less spatial- and/or temporal anticipation, as compared to human drivers. The low parameter sensitivity for IDM parameter b indicates that the ACC system most probably does not consider an intelligent braking strategy. Increasing parameter values k_p in the alternative sACC model in trajectories that contain lower velocities are an indication that accelerations depend on the current velocity. Furthermore, the large overshoot of the sACC model after the cut-out, as compared to the IDM model, indicates that there exists a relation between accelerations and the desired velocity.

The non-linearity of the IDM model allows it to balance the intensity of its reactions. The model behaviour is robust to parameter changes, and the model is not sensitive to overshoot in case strong reactions are needed. Dynamics are preserved when selecting the mean or "best" parameter sets. The calibration trajectory of "best" parameter set includes comfortable driving behaviour and therefore considers the disability to represent this behaviour. As compared to the mean parameter set, the model increases performance on representing these events by compensating for this mismatch. Most errors originate from situations in which the vehicle shows extra comfortable driving behaviour. The linear sACC model is not able to vary the intensity of its reaction. The model is not robust to parameter variations, can in its current form not represent low-velocity conditions and has a high risk of showing velocities above v_{des}. Furthermore, the model must show a trade-off between fitting power and overshoot. This causes the model to show a damped version of the system dynamics when considering calibrated parameter sets, and show overshoot and negative distance-gaps when considering mean or "best" parameter sets. The alternative model, which considers a parameter s_0, decreases variations in obtained parameter values. The model results in similar mean and "best" parameter values for k_p and k_d. The model mostly increases performance at low velocities. In terms of validation errors, its performance is more related to that of the IDM model. However, the model is still linear and lacks a comfort mode.

Chapter 7

Conclusions and Recommendations

7-1 Conclusions

In this research, the sensitivity of the model calibration and capability of representing the driving behaviour of an ACC system using commonly applied parametric car-following models was investigated. The models investigated were the Intelligent Driver Model (IDM) model, the newly introduced sACC model and a variant on this model including a parameter defining the minimum standstill distance.

An analysis on synthetic data has revealed that calibration of the models is characterised by a smooth objective function showing a single optimum, such that gradient-based optimisation algorithms can be applied to obtain parameter estimates. Selecting Root Mean Square Error (RMSE) error-measures and considering more weight on correctly matching the distance-gap signal was found to increase the sensitivity of the model parameters. For high parameter sensitivity, it was furthermore found to be important that the simulation contains continuous intervals sufficiently long to allow the model to develop its dynamics entirely, that model behaviour is in line with the behaviour in the data, and that the data contains all events described by the considered models. Calibration performance was found to decrease when the dynamics are not visible in the calibration data, or when the model is not well in line with the dynamics in the data. Noise was found to reduce the visibility of the dynamics, requiring proper noise reduction techniques before model calibration. In case a model parameter was calibrated incorrectly, other parameters compensate to obtain good model performance. This caused the calibration performance of other parameters in the same mode or even in the complete model to be affected negatively. Resulting in a model that performs well locally, but shows bad results on representing other driving situations.

In the real-world analysis, it was found that the models are not entirely in line with the actual driving behaviour. This mismatch was found to decrease the sensitivity of the model parameters. When calibrating a capable model to a proper calibration trajectory, the order of most sensitive parameters to a correct calibration was found to be equal to the order found in the analysis of synthetic data. The only exception being parameter b from the IDM model, which could not be calibrated. Together with the fact that the alternative sACC model could not represent the driving

behaviour, this indicates that the ACC system does not consider an intelligent braking strategy. Both simplified ACC (sACC) models showed a damped version of the actual vehicle dynamics and were not able to vary the intensity of their reactions. Therefore, the models must show a trade-off between fitting quality and overshoot. The non-linearity of the IDM model allows it to balance the intensity of its reactions. In general, this increased the ability to represent actual driving behaviour. The model furthermore considers a maximum desired velocity, which prevents overshoot in case an opening gap becomes too large. Errors in representation were mainly found during situations in which the Adaptive Cruise Control (ACC) system was showing comfortable driving behaviour.

In terms of overall fitting quality, the best performance was found for the non-linear IDM model, followed by the linear alternative sACC model. As a result, the obtained parameter sets from IDM model calibration to show least variations over the different calibration trajectories, while other models have to adapt their parameters locally to increase performance. As a conclusion, a capable model can describe multiple trajectories considering a single set of optimal parameters, robust overall performance to changes in parameter values and shows high local performance on describing specific events. Therefore, the IDM model and (to a lesser extent) alternative sACC model are capable models to represent the driving behaviour of the ACC system.

7-2 Discussion

In line with the methodology adopted in many papers, this thesis assessed the capability of the considered models on representing the driving behaviour by comparing obtained simulation trajectories with actual vehicle trajectories. Beyond what these papers generally consider, this thesis considered a further division between the overall performance and performance on representing specific events. The analysis based on synthetic data allowed for investigation of the absolute performance on finding the optimal model parameters. Results from the model validation have proven that most findings also apply to the calibration of models to real-world data. The real-world data considered realistic traffic scenarios, enabling the application of the applied methodology and results also outside of the scope of this thesis.

For the investigated ACC system, lower calibration and validation errors indicate that the models are more in line with the driving behaviour of the system. This means that the system shows more deterministic driving behaviour and/or less spatial- and/or temporal anticipation, as compared to human drivers. Various assumptions present in both the sACC models, such as symmetric and velocity independent acceleration, cause parameter values to vary more over the different trajectories and to be dependent on the considered velocity range in the calibration data-set. From a different point of view, this proves that the maximum acceleration of the system depends on the current velocity and the desired velocity. The non-linear IDM model is better in balancing the intensity of its reactions than the linear sACC models, indicating that the driving behaviour of the ACC system is non-linear. Bad model performance on representing the vehicle behaviour at cut-ins indicates that the system contains another objective in the controller enforcing comfortable vehicle behaviour. Finally, as discussed earlier, the ACC system does not consider an intelligent braking strategy. As a result, the system is not able to handle safety-critical situations, and deactivation must occur if such a situation is encountered.

The performed research in this report was limited to only a single ACC system. However, results can be used to hypothesise on the expectations of the performance on modelling other ACC systems

using the studied models. To prevent the driver from deactivating the system, systems should show comfortable, predictable and safe driving behaviour. The non-linear control approach with additional comfort mode allows the vehicle to balance the intensity of its reaction while ensuring comfortable behaviour at cut-ins. As a result, the vehicle can prevent oscillations around the equilibrium distance-gap and avoids most safety-critical events. For these reasons, the found non-linear control towards a constant time-gap found in the Audi ACC system is also expected to be present in other systems. When a safety-critical event does happen, system deactivation is expected in all systems lacking an intelligent braking mode and should be considered in the simulation. The high overall fitting quality obtained in the research was partly the result of limited anticipation of the system. To reduce unnecessary accelerations and hence increase comfort, spatial- and temporal anticipation are expected to improve when ACC systems become more advanced. By default, these are not considered in the models, which will probably cause overall model performance to decrease.

Because the control is expected to remain non-linear, the IDM model will continue to give a better fit. Eventually, it is expected that the systems will also be able to carry out the emergency braking procedure, for which a mode is already built into the IDM model. Currently, most modelling errors are located at times in which the system shows comfortable behaviour. Probably including such a parameter in the model will improve performance. At the same time, this means that the performance of the sACC models will lag behind that of the IDM model. Although these models allow a relatively simple linear stability analysis, there is a chance that the results will be negatively influenced by the damped representation of the dynamics and overshoot in the model response. Also, both models have only limited applicability. In case someone wants to use the models, at least the alternative version will have to be considered.

7-3 Recommendations upon Further Research

The IDM and sACC models show different sensitivity to each of the methodological factors investigated in the analysis of synthetic data. Results from the IDM model have proven that if a model can be considered as the right model to represent the driving behaviour, there must exist a single parameter set obtaining proper performance in most driving situations. Interesting could, therefore, be to research how both models perform in representing the different events considered in this thesis in case they are calibrated to a trajectory which allows for calibration of all parameters using an optimal calibration methodology for that model.

Since the performance of the model calibration process is not equal in case of synthetic data and real-world data, the synthetic analysis only allows for indicative norms defining, for example, the minimum length and system excitation needed in the considered model calibration trajectory. An analysis of the decrease in validation error when varying each of the factors investigated in the synthetic analysis could lead to more insights in the real world sensitivity of the model calibration.

In addition to this, one could investigate the impact on the calibration and validation performance in case parameters which cannot be determined using the selected calibration trajectory are fixed to “common” values in the calibration procedure.

Based on the assessment criteria considered in this research, the IDM model and alternative sACC models are the better model to represent the driving behaviour of ACC systems. The problem with these criteria is that they do not directly reflect their impact on the conclusions which will be

drawn from the application of these models (i.e. traffic stability and equilibrium traffic flow). A final interesting research would be how the performance of the considered models increases when common variations are considered. For the sACC model, a variant taking into account a minimum standstill distance s_0 has been investigated, indicating a significant improvement in overall model performance and applicability. Other variations could, for example, be those that would increase comfortable behaviour after cut-in events.

Bibliography

ADAS Alliantie (2019). Adas convenant: Verhogen veilig gebruik adas door het bevorderen van doorontwikkeling, bekendheid en aanschaf.

Alkim, T. P., Bootsma, G., and Hoogendoorn, S. P. (2007). Field Operational Test "The Assisted Driver". In *2007 IEEE Intelligent Vehicles Symposium*, pages 1198–1203. IEEE.

Blauw, M. (2019). Literature Survey on Heterogeneity in Adaptive Cruise Control Systems. Master's thesis, Delft University of Technology.

Brockfeld, E., Kühne, R., and Wagner, P. (2005). Calibration and Validation of Microscopic Models of Traffic Flow. *Transportation Research Record: Journal of the Transportation Research Board*, 1934(May):179–187.

Ciuffo, B. and Punzo, V. (2014). "No Free Lunch" Theorems Applied to the Calibration of Traffic Simulation Models. *IEEE Transactions on Intelligent Transportation Systems*, 15(2):553–562.

Dogruer, C. U. (2014). Estimating Mobile Robot Odometer Error with LSE Method. pages 1–9.

Gavrila, D. and Kooij, J. (2017). Lecture notes in intelligent vehicles.

Happee, R., de Winter, J., Abbink, D., Vink, P., Shyrokau, B., Stapel, J., Lu, Z., and Irmak, T. (2018). Lecture notes in automotive human factors.

Kesting, A. (2008). *Microscopic Modeling of Human and Automated Driving : Towards Traffic-Adaptive Cruise Control*. PhD thesis, Technical University of Dresden.

Kesting, A., Treiber, M., Schönhof, M., Kranke, F., and Helbing, D. (2006). Jam-Avoiding Adaptive Cruise Control (ACC) and its Impact on Traffic Dynamics. *Traffic and Granular FlowâĂŹ05*.

Liu, H., Kan, X. D., Shladover, S. E., Lu, X.-Y., and Ferlis, R. E. (2018). Modeling impacts of Cooperative Adaptive Cruise Control on mixed traffic flow in multi-lane freeway facilities. *Transportation Research Part C: Emerging Technologies*, 95:261–279.

Magnusson, N. and Odenman, T. (2012). Improving absolute position estimates of an automotive vehicle using GPS in sensor fusion. Master's thesis, Chalmers University of Technology.

Makridis, M., Mattas, K., Borio, D., Giuliani, R., and Ciuffo, B. (2018). Estimating reaction time in Adaptive Cruise Control System. *IEEE Intelligent Vehicles Symposium, Proceedings*, 2018-June(Iv):1312–1317.

Milanés, V. and Shladover, S. E. (2014). Modeling cooperative and autonomous adaptive cruise control dynamic responses using experimental data. *Transportation Research Part C: Emerging Technologies*, 48:285–300.

Milanés, V. and Shladover, S. E. (2016). Handling Cut-In Vehicles in Strings of Cooperative Adaptive Cruise Control Vehicles. *Journal of Intelligent Transportation Systems*, 20(2):178–191.

Montanino, M., Ciuffo, B., and Punzo, V. (2012). Calibration of microscopic traffic flow models against time-series data. In *2012 15th International IEEE Conference on Intelligent Transportation Systems*, pages 108–114. IEEE.

Mullakkal-Babu, F. A., Wang, M., van Arem, B., and Happee, R. (2016). Design and analysis of Full Range Adaptive Cruise Control with integrated collision a voidance strategy. In *2016 IEEE 19th International Conference on Intelligent Transportation Systems (ITSC)*, pages 308–315. IEEE.

Nowakowski, C., Shladover, S. E., Cody, D., Bu, F., O'Connell, J., Spring, J., Dickey, S., and Nelson, D. (2011). Cooperative Adaptive Cruise Control: Testing Drivers' Choices of Following Distances. Technical Report January, University of California, Berkeley, Berkeley, Calif.

Ossen, S. J. (2008). *Longitudinal driving behavior: theory and empirics*. PhD thesis, Delft University of Technology.

Punzo, V., Montanino, M., and Ciuffo, B. (2015). Do We Really Need to Calibrate All the Parameters? Variance-Based Sensitivity Analysis to Simplify Microscopic Traffic Flow Models. *IEEE Transactions on Intelligent Transportation Systems*, 16(1):184–193.

Punzo, V. and Simonelli, F. (2005). Analysis and Comparison of Microscopic Traffic Flow Models with Real Traffic Microscopic Data. *Transportation Research Record: Journal of the Transportation Research Board*, 1934:53–63.

Schakel, W. J., Gorter, C. M., de Winter, J. C., and van Arem, B. (2017). Driving Characteristics and Adaptive Cruise Control ? A Naturalistic Driving Study. *IEEE Intelligent Transportation Systems Magazine*, 9(2):17–24.

Schakel, W. J., van Arem, B., and Netten, B. D. (2010). Effects of Cooperative Adaptive Cruise Control on traffic flow stability. In *13th International IEEE Conference on Intelligent Transportation Systems*, pages 759–764. IEEE.

Shladover, S. E., Su, D., and Lu, X.-Y. (2012). Impacts of Cooperative Adaptive Cruise Control on Freeway Traffic Flow. *Transportation Research Record: Journal of the Transportation Research Board*, 2324(1):63–70.

Treiber, M., Hennecke, A., and Helbing, D. (2000). Congested traffic states in empirical observations and microscopic simulations. *Physical Review E*, 62(2):1805–1824.

Treiber, M. and Kesting, A. (2013a). Microscopic Calibration and Validation of Car-Following Models âĂŞ A Systematic Approach. *Procedia - Social and Behavioral Sciences*, 80(March):922–939.

Treiber, M. and Kesting, A. (2013b). *Traffic Flow Dynamics*. Springer Berlin Heidelberg, Berlin, Heidelberg.

Verhaegen, M. and Verdult, V. (2007). *Filtering and System Identification: A Least Squares Approach*. Cambridge University Press.

Viti, F., Hoogendoorn, S. P., Alkim, T. P., and Bootsma, G. (2008). Driving behavior interaction with ACC: results from a Field Operational Test in the Netherlands. In *2008 IEEE Intelligent Vehicles Symposium*, pages 745–750. IEEE.

Wang, M. (2014). *Generic Model Predictive Control Framework for Advanced Driver Assistance Systems*. PhD thesis, Delft University of Technology.

Wang, X., Jiang, R., Li, L., Lin, Y., Zheng, X., and Wang, F.-Y. (2018). Capturing Car-Following Behaviors by Deep Learning. *IEEE Transactions on Intelligent Transportation Systems*, 19(3):910–920.

Wilson, R. E. (2001). An analysis of Gipps' model of highway traffic. *IMA J. ˜Appl. ˜Math.*, 66(5):509–537.

Xiao, L., Wang, M., Schakel, W. J., and van Arem, B. (2018). Unravelling effects of cooperative adaptive cruise control deactivation on traffic flow characteristics at merging bottlenecks. *Transportation Research Part C: Emerging Technologies*, 96:380–397.

Xiao, L., Wang, M., and van Arem, B. (2017). Realistic Car-Following Models for Microscopic Simulation of Adaptive and Cooperative Adaptive Cruise Control Vehicles. *Transportation Research Record: Journal of the Transportation Research Board*, 2623(1):1–9.

Appendix A

Kalman Filter: Theory for Matlab Implementation

In the Kalman filter problem from this thesis, the aim is to obtain the state of a system by applying a state observer. The schematic of the Kalman filter is shown in Figure 3-3 on page 11. It is assumed that the plant dynamics are defined as

$$\begin{aligned} \mathbf{x}(t+\Delta t) &= A\mathbf{x}(t) + Bu(t) \\ \mathbf{z}(t) &= C\mathbf{x}(t) + Du(t) \end{aligned} \tag{A-1}$$

where $\mathbf{x} = [x,\ v,\ \dot{v}]^T$, A and C are as defined in Equation 3-4 on page 10 and $B = D = \mathbf{0}$ (no input is considered). For notation simplicity, subscript i is dropped in all equations. Considering a measurement model equivalent to the plant, one can use the state observer (Equation A-2) to define the error and error dynamics between the estimated state and actual state of the system (Equations A-3 and A-4).

$$\hat{\mathbf{x}}(t+\Delta t) = A\hat{\mathbf{x}}(t) + K(t)\left(\mathbf{z}(t) - C\hat{\mathbf{x}}(t)\right) \tag{A-2}$$

$$\mathbf{x}_e(t) = \hat{\mathbf{x}}(t) - \mathbf{x}(t) \tag{A-3}$$

$$\mathbf{x}_e(t+\Delta t) = (A - K(t)C)\mathbf{x}_e(t) \tag{A-4}$$

Given that the pair (A, C) is observable and $(A - K(t)C) < \mathbf{I},\ \forall t$, it follows that

$$\lim_{t\to\infty} (\hat{\mathbf{x}}(t) - \mathbf{x}(t)) = 0$$

which means the actual model state is observed by the Kalman filter. However, both the plant dynamics and measurements are subject to noise. Due to this noise, $\mathbf{x}_e(t) = 0$ cannot be reached. Including the noise in the plant model and error dynamics results in the following set of equations:

$$\mathbf{x}(t+\Delta t) = A\mathbf{x}(t) + Bu(t) + \mathbf{w}(t) \tag{A-5}$$

$$\mathbf{z}(t) = C\mathbf{x}(t) + Du(t) + \mathbf{v}(t) \tag{A-6}$$

$$\mathbf{x}_e(t+\Delta t) = (A - K(t)C)\mathbf{x}_e(t) - \mathbf{w}(t) + K(t)\mathbf{v}(t) \tag{A-7}$$

The goal is now to define $K(t)$ in such a way that the approach rate of $\hat{\mathbf{x}}$ to $\mathbf{x}$ is optimal. The noise covariance matrices are defined as $\mathbb{E}\left[\mathbf{w}(t)\mathbf{w}^T(t)\right] = Q$ and $\mathbb{E}\left[\mathbf{v}(t)\mathbf{v}^T(t)\right] = R$. The best possibility is to obtain $\mathbf{x}_e$ as such, that it yields a minimum variance ($\mathbb{E}\left[\mathbf{x}_e(t)\mathbf{x}_e(t)^T\right] = P(t)$) and unbiased ($\mathbb{E}[\mathbf{x}_e(t)] = 0$) estimation of the actual state. Here, $P(t|t)$ denotes the state covariance matrix at time t using all information up to time t.

A measurement update gives the current filtered state estimate $\hat{\mathbf{x}}(t|t)$ based on the current measurements and all prior information as:

$$K^T(t) = P(t|t-\Delta t)C^T\left(R + CP(t|t-\Delta t)C^T\right)^{-1} \tag{A-8}$$

$$P(t|t) = \left(\mathbf{I} - K^T(t)C\right)P(t|t-\Delta t) \tag{A-9}$$

$$\hat{\mathbf{x}}(t|t) = \hat{\mathbf{x}}(t|t-\Delta t) + K^T(t)\left(\mathbf{z}(t) - C\hat{\mathbf{x}}(t|t-\Delta t)\right) \tag{A-10}$$

After advancing in time ($t = t + \Delta t$), this state estimate and the state covariance matrix are updated using a time-update, defined as:

$$\hat{\mathbf{x}}(t|t-\Delta t) = A\hat{\mathbf{x}}(t-\Delta t|t-\Delta t) \tag{A-11}$$

$$P(t|t-\Delta t) = AP(t-\Delta t|t-\Delta t)A^T + Q \tag{A-12}$$

After taking these steps, the cycle will repeat again starting from Equation A-8.

To remove bias from the measurement signals an additional bias state $\dot{v}_{bias}$ is introduced, such that $\hat{\mathbf{x}} = [x,\ v,\ \dot{v},\ \dot{v}_{bias}]^T$. Matrices A and C in Equations A-8 - A-12 are be updated as:

$$A = \begin{bmatrix} & A & & 0 \\ & & & 0 \\ & & & 1 \\ 0 & 0 & 0 & 1 \end{bmatrix}, \quad C = \begin{bmatrix} & & 0 \\ C & & 0 \\ & & 1 \end{bmatrix}$$

which makes it possible to filter the bias from the measurement signals.

For a more elaborate introduction on the Kalman filter, bias filtering using a Kalman filter, and a proof of its workings, see Verhaegen and Verdult (2007) and Magnusson and Odenman (2012).

Appendix B

Moving Average Filter: Theory and Results

B-1 Theory

Considering a case in which a measurement sequence of infinite length only contains zero-mean white noise, taking the mean of all measurement values results in a zero value (since $\mathbb{E}[X] = 0$, this leads to: $\frac{1}{N}\lim_{N\to\infty}\sum_{n=1}^{N} X[n] = 0$). The moving average filter utilises this to filter noise from a measurement signal. Actual measurement signals contain noise, as well as information about the dynamics of the system. Taking the (weighted) average over a relatively small number of measurement values preserves the dynamics of the signal, but at the same time approaches taking the limit of the noise sequence and thus removing noise from the measurement signal. The moving average filter replaces measurement i by the average over the last $(N-1)/2$ to the next $(N-1)/2$ measurement values. The moving average filter is defined as

$$z(t) = \frac{1}{N}\sum_{n=0}^{N-1} z\left(t + \left(n - \frac{N-1}{2}\right)\Delta t\right) \tag{B-1}$$

B-2 Results

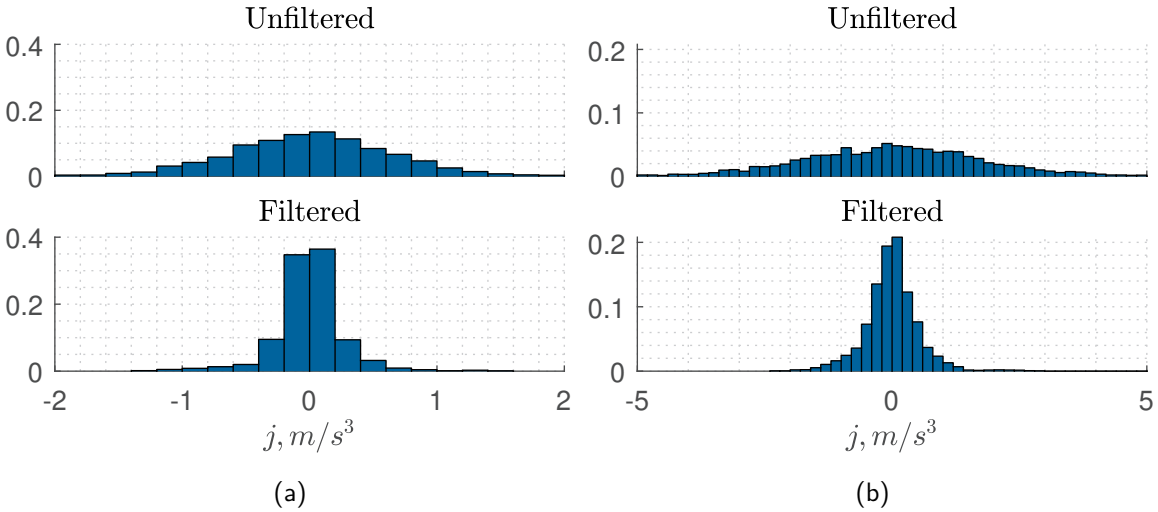

(a) (b)

Figure B-1: Figure showing a histogram containing final jerk values before and after the smoothing of measurement signals from the ego- (a) and lead-vehicle (b) using a window size of 4 and 9 measurement samples, respectively.

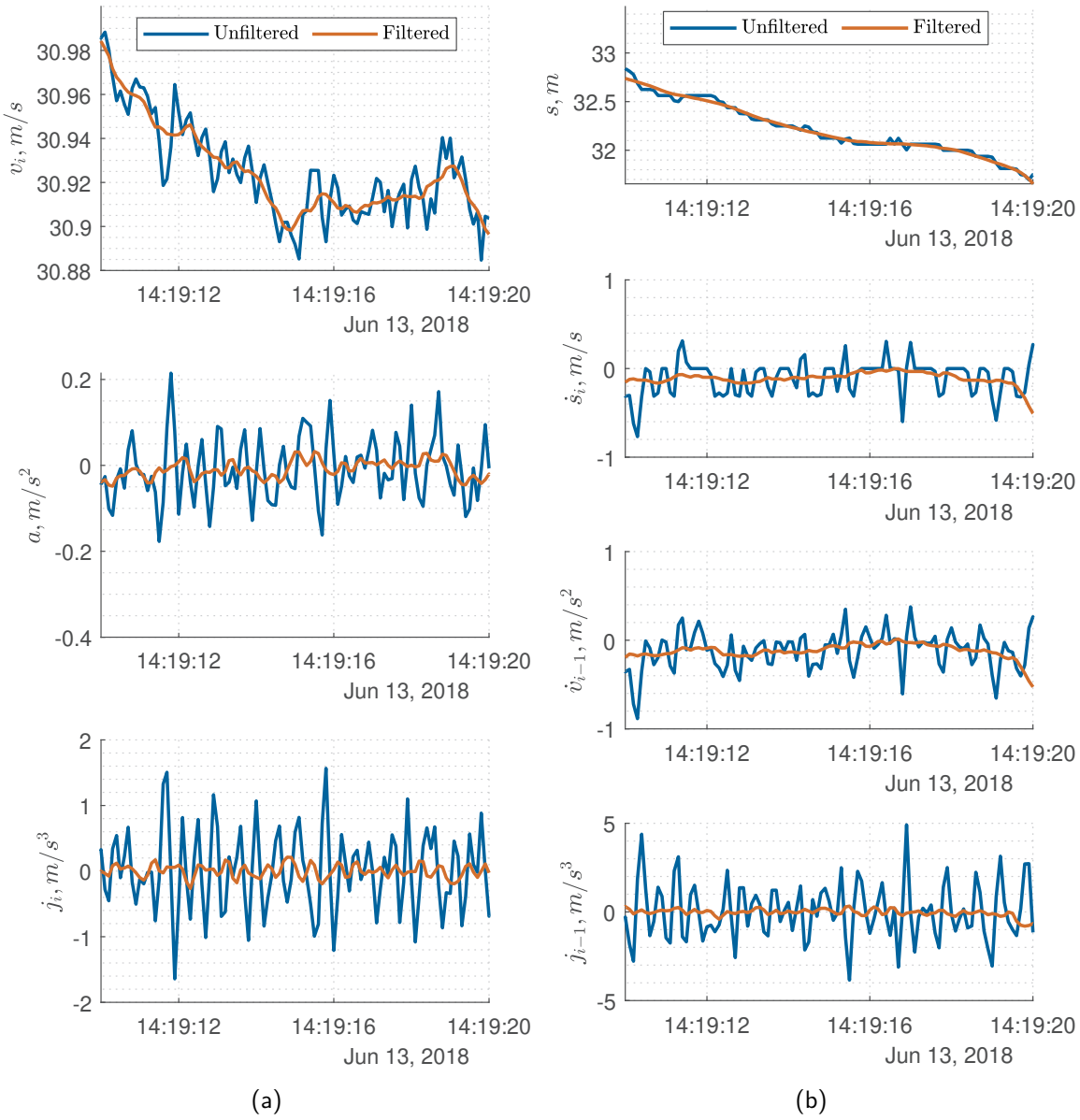

Figure B-2: Figure showing the final results of the smoothing of measurement signals from the ego- (a) and lead-vehicle (b) using a window size of 4 and 9 measurement samples, respectively.

Appendix C

Data Selection

C-1 ACC Operating Times

In order for vehicle data to be suitable to be used within the research, accurate empirical evidence on when the Adaptive Cruise Control (ACC) system is active and the input variables to which the ACC system reacts must be known. The following set of criteria is defined to determine whether data from a vehicle can be used within the research

1. Distance-gaps between the ego vehicle and the vehicle driving in front must be known
2. The velocity of the ego vehicle must be known
3. The ACC status of the ego vehicle must be known. This involves having evidence on
   (a) (De)activation times of the ACC system
   (b) Whether the driver or ACC system is braking
   (c) Whether the driver or ACC system is throttling
   (d) The (desired) gap between the ego vehicle and the vehicle driving in front

In Figures C-1 and C-2, an overview of the logged data for the Audi vehicle is shown. The numbers included in the figures indicate different events that can be used as proof of the data meeting the criteria from the above list. Distance gaps *(1)* and velocities *(2)* are logged at all times for the Audi. In Figure C-1, *(3a)* points to locations at which the ACC system is being (de)activated. A 0 value indicates the system is not active, whereas 2 indicates the system is active. From *(3b)*, it can be seen that during times at which the ACC system is activated, brake lights are turned on without brake pedal positions to be logged. Therefore, it can be concluded that only manual braking is logged within the data. Similar reasoning yields for the throttle pedal *(3c)*, making it very easy to observe overruling of the ACC system by throttling while the system is active. In this case, throttle positions different from zero will be observed while the ACC state is logged as active. The (desired) gap can be obtained from a point in time at which steady-state (or close-to steady state) car-following behaviour is observed *(3d)*.

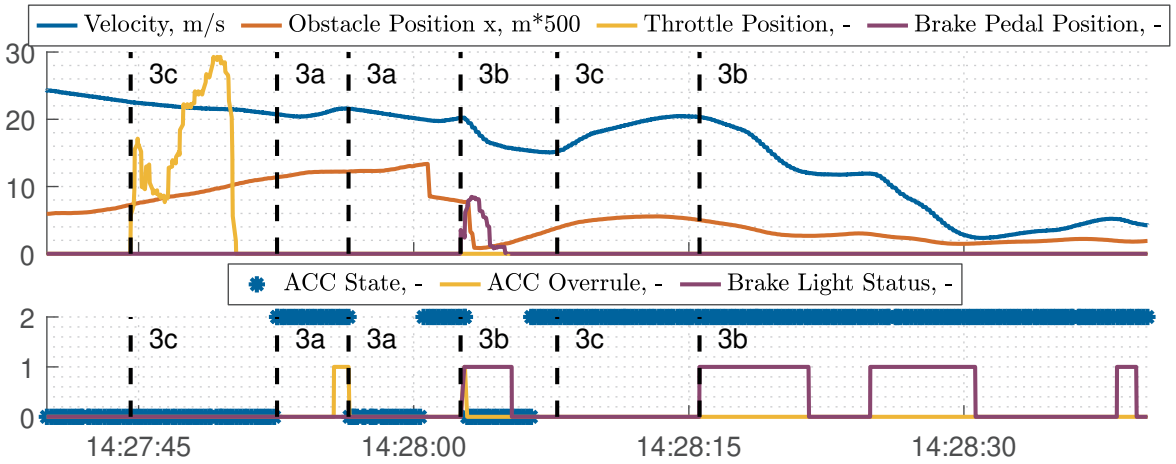

Figure C-1: Figure showing logged evidence for the ego vehicle.

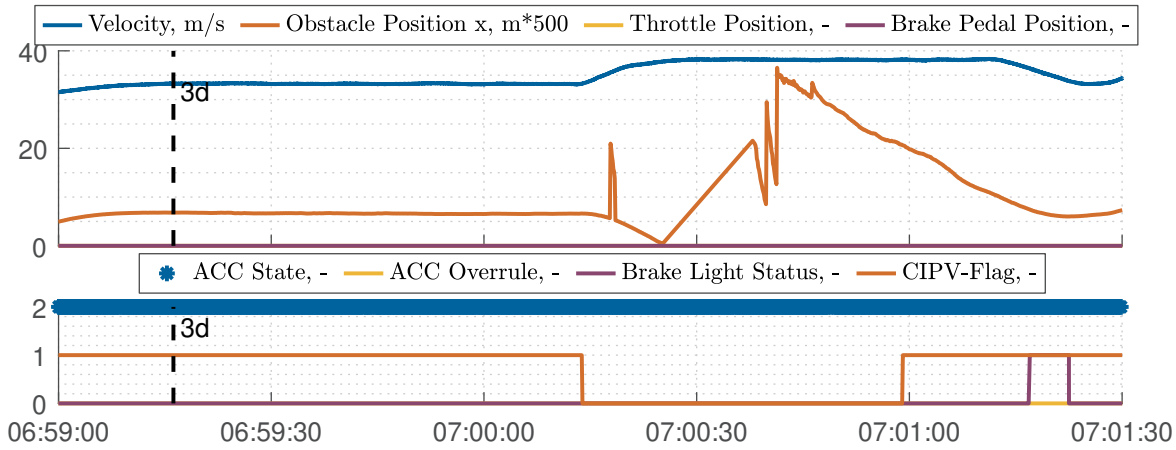

Figure C-2: Figure showing logged evidence for the lead vehicle.

C-2 Results

In each of the Figures C-3 - C-4, the “flags” indicate whether a certain event is considered as “true”. Therefore, data with the following flags is removed from the dataset: ACC overrule, manual throttle, manual brake, left (L) lane-change, right (R) lane-change, left (L) indicator and right (R) indicator.

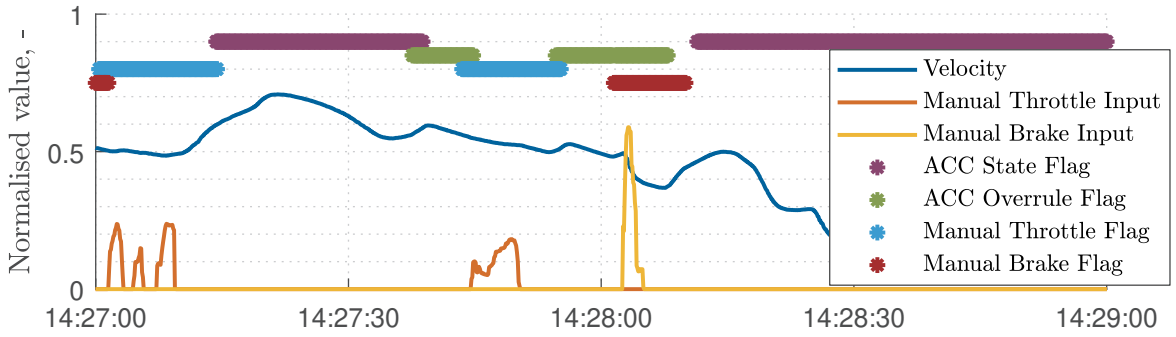

Figure C-3: Figure showing detection of ACC system (de)activation and overruling using data from the CAN bus.

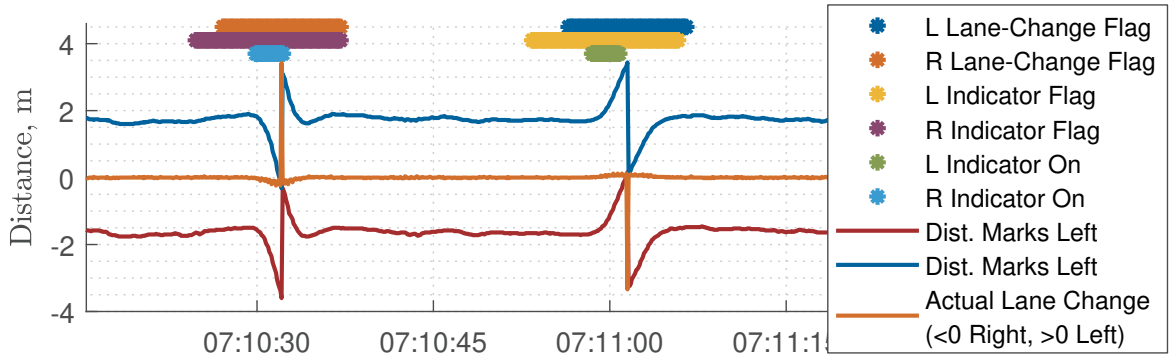

Figure C-4: Figure showing detection of a lane-change using data from the MobilEye and CAN bus.

Appendix D

Sensitivity of the Model Calibration: More Results

D-1 Creation of Synthetic Data

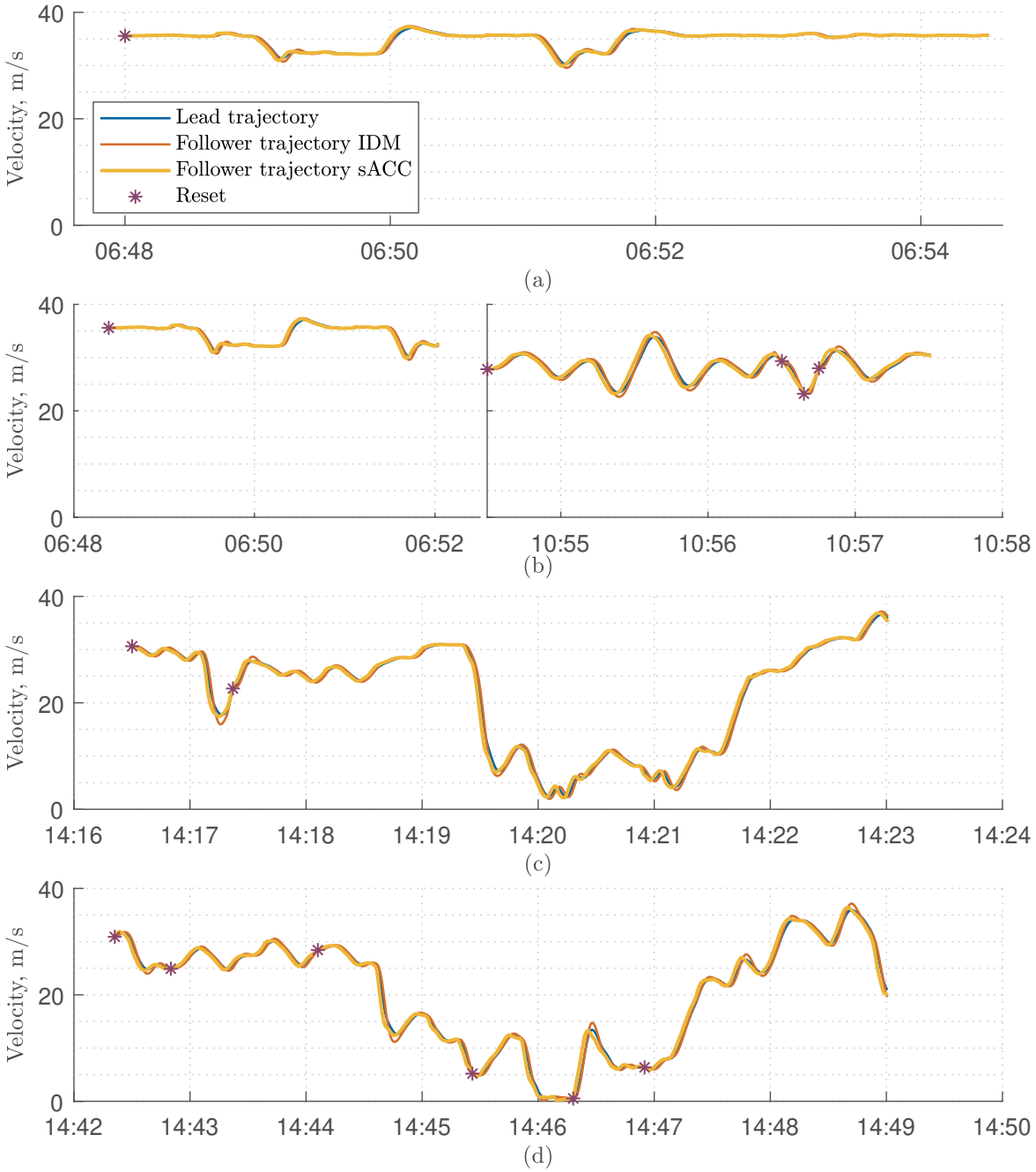

Figure D-1: Plot showing an example of generated follower trajectories on the CF (a), OSC (b), SG1 (c) and SG2 (d) trajectories for the IDM model using parameters $p_{IDM} = [2.63,\ 2.81,\ 1.33,\ 54.13,\ 3.53]^T$ and sACC model using parameters $p_{sACC} = [0.28,\ 0.09,\ 1.33]^T$.

D-2 Impact of Calibration Methodology

D-2-1 Error-Measure

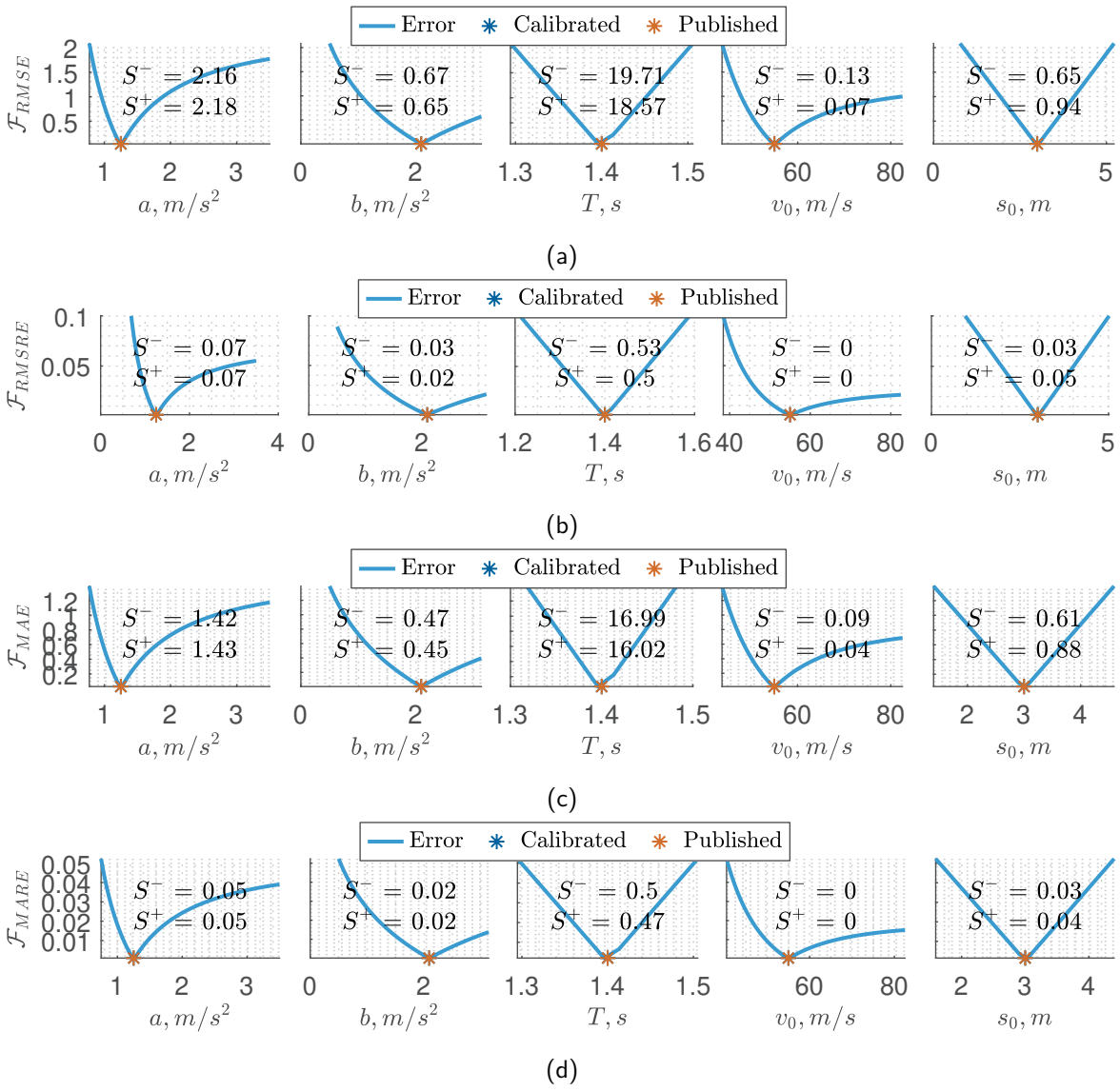

Figure D-2: Figure showing the parameter sensitivity of the IDM model for different error measures: RMSE (a), RMSRE (b), MAE (c) and MARE (d). The calibration was performed on the noise-free SG1 trajectory using full weight on the distance-gap ($w_s = 1$).

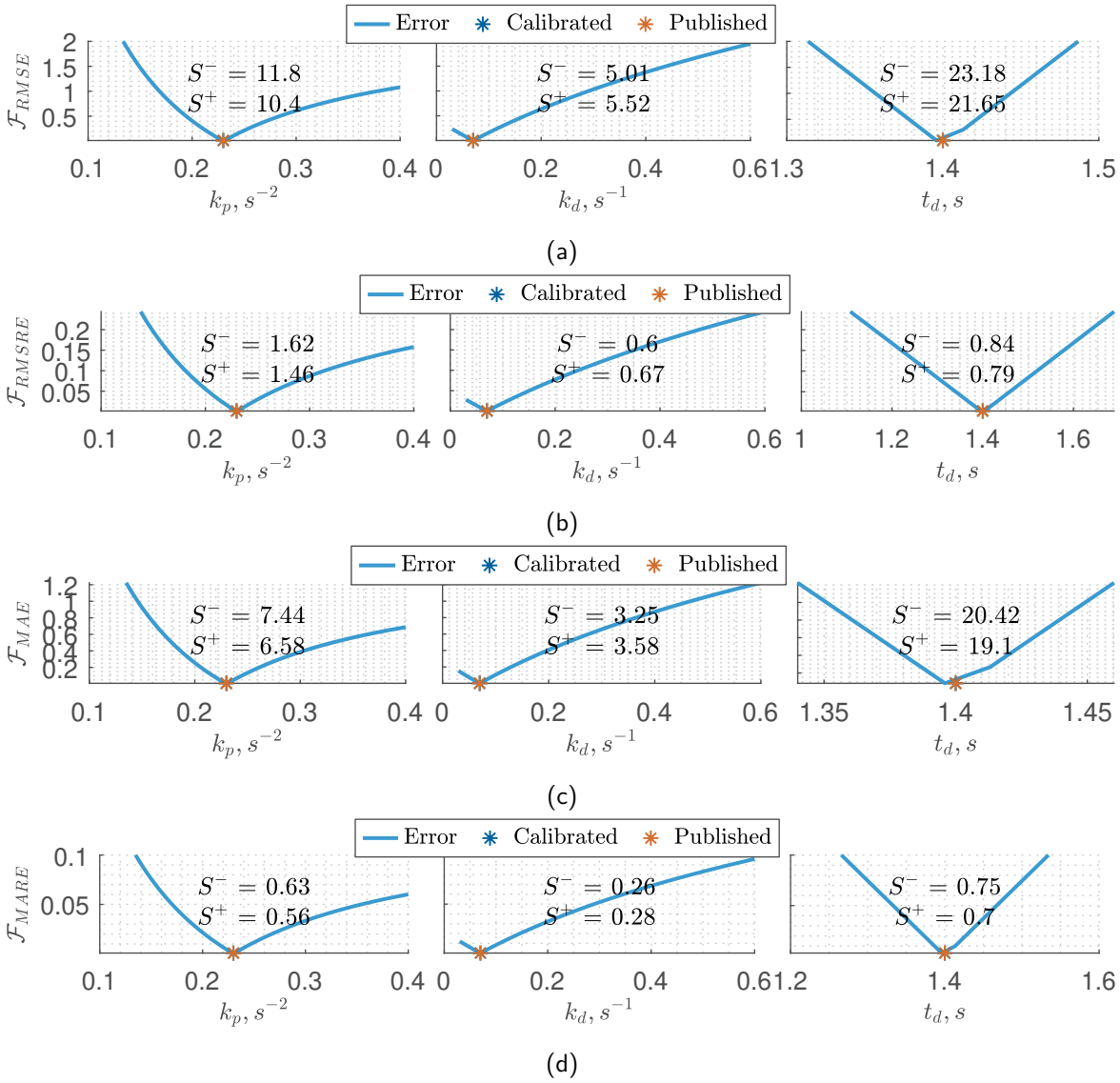

Figure D-3: Figure showing the parameter sensitivity of the sACC model for different error measures: RMSE (a), RMSRE (b), MAE (c) and MARE (d). The calibration was performed on the noise-free SG1 trajectory using full weight on the distance-gap ($w_s = 1$).

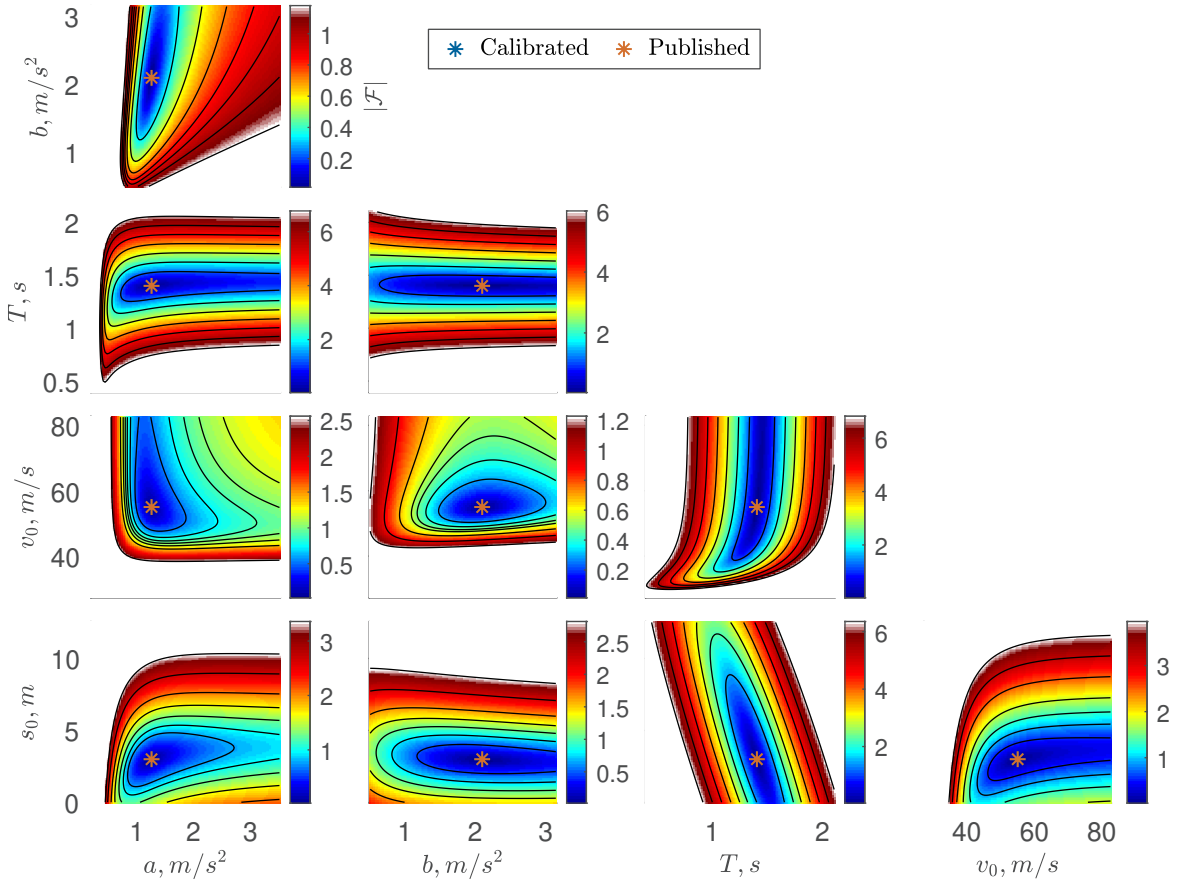

(a)

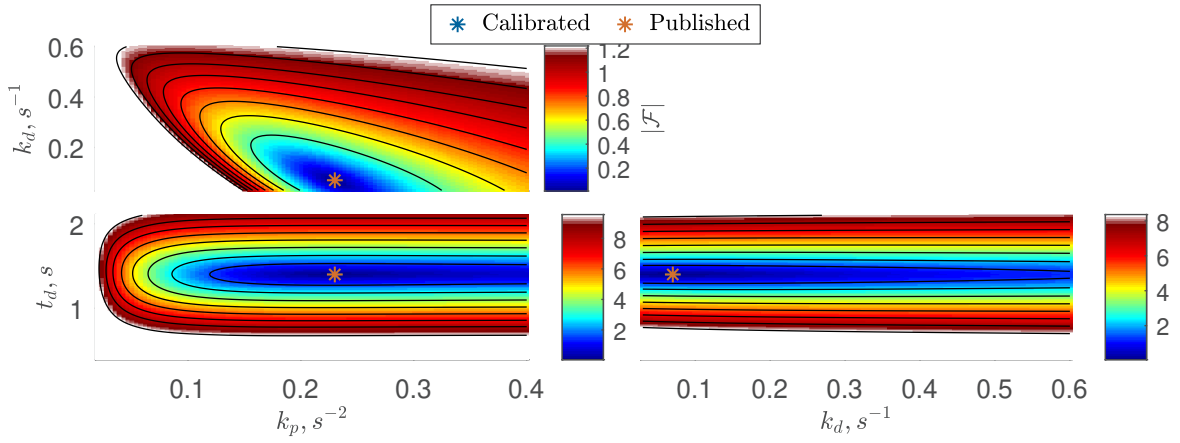

(b)

Figure D-4: Figure showing the fitness landscape of the IDM (a) and sACC (b) models. The analysis was performed using the RMSE error-measure with equal weight on the distance-gap and velocity ($w_s = w_v = 0.5$).

D-2-2 Reset Interval

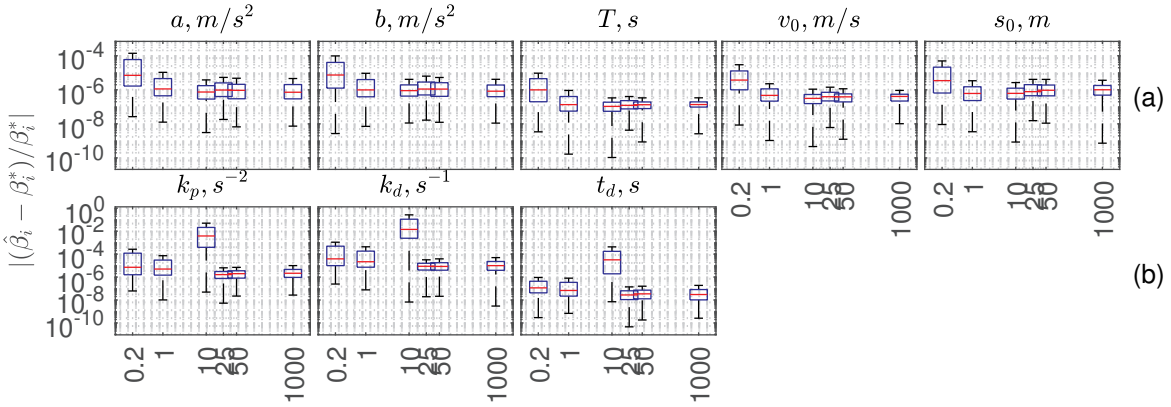

Figure D-5: Figure showing the distribution of the distances of the calibrated parameters to the actual model parameters of the IDM (a) and sACC (b) models for different simulation reset intervals. The calibration was performed on the noise-free SG1 trajectory using the RMSE error-measure with equal weight on the distance-gap and velocity ($w_s = w_v = 0.5$).

D-3 Impact of Varying Data Quality

D-3-1 Noise: Lead Vehicle

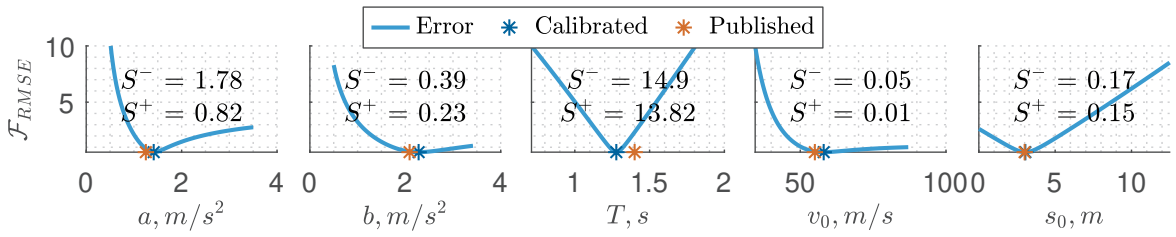

Figure D-6: Figure showing the parameter sensitivity of the IDM model for the case where noise ($\mathcal{N}(0,0.1)$) is injected to the distance-gap measurements. The calibration was performed on the SG1 trajectory using the RMSE error-measure with full weight on the distance-gap ($w_s = 1$).

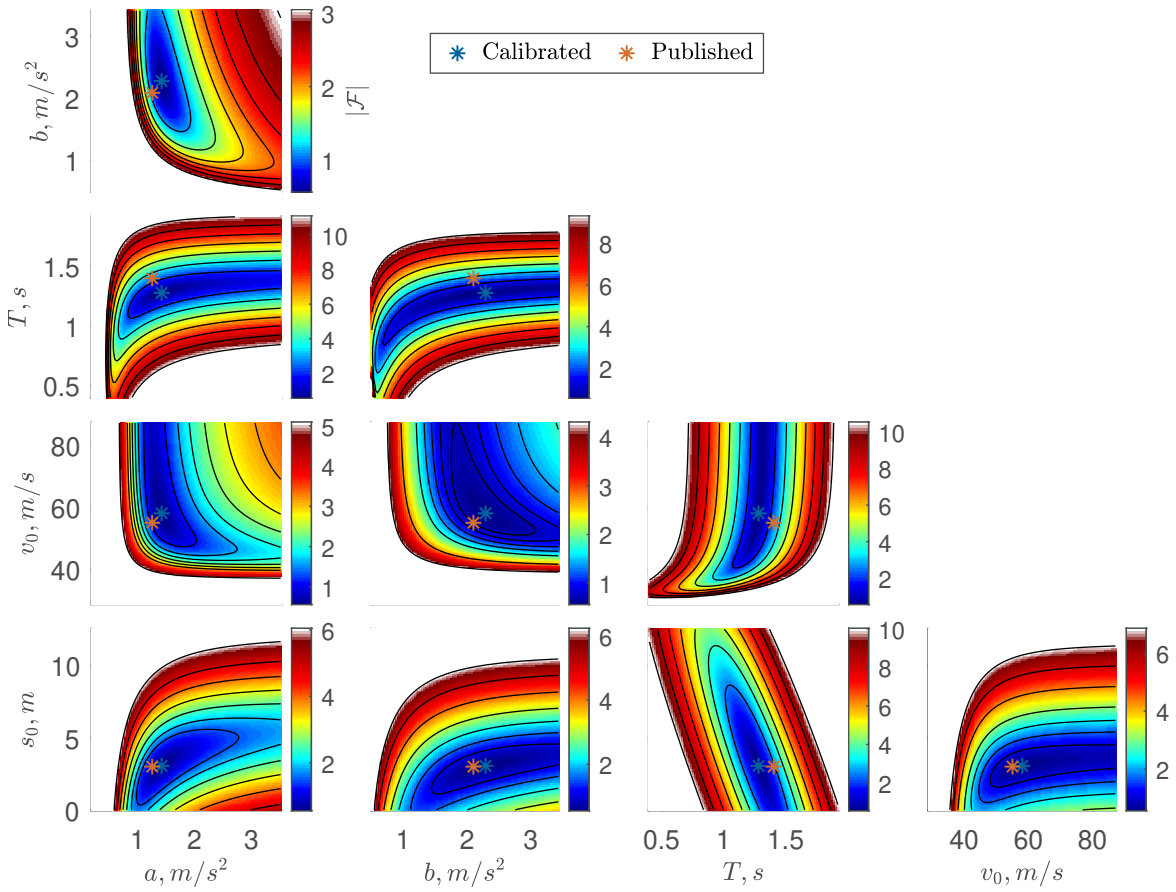

Figure D-7: Figure showing the fitness landscape of the IDM (a) and sACC (b) models in case noise ($\mathcal{N}(0,0.1)$) is injected to the distance-gap measurements. The analysis was performed using the RMSE error-measure with full weight on the distance-gap ($w_s = 1$).

D-3-2 Incorrect Car-Following Model

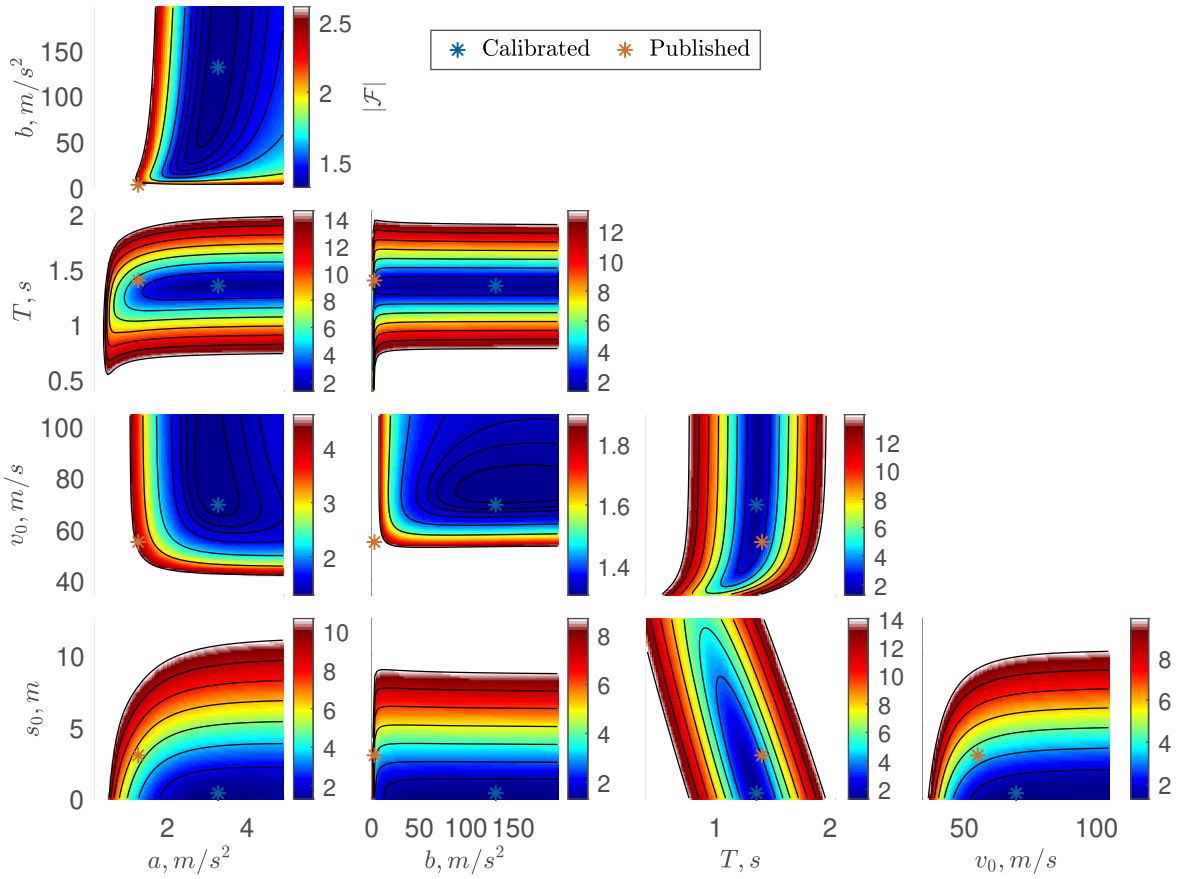

(a)

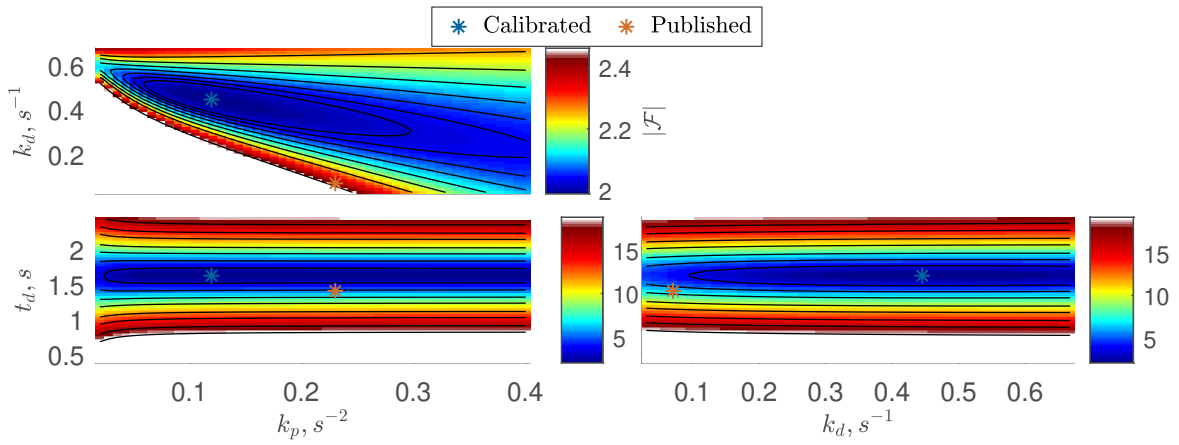

(b)

Figure D-8: Figure showing the fitness landscape of the IDM (a) and sACC (b) models, where the trajectories are created using the other model. The analysis was performed using the RMSE error-measure with full weight on the distance-gap ($w_s = 1$).

D-4 Impact of Varying Data Quantity

D-4-1 Trajectory Length

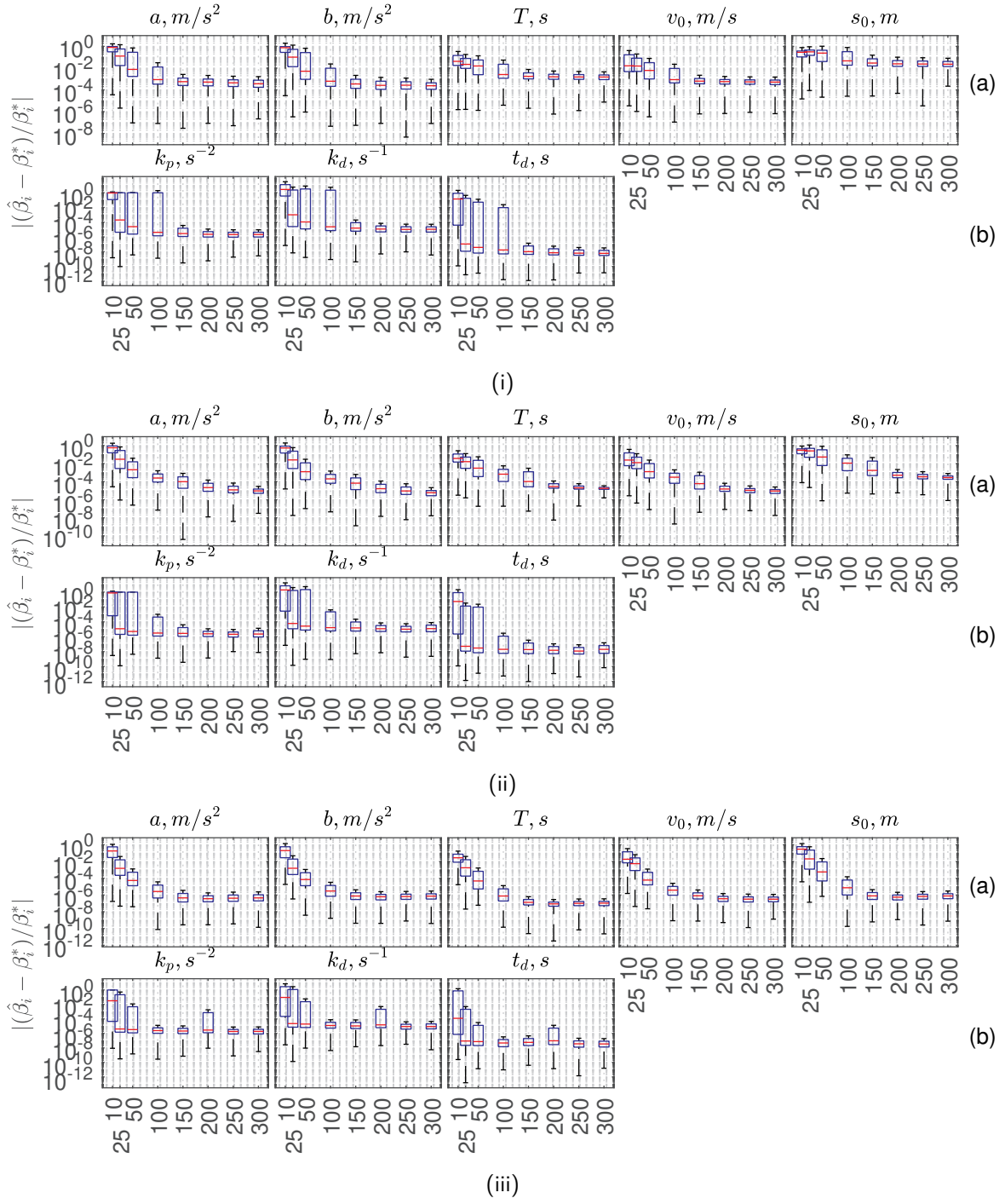

Figure D-9: Figure showing the distribution of the distances of the calibrated parameters to the actual model parameters of the IDM (a) and sACC (b) model for different trajectory lengths. The calibration was performed on the noise-free CF (i), OSC (ii) and SG2 (iii) trajectories using the RMSE error-measure with full weight on the distance-gap ($w_s = 1$).

D-4-2 System Excitation

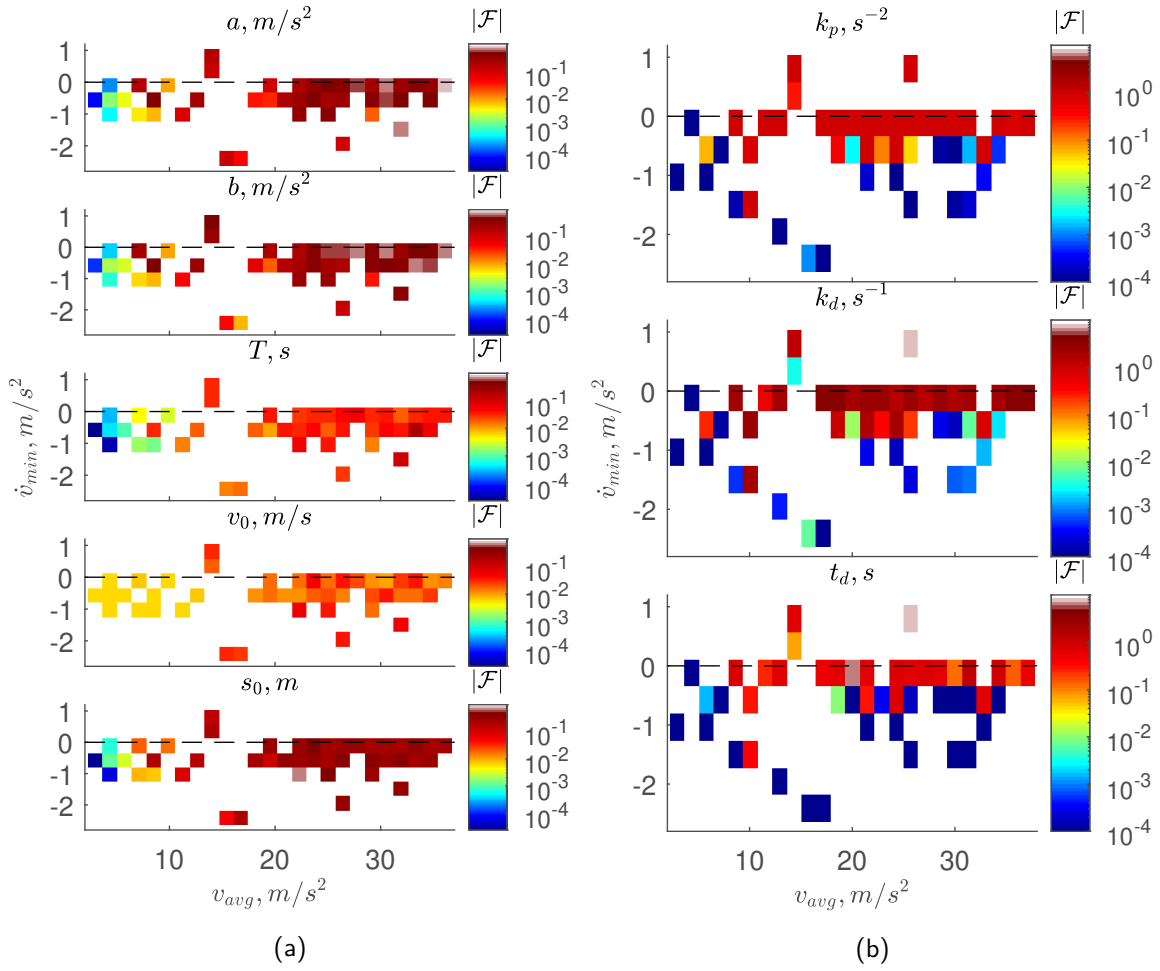

Figure D-10: Figure showing the median distance of the calibrated parameters to the actual model parameters of the IDM (a) and sACC (b) models for different excitation levels. The calibration was performed on all data-sets using a trajectory length of 10 seconds and using the RMSE error-measure with full weight on the distance-gap ($w_s = 1$).

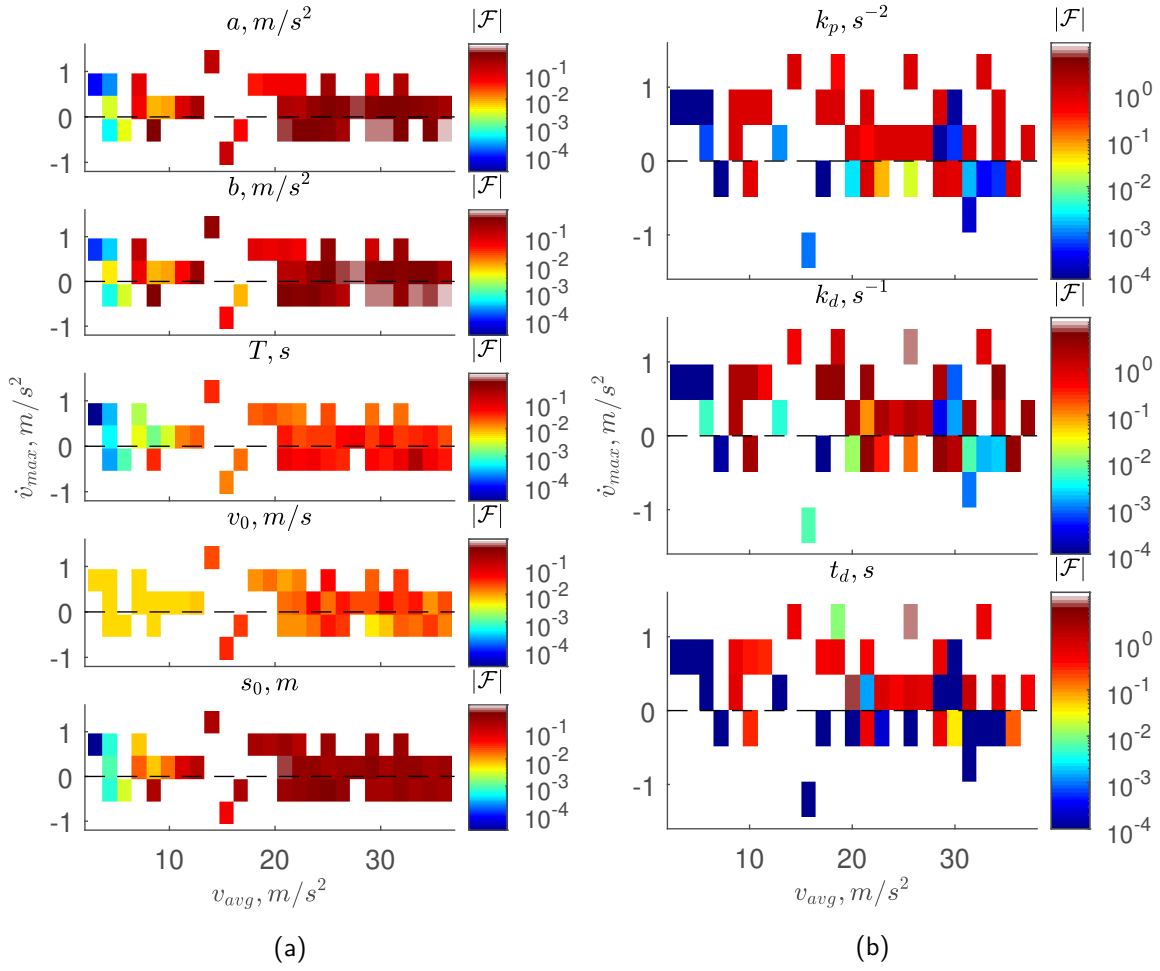

Figure D-11: Figure showing the median distance of the calibrated parameters to the actual model parameters of the IDM (a) and sACC (b) models for different excitation levels. The calibration was performed on all data-sets using a trajectory length of 10 seconds and using the RMSE error-measure with full weight on the distance-gap ($w_s = 1$).

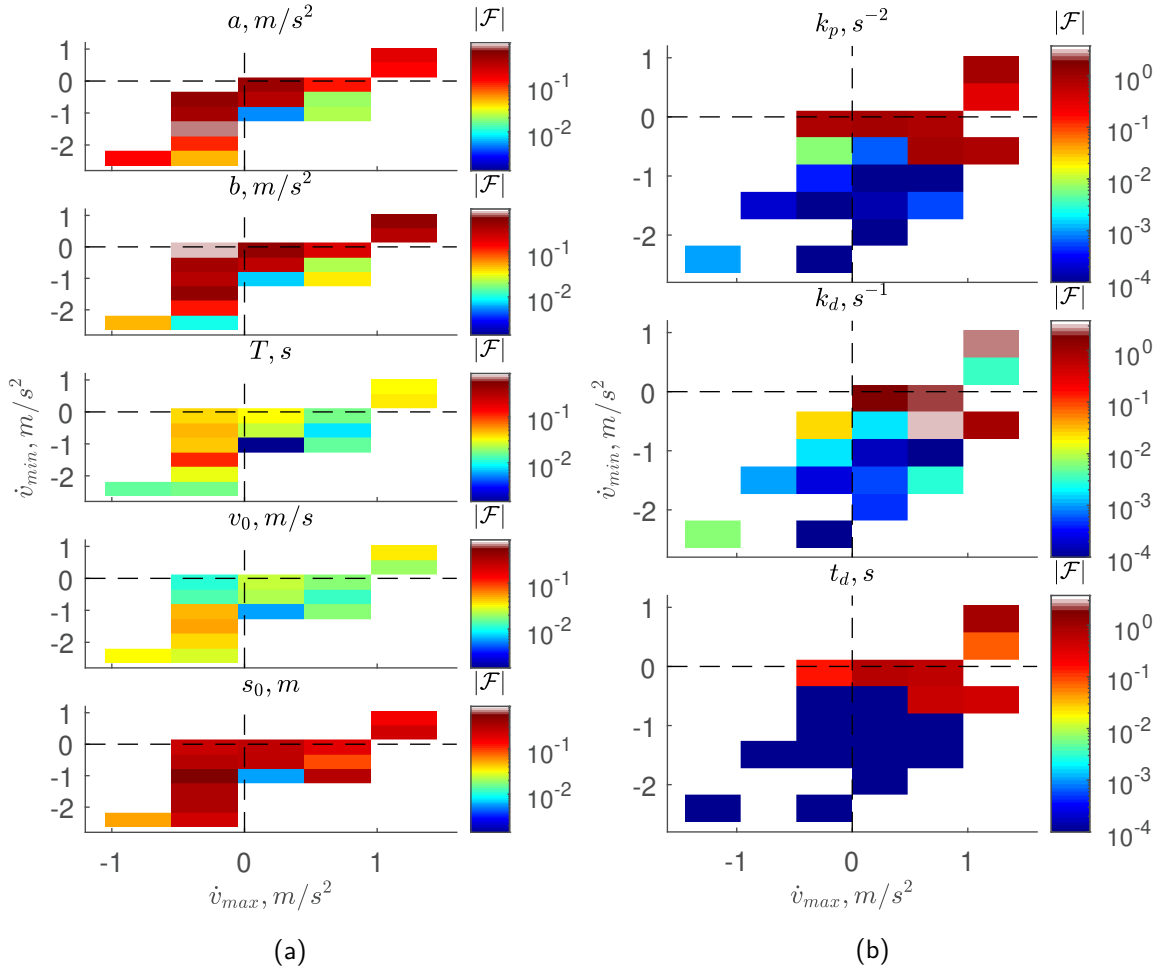

Figure D-12: Figure showing the median distance of the calibrated parameters to the actual model parameters of the IDM (a) and sACC (b) models for different excitation levels. The calibration was performed on all data-sets using a trajectory length of 10 seconds and using the RMSE error-measure with full weight on the distance-gap ($w_s = 1$).

Appendix E

Real World Validation of Adaptive Cruise Control (ACC) Models: More Results

E-1 Steady-State Car-Following

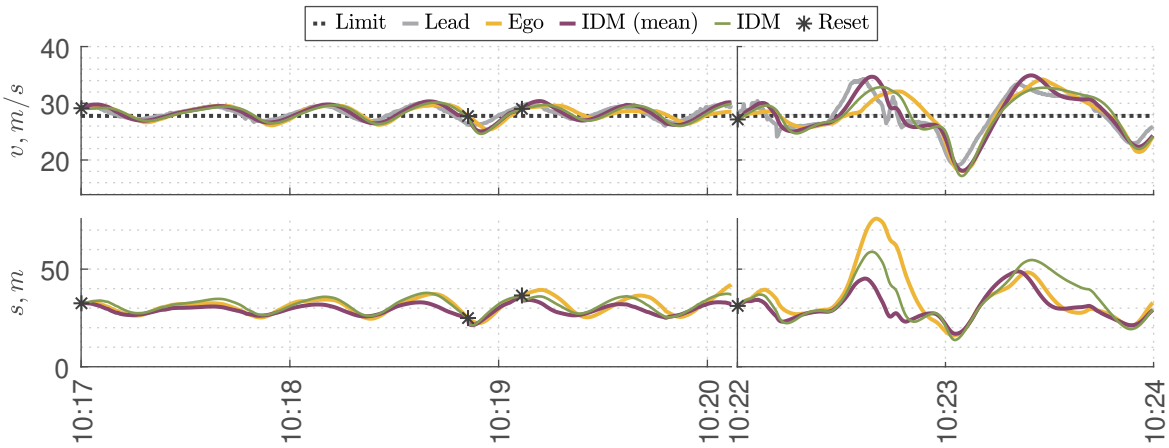

Figure E-1: Figure showing the response of the IDM model on the CF trajectory using mean parameters from the CI2, HB and SG trajectories. The model is calibrated using the RMSE error-measure with equal weight on the distance-gap and velocity ($w_s = w_v = 0.5$).

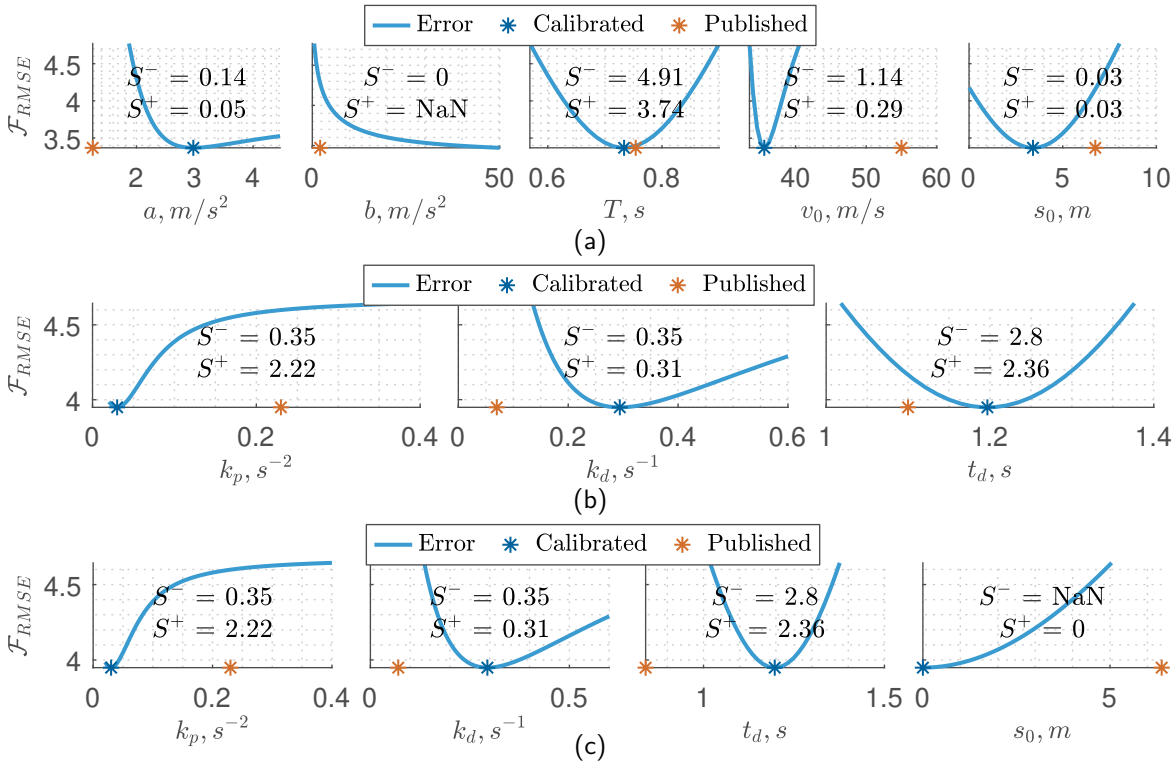

Figure E-2: Figure showing the parameter sensitivity of the IDM (a), sACC (b) and alternative sACC (c) models on real world vehicle data of the CF trajectory. The analysis was performed using the RMSE error-measure with equal weight on the distance-gap and velocity ($w_s = w_v = 0.5$).

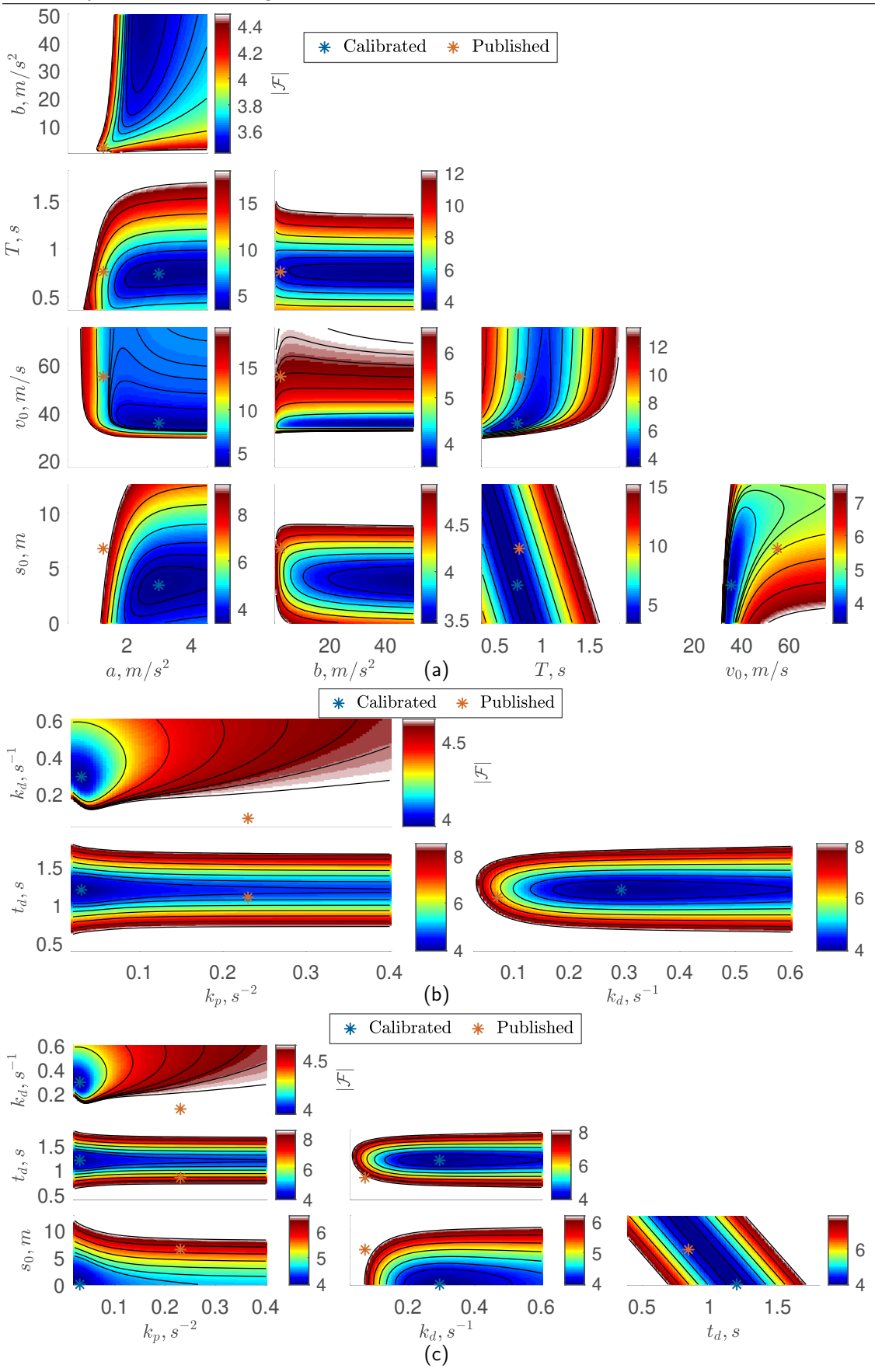

Figure E-3: Figure showing the fitness landscape of the IDM (a), sACC (b) and alternative sACC (c) models on real world vehicle data of the CF trajectory. The analysis was performed using the RMSE error-measure with equal weight on the distance-gap and velocity ($w_s = w_v = 0.5$).

E-2 Cut-In

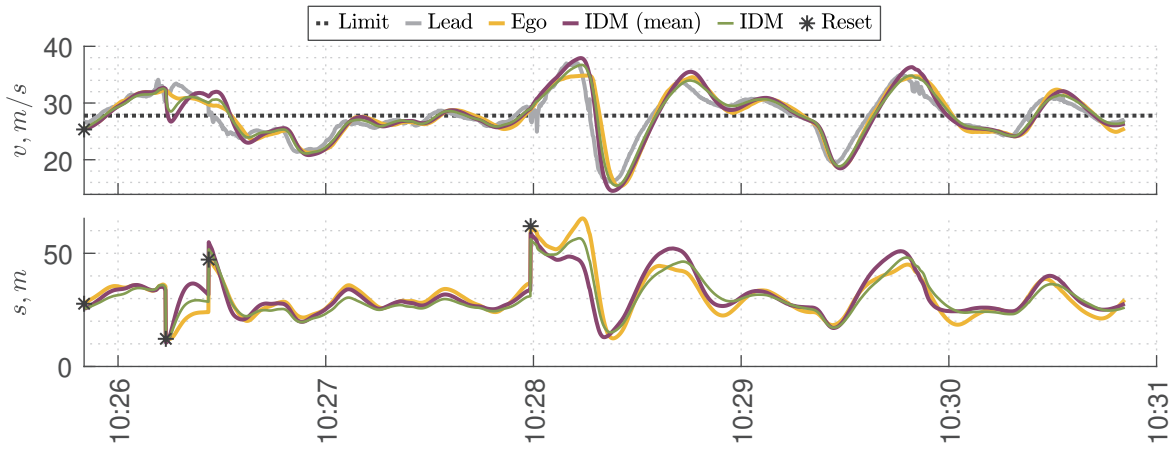

Figure E-4: Figure showing the response of the IDM model on the CI trajectory using mean parameters from the CI2, HB and SG trajectories. The model is calibrated using the RMSE error-measure with equal weight on the distance-gap and velocity ($w_s = w_v = 0.5$).

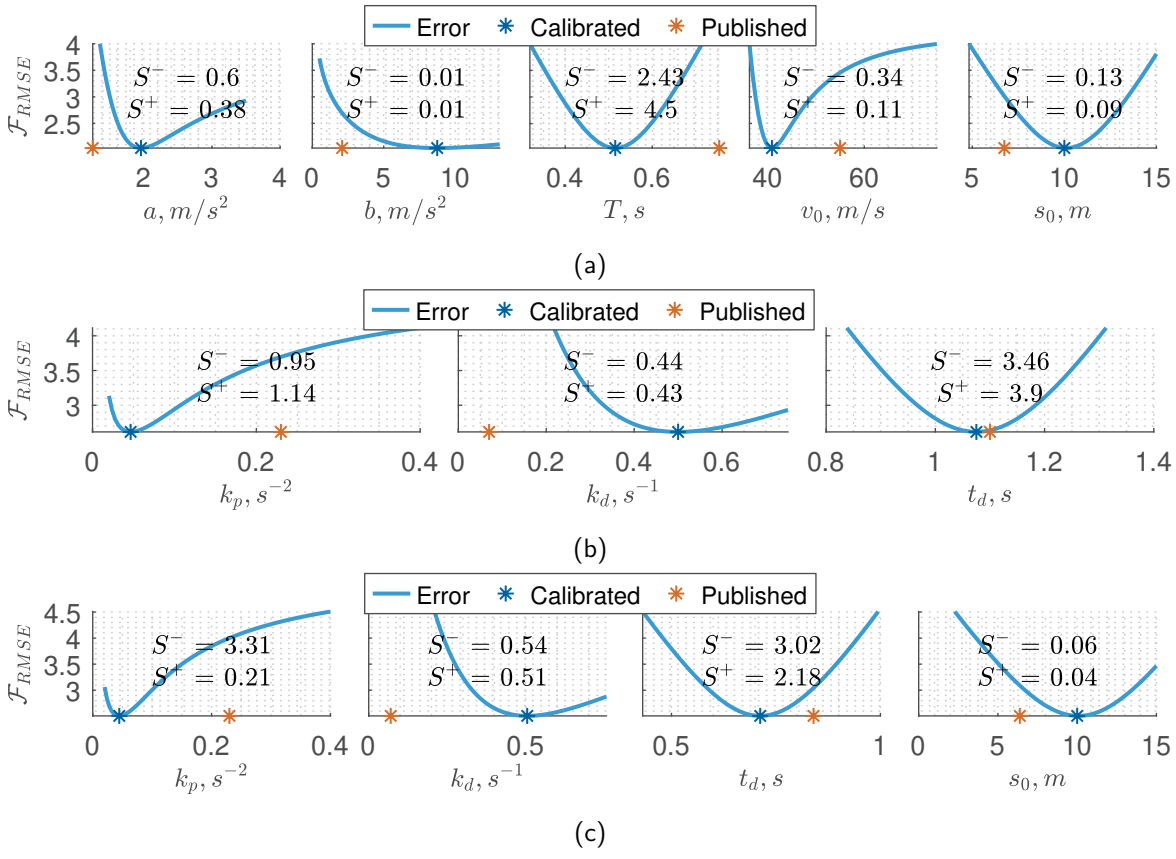

Figure E-5: Figure showing the parameter sensitivity of the IDM (a), sACC (b) and alternative sACC (c) models on real world vehicle data of the CI trajectory. The analysis was performed using the RMSE error-measure with equal weight on the distance-gap and velocity ($w_s = w_v = 0.5$).

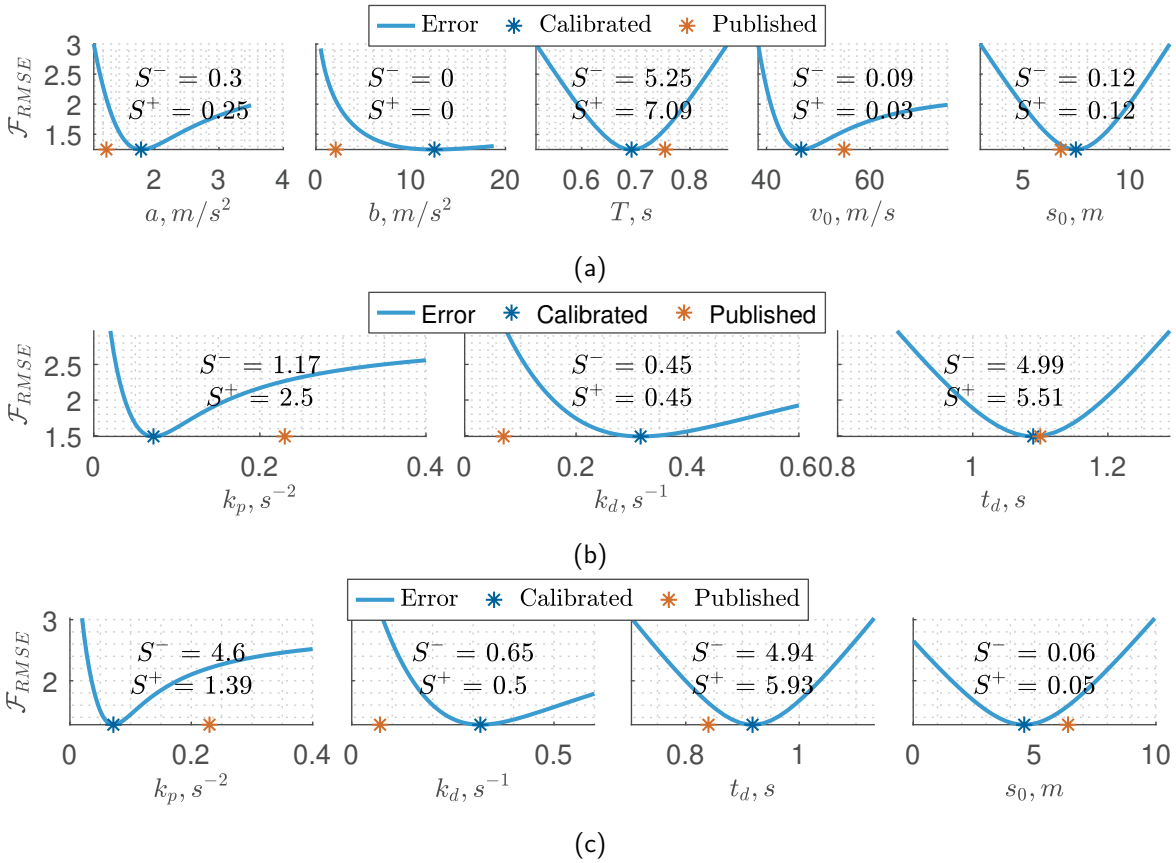

Figure E-6: Figure showing the parameter sensitivity of the IDM (a), sACC (b) and alternative sACC (c) model on real world vehicle data of the CI2 trajectory. The analysis was performed using the RMSE error-measure with equal weight on the distance-gap and velocity ($w_s = w_v = 0.5$).

E-3 Hard-Braking

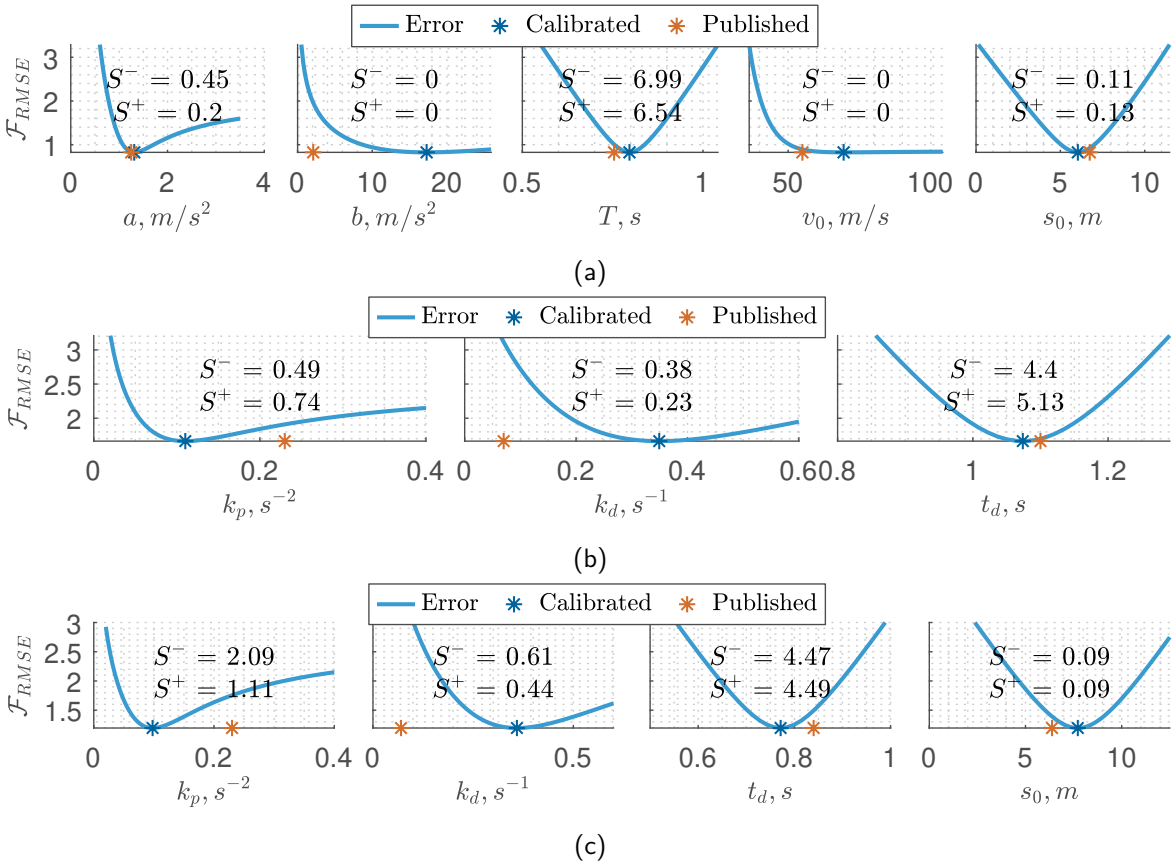

Figure E-7: Figure showing the parameter sensitivity of the IDM (a), sACC (b) and alternative sACC (c) models on real world vehicle data of the HB trajectory. The analysis was performed using the RMSE error-measure with equal weight on the distance-gap and velocity ($w_s = w_v = 0.5$).

E-4 Stop-and-Go

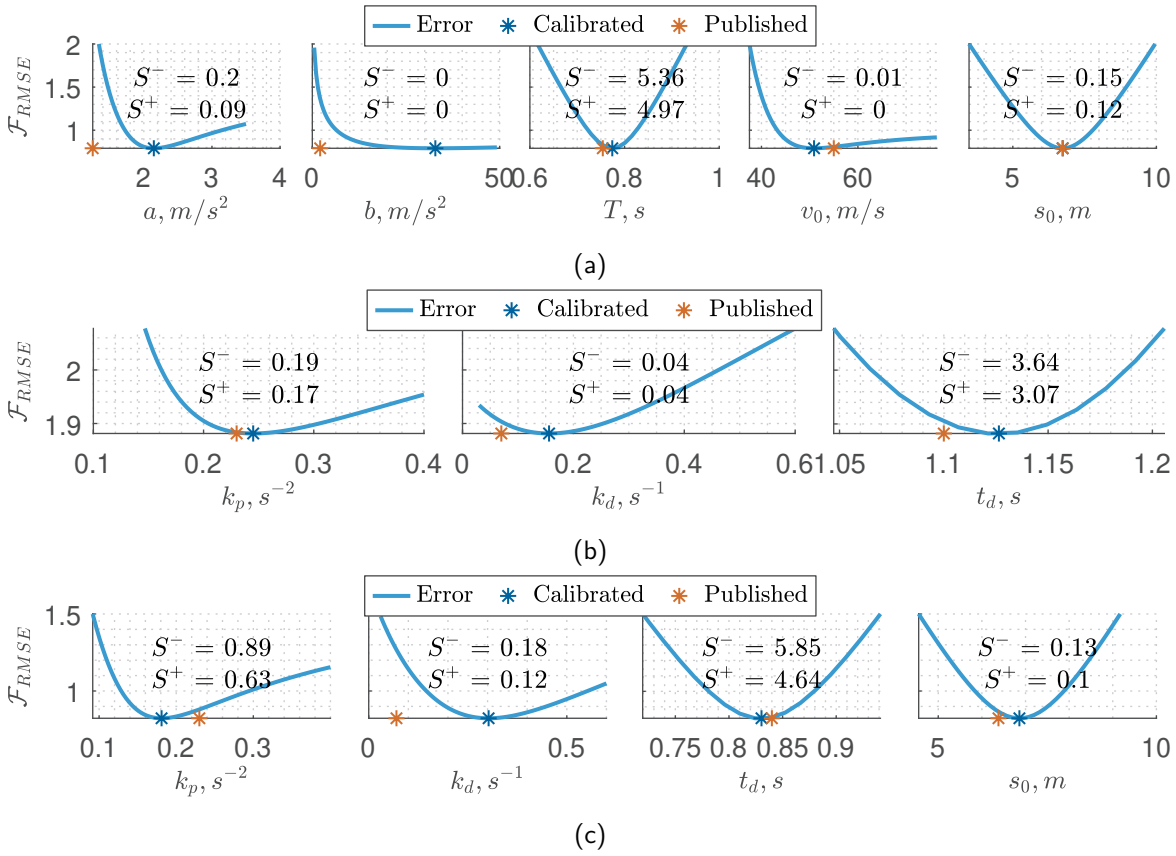

Figure E-8: Figure showing the parameter sensitivity of the IDM (a), sACC (b) and alternative sACC (c) models on real world vehicle data of the SG trajectory. The analysis was performed using the RMSE error-measure with equal weight on the distance-gap and velocity ($w_s = w_v = 0.5$).

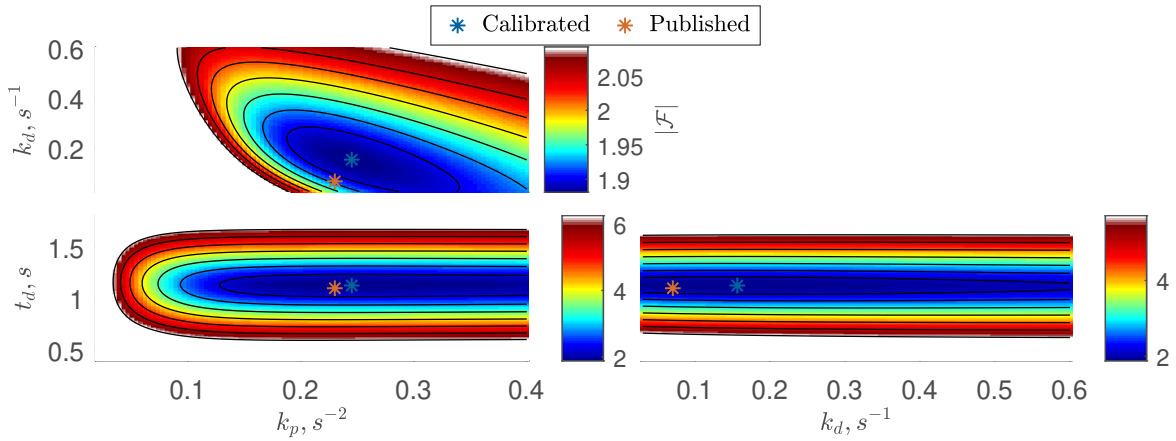

Figure E-9: Figure showing the fitness landscape of the IDM (a) and sACC (b) models on real world vehicle data of the SG trajectory. The analysis was performed using the RMSE error-measure with equal weight on the distance-gap and velocity ($w_s = w_v = 0.5$).

E-5 Cross-Comparing Results from the IDM Model

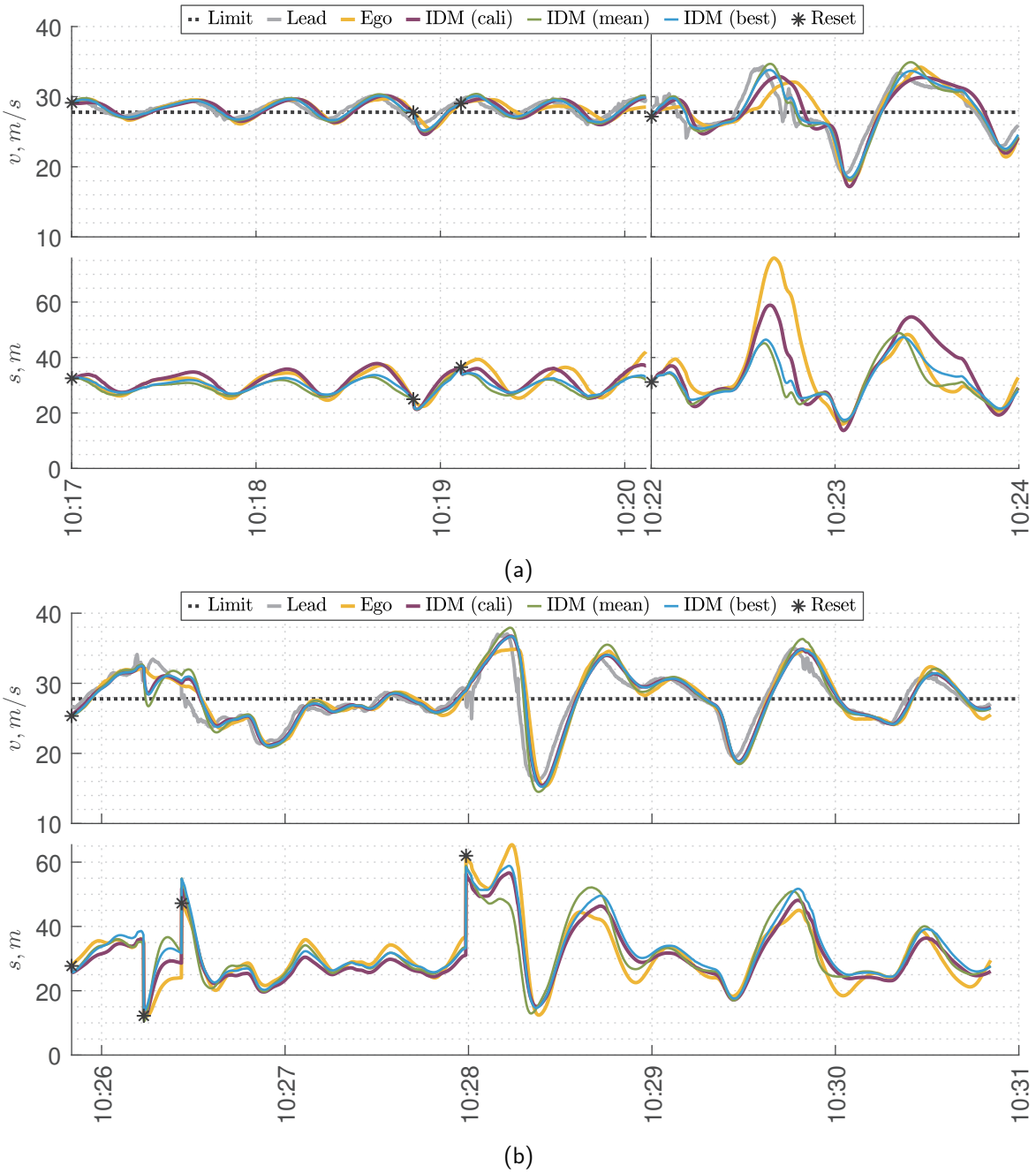

Figure E-10: Figure showing the response of the IDM model on the CF (a) and CI (b) trajectories using the calibrated, mean and "best" calibration parameters. The figures indicate an overshoot of the desired velocity in both figures and too sensitive response at the cut-in and second cut-out in Figure E-10b.

E-6 Cross-Comparing Results from the sACC Model

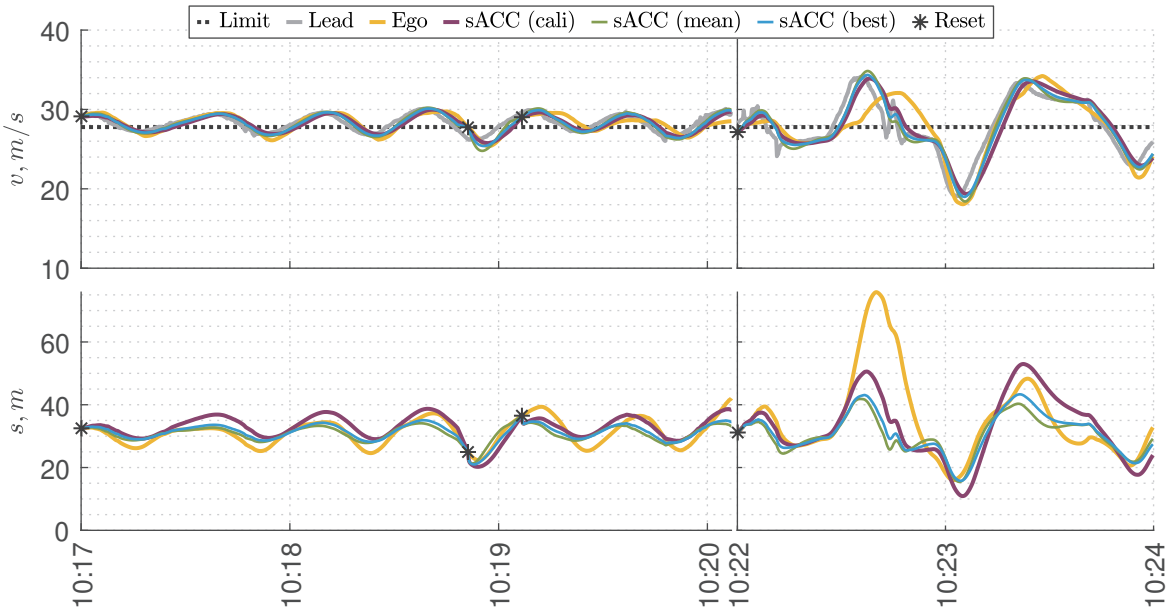

(a)

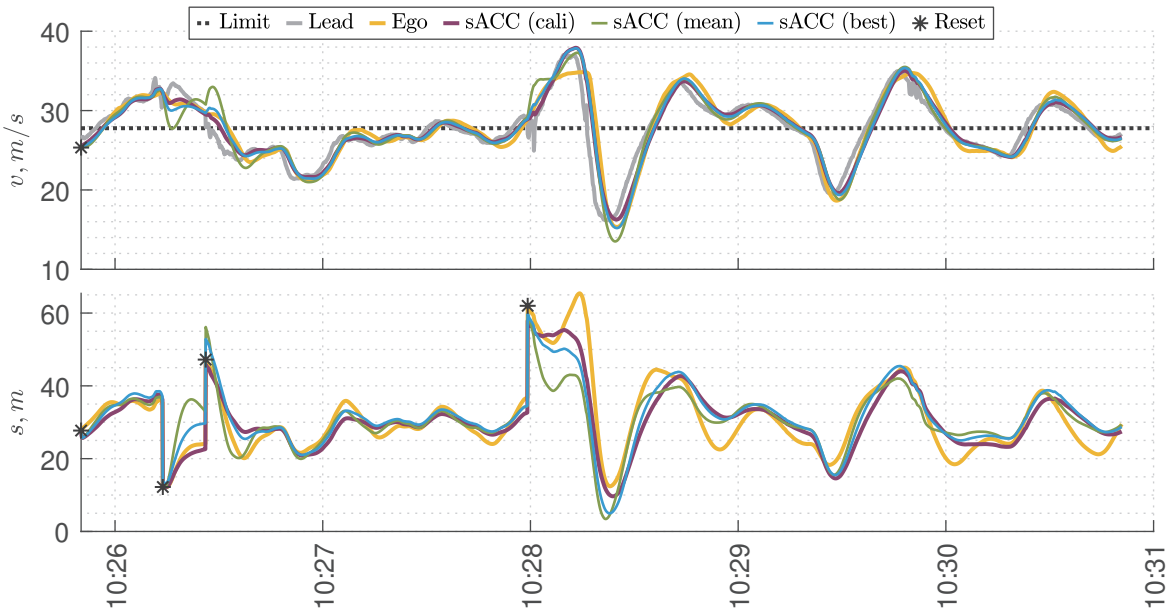

(b)

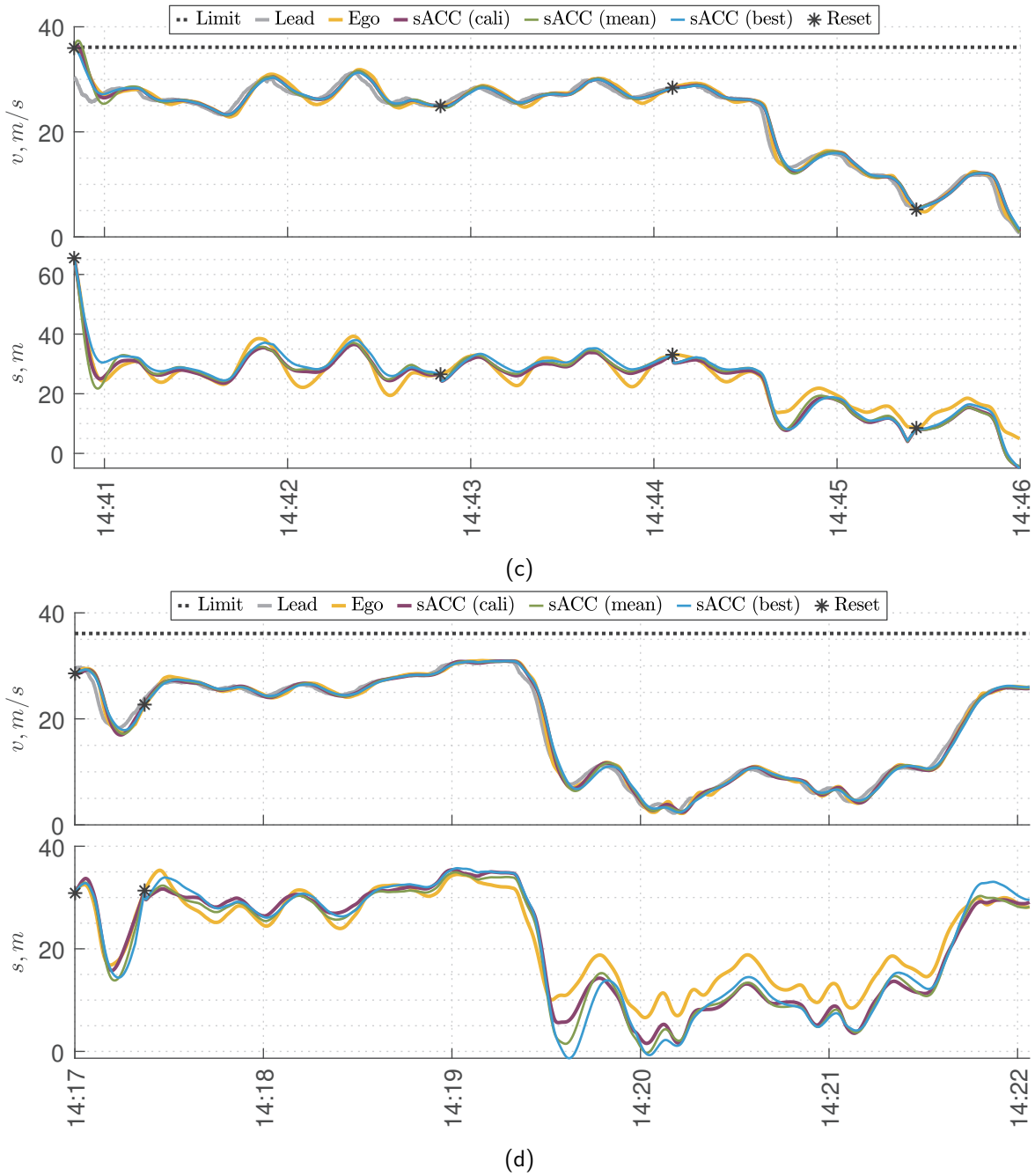

Figure E-11: Figure showing the response of the sACC model on the CF (a) CI (b) and SG (c) trajectories using the calibrated, mean and "best" calibration parameters. The figures indicate an overshoot of the desired velocity in Figures E-11a and b, negative distance-gaps for the "best" parameter set in Figure E-11c too sensitive response at the cut-in and second cut-out in Figure E-11b and zero distance-gap in Figure E-11d.

E-7 Cross-Comparing Results from the Alternative sACC Model

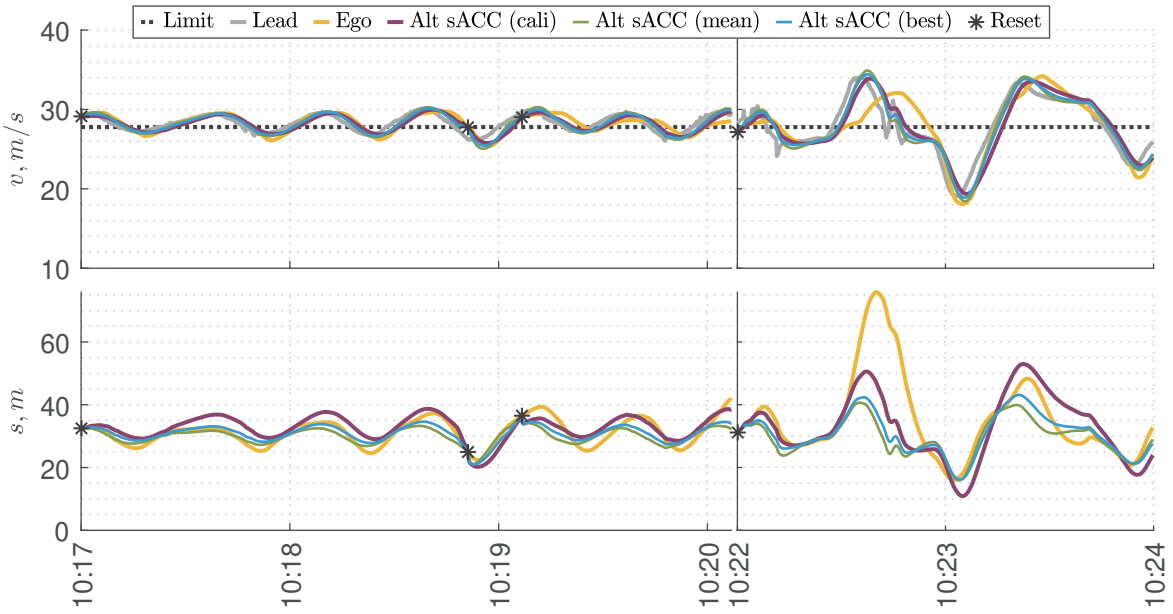

(a)

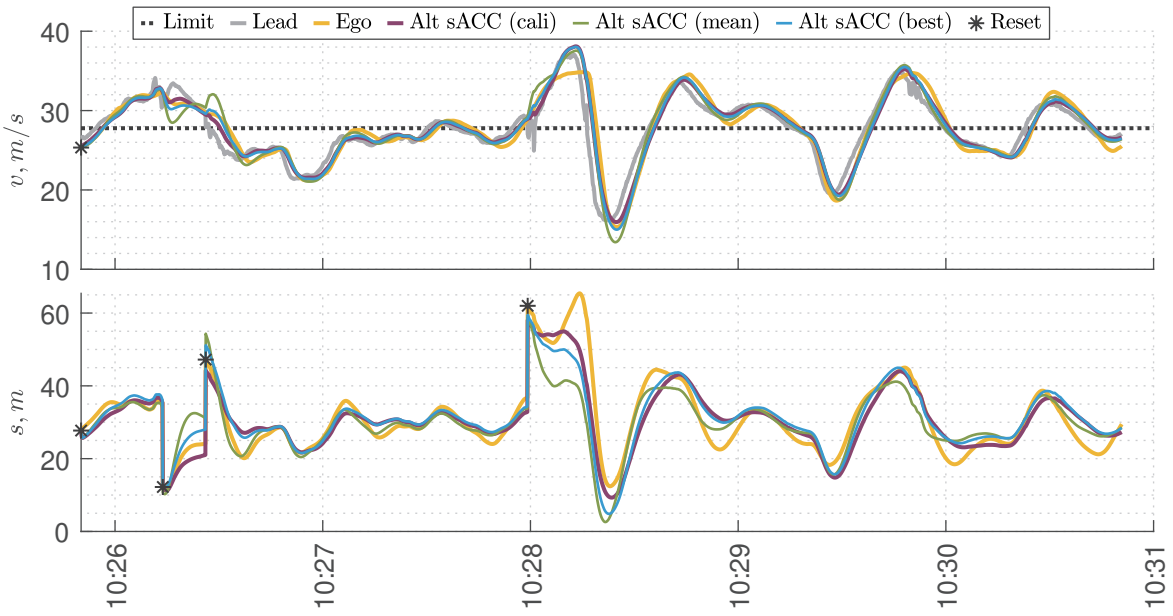

(b)

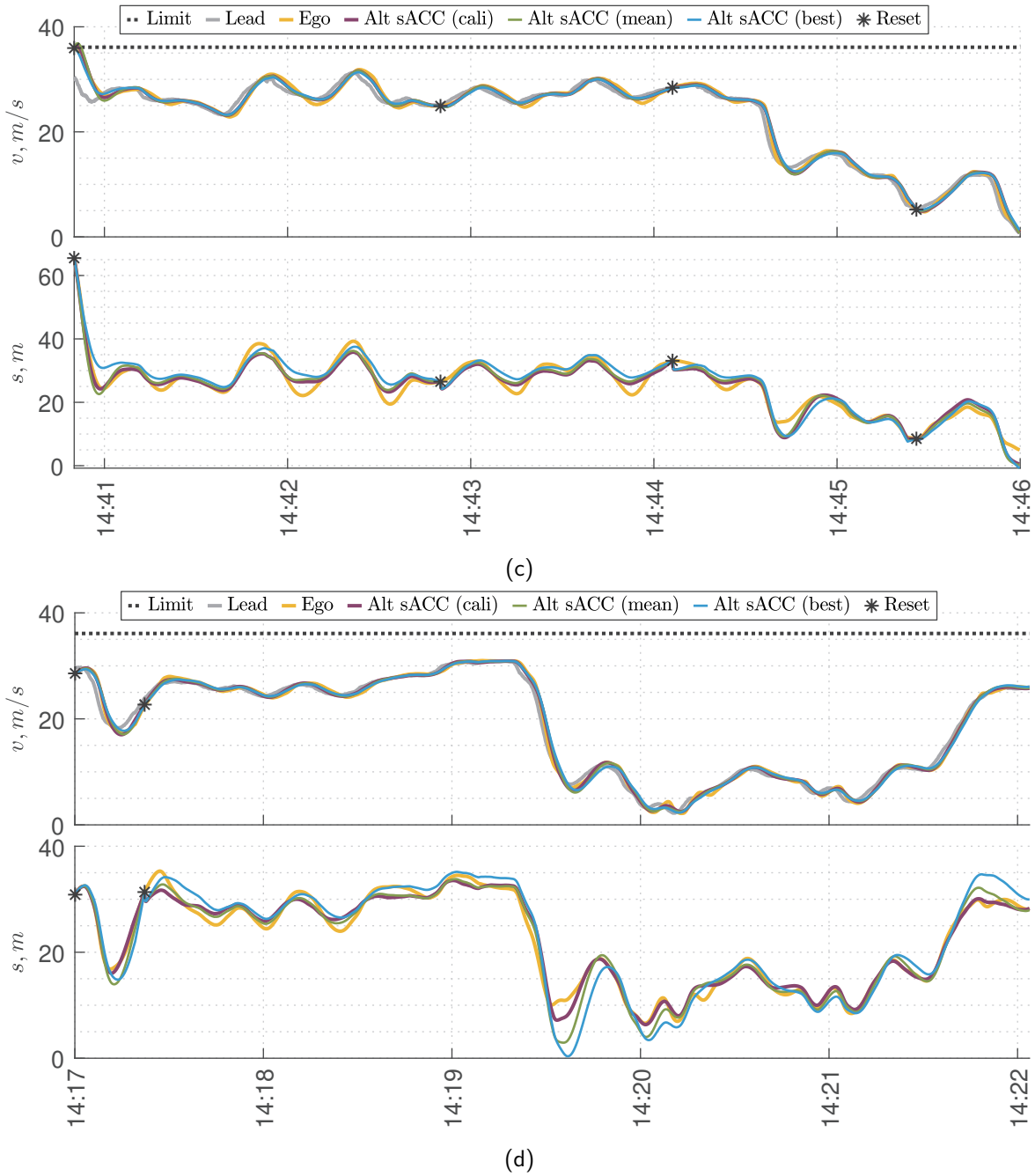

Figure E-12: Figure showing the response of the alternative sACC model on the CF (a) CI (b) and SG (c) trajectories using the calibrated, mean and "best" calibration parameters. The figures indicate an overshoot of the desired velocity in Figures E-12a and b, negative distance-gaps for the "best" parameter set in Figure E-12c and too sensitive response at the cut-in and second cut-out in Figure E-12b and zero distance-gap in Figure E-12d.

Glossary

List of Acronyms

ADAS	Advanced Driving Assistance Systems
ACC	Adaptive Cruise Control
sACC	simplified ACC
IDM	Intelligent Driver Model
OBD	On-Board Diagnostics
CAN	Controller Area Network
RMSE	Root Mean Square Error
RMSRE	Root Mean Square Relative Error
MAE	Mean Absolute Error
MARE	Mean Absolute Relative Error
SQP	Sequential Quadratic Programming
CF	Refers to the “Car-Following” trajectory
OSC	Refers to the “Oscillating” trajectory
SG1	Refers to the “Stop-and-Go 1” trajectory
SG2	Refers to the “Stop-and-Go 2” trajectory
CI	Refers to the “Cut-In” trajectory
HB	Refers to the “Hard-Braking” trajectory
SG	Refers to the “Stop-and-Go” trajectory
DDT	Dynamic Driving Task
VMC	Vehicle Motion Control

List of Symbols

Model Calibration		
Δt	Simulation time-step / sampling-interval	s
e_s	Distance-gap representation error	m
e_v	Velocity representation error	m/s
S^+	Parameter sensitivity overestimation (right)	–
S^-	Parameter sensitivity underestimation (left)	–
t^+	Measurement immediately after time	s
t_0	Initial time	s
t_e	End time	s
w_s	Calibration weight, distance-gap	–
w_v	Calibration weight, velocity	–
Data Analysis		
$\boldsymbol{\delta}^*_{\boldsymbol{GPS}}$	GPS lag	s
$\mathbf{A}, \mathbf{C}$	Kalman state matrices	–
$\mathbf{K}$	Kalman gain	–
$\mathbf{v}$	Measurement noise	–
$\mathbf{w}$	Process noise	–
$\mathbf{z}$	Sensor measurements	–
δ^*_{CAN}	Speedometer bias factor	s
Notation		
$\hat{\beta} = \arg\min_{\beta} \mathcal{F}(z, \hat{z})$	Optimisation problem	
Model Parameters		
$\boldsymbol{\beta}$	Set of model parameters	–
a	Maximum comfortable acceleration (IDM)	m/s^2
b	Maximum comfortable deceleration (IDM)	m/s^2
k_d	Velocity gain ((alternative) ACC)	s^{-1}
k_p	Distance-gap gain ((alternative) ACC)	s^{-2}
s_0	Minimum standstill distance (IDM)	m
s_0	Minimum standstill distance (alternative ACC)	m
T	Desired time-gap (IDM)	s
t_d	Desired time-gap ((alternative) ACC)	s
v_0	Desired velocity (IDM)	m/s
State Variables		
$\dot{v}$	Acceleration	m/s^2
j	Jerk	m/s^3
l	Vehicle length	m
s	Distance-gap	m
v	Velocity	m/s
x	Driven distance	m
Subscripts		
ACL	Accelerometer variable	–
CAN	CAN-bus variable	–
GPS	GPS variable	–
i	Ego-vehicle	–
$i-1$	Lead-vehicle	–